Extracellular Matrix as a Key Mediator of Mammary Tumor Cell Normalization

Donald E. Ingber Ashley Gibbs Bischof

Extracellular Matrix as a Key Mediator of Mammary Tumor Cell Normalization

Abstract

Some epithelial cancers can be induced to revert to quiescent differentiated tissues when combined with embryonic mesenchyme; however, the mechanism of this induction is unknown. This dissertation is based on the hypothesis that because extracellular matrix (ECM) plays a critical role during organ development in the embryo, it also may mediate the differentiation-inducing effects of embryonic mesenchyme on cancer cells. To test this hypothesis, I first optimized methods to isolate ECMs from whole tissues or cultured cells, and to repopulate them with cultured cells, using embryonic tooth as a model system. In Chapter 2, I describe these studies and use them to demonstrate that embryonic ECM is sufficient to regulate odontogenic signaling, cell fate decisions and histodifferentiation during normal tooth development. In Chapter 3, I adapt these methods to show that culture of breast cancer cells with ECM derived from embryonic mammary mesenchyme decreases tumor cell proliferation, and stimulates differentiation, including formation of hollow acini and ducts as well as enhanced expression of estrogen receptor-α and decreased migration. Further, when the inductive ECMs were injected into fast-growing breast tumors in mice, they significantly inhibited cancer expansion. Critically, the differentiation observed with ECM was the same as that observed in co-culture with mammary mesenchyme cells, showing that ECM is playing a dominant role in tumor cell normalization. In Chapter 4, I then set out to determine the mechanism by which embryonic ECM normalizes tumor cells, I analyzed the contributions of bound cytokines, ECM composition and mechanics. Western blot analysis revealed several bound growth factors, which remained following decellularization; however, removal of these growth factors using

high salt washes had no effect on ECM-mediated normalization of tumors. Further, using proteomics analysis I identified eleven ECM proteins present only within inductive ECMs and by testing these proteins in 3D culture, I found three proteins – collagen III, biglycan and SPARC – that increased lumen formation to a similar extent as embryonic ECM. These data confirm that mesenchyme-induced tumor cell normalization is mediated by the insoluble ECM, and reveal the identity of some of the inductive molecules responsible for these effects.

Contents

List of Figures

List of Tables

Acknowledgments

There are many people without whom this work would not have been possible. The few lines here can only express a fraction of my gratitude to a fraction of the people. I hope I am able to repay the rest in the years to come.

First, I would like to thank my thesis advisor, Dr. Donald Ingber, for his patience and guidance throughout my dissertation. Don accepted me into the lab at an exciting time, giving me the opportunity to grow up scientifically along side the start of the Wyss Institute. Don has given me the freedom to explore research ideas while at the same time pushing me to do the highest possible quality of science. Don's passion for translational research is infectious and I will always admire his talent for bringing challenging ideas to fruition. I am grateful for his mentorship throughout the years.

My dissertation advisory committee, Drs. Dave Mooney, Marsha Moses, David Weitz, Jack Lawler, and Jim Hogel consistently supplied a fresh perspective and fruitful discussions. I am thankful for their time and effort over the years, which helped to mold my thesis work into its current form. Dr. Jim Hogel and Michele Jakoulov from the Harvard Biophysics Program also supplied helpful guidance and support.

I have been fortunate to work with and learn from many talented individuals in the Ingber lab. Specific contributions to each chapter are listed at the end in the separate "Acknowledgements" sections. In particular, I want to thank Drs. Akiko Mammoto and Tada Mammoto who provided scientific guidance and moral support as well as teaching me many experimental techniques throughout my graduate career. I would also like to thank Dr. Kaustabh Ghosh, my post-doc mentor upon entering the lab, Kaustabh always pushed me to think deeply about science but also became a great

friend and provided much needed support and advise. I have also been lucky to work closely with Dr. Deniz Yuksel who helped me to get over the middle of graduate school slump, and in the process became a wonderful friend. Dr. Mariko Kobayashi has taught me a number of molecular biology techniques as well as being an excellent lunch buddy, friend and source of moral support. Dr. Elaine Gee was also a source of fruitful discussions and friendship, our nights and weekends at the AFM will not soon be forgotten. I am also grateful for the support and friendship of my bench mates, Dr. Ben Matthews, Sam Jurek, and Alex German as well as other members of the Ingber lab both past and present. Additionally, thanks to my friends and members of my cohort: Alison Hill, Andy Leifer, Nate Derr, Bryan Harada, Dan Chonde, Xavier Rios, Peter Stark and Kevin Takasaki.

I would like to thank my family for their patience and support. Thanks to my parents, Marvin and Barbara Gibbs, for their encouragement, and endless moral support from day one. You have instilled in me the importance of education, and you have been there to pick me up every time things got rough. Thanks to my sister, Summer, who has always encouraged and pushed me.

Finally, I would like to thank my husband, Jon. We embarked on graduate school together and I could not have imagined a better person to have by my side throughout this process. I look forward to many adventure in our future!

1

Introduction

Cancer is generally viewed as an irreversible genetic disease of uncontrolled cell growth and hence most of the current treatment options focus on the use of toxic and/or anti-proliferative therapies. However, some epithelial cancers have been shown to revert to normal tissue when combined with embryonic mesenchyme. For example, 40 years ago DeCosse *et al.* showed that embryonic mammary mesenchyme can induce morphological normalization of mammary tumors, effectively reversing cancer [1], and similar results have been obtained in multiple experimental models [2–4]. The mechanism of this cancer reversion remains unclear; however, it appears

to be mediated, at least in part, through changes in extracellular matrix (ECM). For instance, insoluble ECM materials deposited at the normal epithelial-mesenchymal interface (laminins, collagens, and various proteoglycans) during development can similarly induce normalization of cancer [5–8]. Separate studies show that alterations in ECM structure and composition can also drive epithelial cancer formation [9–11]. Thus, an understanding of the properties of the mesenchyme and ECM that regulate tumor progression could provide new targets for anti-cancer therapies.

In this thesis, I set out to test the hypothesis that embryonic ECM plays a critical role in histodifferentiation and cell fate decisions that may drive tumor cell normalization *in vitro* and *in vivo*, with a focus on breast cancer. I did this by exploring whether embryonic ECM is responsible for the tumor normalization behavior of mesenchymal cells, and by defining key features of the embryonic ECM that are necessary for tumor cell normalization. In this Chapter, I begin by reviewing the molecular and biophysical properties of ECM, and the role they play during embryonic development and tumor progression. In Chapter 2, I describe the development of methods to isolate intact ECM from embryonic tissue sections and cultured embryonic mesenchymal cells, and to culture cells on these substrates using mesenchyme isolated from embryonic tooth germ as a simple model system. Using this approach, I was able to demonstrate that embryonic ECM is sufficient to stimulate histodifferentiation and cell fate decisions during normal development. Chapter 3 adapts these methods to show that these same insoluble ECMs, isolated from early embryonic mammary mesenchyme, are sufficient to induce normalization of tumor epithelial cells both *in vitro* and *in vivo*. In Chapter 4, I use proteomics, western blot, and atomic force microscopy (AFM) studies to define features of inductive embryonic ECMs that are critical for their inductive activity. This work led to the identification of three ECM proteins that are sufficient to induce tumor normalization *in vitro*. Finally, in Chapter 5, I

discuss the implications of this work, consider potential limitations, and explore how these insights might facilitate the development of a tissue engineering approach to tumor therapy in the future.

1.1 Regulation of Cell Behavior by Extracellular Matrix

ECM scaffolds have unique physical, biochemical, and biomechanical properties that are essential for regulating cell behavior (reviewed in [12–14]). The physical properties of the ECM (*i.e.*, rigidity, porosity, insolubility, topography, and mechanics) determine its role as a scaffold that supports tissue architecture and integrity [15, 16], as well as directs cell migration [17–19] and cell fate [20–22]. The biochemical properties of the ECM allow cells to sense and interact with their environment using various receptor-mediated signal transduction cascades emanating from the cell surface to the nucleus, resulting in changes in gene expression and cell behavior [23–25]. The highly charged ECM network, rich in polysaccharide modifications can also bind growth factors, limiting the diffusive range, accessibility, and signaling of ligands [26, 27]. Additionally, it is important to note that these signals are highly dynamic, intertwined and reciprocal. The ECM is constantly being synthesized, remodeled, and degraded which alters both matrix composition as well as structure and mechanics, and these changes in turn regulate cell behavior as well as ECM protein metabolism.

1.1.1 Extracellular matrix composition

The ECM is composed of several distinct families of molecules including collagens and non-collagenous glycoproteins, glycosaminoglycans (GAG), and proteoglycans with different physical and biochemical properties. These components make up the basement membrane, produced jointly by the epithelium or endothelium and stroma,

as well as the interstitial matrix, primarily made by the stromal cells. The basement membrane, which is made up of type IV collagen, laminins, fibronectin, and liner proteins such as nidogen, enactin and tubulointerstitial nephritis antigen (TIN-ag), is more compact and less porous than interstitial matrix, functioning as a barrier between epithelial and stromal compartments. The interstitial matrix is highly charged, hydrated and contributes greatly to the tensile strength of the tissue; it is rich in fibrillar collagens, proteoglycans, like biglycan, and various glycoproteins such as tenascin C, fibronectin, vitronectin, and fibrillin.

The most abundant proteins in the human body are collagens. There are at least 28 collagens, classified into both fibrillar and non-fibrillar forms, that share a common structural motif of helical fibrils formed by three protein subunits [28]. The primary function of the collagens is to act as the structural support and binding partners for other ECM proteins. There is also a diverse array of non-collagenase glycoproteins represented by several families of proteins with diverse origins. Many of these molecules are composed of multiple chains (*e.g.*, laminin trimer, fibronectin dimer) that further undergo alternative splicing depending on the developmental stage and tissue-specific context of their expression. However, despite the wide variation in ECM glycoprotein structure, many share analogous functions and common structural motifs, such as the adhesive Arg-Gly-Asp (RGD) sequence.

GAGs are linear, unbranched polymers of repeating disaccharides composed of a hexosamine and uronic acid. The abundance of carboxyl, hydroxyl, and sulfate groups (*e.g.*, chondroitin, dermatin, keratin and heparin-sulfates) give GAGs a net negative charge, which attracts Na^+. This draws water in creating swelling which opens pathways to promote invasion and migration of cells [29]. Most GAGs, with the exception of hyaluronan, are further covalently linked to a core protein to form proteoglycans. Biglycan, for example, consists of a core protein of 331 amino acids

covalently bound to two chondroitin sulphate- or dermatan sulphate-containing GAG side chains [30].

Another class of ECM molecules, called matricellular proteins, including thrombospondin, SPARC (secreted protein, acidic and rich in cysteine), galectin, tenascin-C, periostin, and osteopontin, do not function as structural elements but interact with ECM proteins and cells to modulate cell-matrix interaction [31, 32]. For example, SPARC binds rapidly to precise components of the ECM, such as collagens [33], and modulates the interaction of cells, inhibiting cell adhesion and cell cycle progression [34, 35]. Through these activities SPARC has been shown to inhibit both adipogenesis and tumor progression [36].

The diverse array of ECM proteins support the physical structure of the cell and various biological functions, largely through their ability to bind different partners such as other ECM proteins, growth factors, signal receptors and adhesion molecules, mediated by multiple, specific domains present within each protein. Fibronectin, for example, contributes to the structural framework by binding to collagens and heparin sulphate proteoglycans (HSPGs) through its type I and type II domains [16], as well as binding to cells through its short RGD motif in the type III domain [37]. Interaction of ECM proteins can be critical for the formation of the scaffold, for example, fibrillin-1 binds with itself and other ECM proteins to form microfibrils, which provide a scaffold for deposition of elastin [15], a major structural fiber in ECM. Fibrillin-1 further binds cell surface integrins and transforming growth factor β (TGFβ), limiting the bioavilability [38].

1.1.2 Growth factor signaling

ECM proteins also influence cell behavior by immobilizing growth factors that can induce cell surface receptor signaling when they come in contact with adjacent cells,

or when they are released in a soluble form. ECM-bound growth factors can be released locally and bind to their canonical receptors, creating gradients of the soluble diffusible morphogen [26, 27]. Alternatively, many ECM proteins have binding sites for both cells and growth factors creating a local increase in concentration adjacent to cell surface receptors and in some cases serving as a cofactor. For example, fibroblast growth factor (FGF) binds HSPG and can be cleaved off by heparanase to be released as a soluble ligand or FGF can bind both its receptor and HS creating a higher affinity bond in the complex [39]. ECM proteins can also bind growth factors and sequester them from cells, releasing them only when triggered during physiological events such as wound healing [40], thereby controlling growth factor availability.

1.1.3 Extracellular matrix mechanics

The mechanical properties of ECM scaffolds have also been shown to play a critical role in controlling cell behavior. AFM has been used to image and characterize mechanical properties of living materials such as cells and tissue sections at high resolution [41] showing that the cell niche varies from 100 Pascal (Pa) for brain tissue to more than 30 kPa for calcified bone. These differences are critical for cell behavior, for example, undifferentiated mesenchymal stem cells grown on polymer gels mimicking the ECM elasticity of brain, muscle, or bone begin to express neuronal, skeletal muscle, or bone makers respectively [22]. Differentiation can be blocked using pharmacological inhibitors of myosin motor proteins [22], which are responsible for generating traction forces against the matrix and modifying the tension within the cell based on the substrate stiffness [42].

Multiple mechanisms have been identified through which mechanical forces applied at the cell surface or generated within the contractile cytoskeleton can alter cellular biochemistry and produce transcriptional alterations [43]. Mechanical signals are

sensed by integrins, which transfer the physical forces across the plasma membrane, converting them to biochemical signals within cell surface focal adhesions to trigger transcriptional changes in the nucleus through modulation of downstream signaling cascades [44, 45]. One of the most rapid mechanical signaling pathways upstream of transcription involves activation of mechanosensitive ion channels on the cell surface triggered through mechanical strain applied to ECM-bound integrin [46]. Mechanical cues transmitted through focal adhesions also facilitate chemical signals that modulate the Rho signaling pathway, which feeds back to control phosphorylation of myosin II and the generation of cytoskeleatal tension [47, 48]. Signaling pathways affected by these factors are involved in controlling multiple cellular processes, including migration, growth, differentiation, and matrix remodeling [25, 45, 49, 50].

1.2 Extracellular Matrix and Organogenesis

Branching morphogenesis is one of the most common processes in epithelial organ development as it allows tissues to maximize their surface area to overcome space constraints posed by organ size. This process occurs in the lung, kidney, mammary and salivary glands as well as skin appendages, such as teeth and hair follicles. Although the mature form of these organs diverge greatly in size, shape, and function, their early developmental stages are remarkably similar at the morphogenetic and molecular levels [51]. In each case, the initiation of organogenesis is marked by the localized thickening in the surface epithelium to form a placode that subsequently invaginates into the underlying mesenchyme to form a bud. The formation of each of these organs is regulated by reciprocal and sequential interactions between the epithelial and mesenchymal tissues, which is mediated by signaling pathways, including Wnt, bone morphogenetic protein (Bmp), FGF, TGFβ, hedgehog (Hh), and tumor

necrosis factor (Tnf) and their downstream transcription factors.

One of the simplest examples of organ development is the tooth as it only undergoes a series of two budding or folding events rather than an extensive series of such events as observed in other developing organs. Because of its simplicity, I began my studies using embryonic tooth development as a model system. In the mouse embryo, tooth formation is preceded by the formation of the dental lamina, a horseshoe shaped stripe of thickened epithelium, from which all mammalian teeth bud. Odontogenesis begins with a local thickening of the dental epithelium to form a placode at embryonic day 10 to 11 (E10-E11). At E12, the dental epithelium buds into the underlying mesenchyme, which signals the underlying mesenchyme to condense around the bud by E12-E13. During subsequent morphogenesis, the epithelium folds and grows to surround the dental papilla mesenchyme called the cap stage and the final shape of the tooth crown becomes fixed during the bell stage [52].

Throughout branching morphogenesis, sequential and reciprocal interactions between the epithelial and mesenchymal tissues are critical for regulating appropriate organ formation. During tooth development in the mouse, the early (E10-11) dental epithelium contains all of the information necessary to reprogram adjacent early dental mesenchyme. However, this ondontogenic potential shifts from the dental epithelium to the mesenchyme after E12.5, corresponding with formation of the epithelial bud and the condensation of the underlying mesenchyme [53–55].

This process of cell compaction, known as 'mesenchymal condensation', has long been known to be a key step in the formation of many specialized organs (*e.g.*, tooth, breast, liver, lung, kidney, etc.; [56, 57]) and it was recently discovered by Dr. Tadanori Mammoto in the Ingber laboratory that this mechanical compaction results in changes in cell shape, which induce expression of critical odontogenic transcription factors (Pax9, Msx1) and a molecular morphogen (BMP4) [58]. When

undifferentiated (E10) dental mesenchyme cells were cultured on ECM islands at high plating density, leading to similar cell compaction to that seen at E13 *in vivo*, expression of these critical odontogenic factors increased significantly even in the absence of exogenous morphogens, showing that physical cell compaction dictates cell fate during embryonic tooth organ formation. Further, it has been suggested that mesencymal condensation is supported in part by ECM accumulation; both collagen VI and tenascin C are upregulated within the condensed mesenchyme as well as high density cultures of dental mesenchyme [58].

As I focus on breast cancer as a developmental disease in this dissertation, it is important to understand normal breast anatomy and development. The mammary gland is composed of two main tissues: the epithelium and the stroma, called mesenchyme in the embryo. In the adult, columnar luminal epithelial cells line the mammary ducts and are surrounded by specialized, contractile myoepithelial cells. Outside the myoepithelial cells is the basement membrane, a specialized layer of extracellular matrix molecules which separates the epithelium from the stroma. The stroma consists of both cellular and acellular components. Stromal cell types include fibroblasts, adipocytes, endothelial cells as well as cells of the immune system [59]. The most predominant component in the mammary gland ECM is type I collagen, however, the ECM also includes other fibrillar collagens type III, and V, bead-filament collagen VI and IX as well as basal lamina collagen IV, laminins and proteins known to effect crosslinking, such as elastin, fibrillin 1, decorin, lumican, and biglycan [60].

In the embryo, the formation of the mouse mammary gland begins at E10 with the formation of two milk lines, which run in an anteroposterior direction ventrally along each flank of the embryo. Between E10 and E11 five mammary placodes appear at reproducibly precise positions on each milk line. During the following day the epithelial thickening invades into the underlying dermal mesenchyme to form buds. From

E12.5-E14.5 the epithelial bud experiences a period of relative morphogenetic quiescence, growing slightly in size but not changing shape. The mesenchymal cells directly surrounding the epithelial bud become more densely packed and orient themselves in concentric layers, becoming the mammary mesenchyme while the deeper mesenchyme under the mammary bud differentiates into the dense fat pad precursor by E14.5. By E15 epithelial cell proliferation increases, and the buds begin to elongate at the tip and push through the dense mesenchymal layer towards deeper layers of the dermal mesenchyme and the fat pad precursor. Up until birth (∼E19) the epithelial tissue undergoes further proliferation and bifurcation at the leading tips of the ducts to form a simple ductal tree, which is present in the neonate [61, 62].

As with other ectodermal appendages, the mammary gland is formed by reciprocal and sequential interactions between the epithelium and the mesenchyme. Studies by Propper *et al.*, as early as 1968, suggested that mammary mesenchyme induces the overlying ectoderm to form epithelial buds using *in vitro* cocultures of mammary mesenchyme and non-mammary ectoderm [63, 64]. However, it was only confirmed much later by Cunha *et al.* that E13 embryonic mouse mammary mesenchyme can instruct midventral epidermis of E13 rat embryos to form functioning mammary ducts in adult female mice [65]. When grown in lactating female hosts, induced mammary epithelial cells form lobuloalveolar structures and express casein and α-lactalbumin, demonstrating that embryonic mammary mesenchyme can induce mammary epithelial differentiation both morphologically and functionally. However, mammary gland identity within the embryo appears to be determined as early as E12. Heterotypic recombination of salivary gland mesenchyme with mammary epithelium results in ductal branching patterns resembling the salivary gland, but displays functional cytodifferentiation of the mammary epithelium [66].

The two different mammary mesenchymes, which arise at E14.5, appear to have

separate regulatory roles during embryonic development. The densely packed mammary mesenchyme just adjacent to the epithelial bud induces embryonic or adult mammary epithelium to undergo atypical compact ductal branching, giving rise to ductal patterning similar to the salivary gland [67]. In contrast the fat pad precursor cells elicit a more diffuse pattern of ductal branching characteristic of the adult mammary gland [68]. However, so far only the mammary mesenchyme has been shown to induce non-mesenchyme embryonic epidermis to undergo mammary morphogeneisis as well as functional differentiation [65]. It has been proposed that these differences in epithelial behavior are caused, in part, by ECM composition. The fat pad mesenchyme, which appears in close apposition to regions of the epithelial rudiment that undergo elongation and branching in the embryo, induces expression of laminin and protoheparan sulphate that are also found abundantly in the developing mammary gland during puberty [69]. These results suggest that the abundance, composition, organization and remodeling of ECM all act as crucial regulators of epithelial cell behavior.

1.2.1 Extracellular matrix as a control element during morphogenesis

Most past work on embryonic development and cancer has focused on the role of soluble chemical factors, genes and signaling molecules. However, the development of branched organs involves the invasion of epithelial tissues into surrounding embryonic mesenchyme rich in ECM. During organ morphogenesis, the ECM is constantly changing its composition and spatial distribution and it is the combinatorial effect of multiple ECM molecules as well as their dynamic regulation that instructs morphogenesis. In fact, manipulations to either reduce or promote deposition of individual ECM proteins can inhibit branching. In *ex vivo* organ cultures of the salivary gland, for example, addition of either synthetic laminin α1 G-domain peptides or of a

function-blocking antibody directed against laminin α1 G-domain inhibits branching [70], and similar results have been seen with collagen in the embryonic mammary gland [71–73]. Thus, a single ECM component can have functions that both promote and attenuate cell behaviors important for branching depending on the spatiotemporal context.

The organization of the ECM within the branching structures of the mammary terminal end buds is critical for normal morphogenesis, and gives clues regarding the function of different ECM molecules. The tips of terminal end buds have a thin ECM rich in hyaluronic acid [74], and enhancing ECM binding using β1 integrin activating antibody inhibits branching [75], suggesting that reduced adhesion to ECM in this region is required for epithelial invasion. Conversely, thick ECM composed primarily of collagen IV, laminin 1, laminin 5, and HSPG [71] surrounds the bud flanks, providing a fibrous ECM to maintain the tubular architecture [76]. However, this fibrous ECM is not just a physical barrier, it is also required for signaling. Discoidin domain receptor 1 (DDR1) is a receptor tyrosine kinase which when lost in the mammary gland causes branching defects, in part due to hyperproliferation [77]. Interestingly, DDR is phosphorylated only when ligated by fibrillar collagen and not denatured collagen fragments [77], thus the fibrous ECM in the bud flanks promotes a quiescent state likely required for stabilization of these structures.

Expression patterns of ECM molecules in branching organs have also highlighted the difficulty of analyzing contributions of ECM to morphogenesis. Unique and transient expression patterns of combinations of ECM proteins and their receptors have been described in the kidney, however, they have been seen to vary widely between species [78]. Further, knockout mice for a single ECM component often do not result in kidney defects *in vivo*, suggesting that there is extensive functional compensation. On the other hand, the function of a single integrin can vary depending on

the ECM composition. When $\alpha 3\beta 1$ integrin is blocked in cultures of mammary epithelium branching is enhanced in collagen I gels [79] and inhibited on laminin-rich basement membrane gels [80], showing the complex role of matrix proteins in organ morphogenesis.

ECM also provides structural and mechanical regulation during organ development; elastic and rigid elements, which propagate and resist forces, sculpt tissues into functioning organ structures. Local anisotropies in the distribution of tension may determine where branch points occur. In the mammary gland, asymmetric induction of sulfated GAGs at the terminal end bud, followed by accumulation of collagen creates a thickened, rigid ECM thought to be responsible for bifurcation and branch direction [76]. Further, epithelial morphogenesis can be altered in developing lungs by directly modulating cytoskeletal tension generation using inhibitors of the Rho-ROCK pathway [81], showing the critical role of mechanics in organ formation.

1.3 Extracellular Matrix and Mammary Tumor Formation

Epithelial cancers or carcinomas that comprise more than 90% of all cancers are commonly thought to arise from a progressive accumulation of random genetic mutations, which lead to uncontrolled cell growth. However, it is only when growth results in disorganization of normal epithelial architecture that the tissue is defined as neoplastic. Moreover, epithelial tumors only become malignant once their ECM boundary (basement membrane) becomes physically compromised so that the tumor cells are free to invade into surrounding connective tissues and metastasize throughout the body. Thus, cancer also can be viewed as a disease of developmental control as it results from a breakdown of the fundamental rules that govern how cells stably organize within tissues, organs and ultimately living organisms [82]. Thus, just as

epithelial-mesenchymal interactions control epithelial growth in the embryo, a break down of epithelial-stromal regulation contributes to tumor progression.

While fibroblasts are often thought to be a passive participant in neoplastic transformation, it has become increasingly clear that cancer associated fibroblasts (CAFs) actively contribute to tumor growth, expansion and dissemination [83–85]. Using tissue recombination it was shown that irradiated or carcinogen treated mammary stroma can promote formation of epithelial carcinomas, while carcinogen-treated mammary epithelial cells failed to form tumors adjacent to untreated stroma [86, 87]. Similarly, CAFs isolated from either human prostate or breast cancer patients can stimulate cell growth and tumor formation in nontumorigenic epithelial cells [88, 89]. These results show that fibroblasts can be activated either by treatment with carcinogen or irradiation, or through interaction with the tumor microenvironment, and that activation of the stroma alone is sufficient to induce tumor formation in an adjacent healthy epithelium. Activated fibroblasts, or CAFs, are typically more proliferative, express α-smooth muscle actin and are surrounded by a dense accumulation of fibrillar collagen [90, 91].

1.3.1 Extracellular matrix contributes to breast cancer

Abnormal ECM dynamics are well documented in clinical studies of many diseases and are a hallmark of cancer [92]. Various collagens (*e.g.*, collagen I, II, III, V, and IX) show increased deposition during mammary tumor formation [93–95], which correlates with an adverse prognosis [96]. Further, while normal tissue contains primarily relaxed nonoriented ECM fibrils, collagen I fibrils in breast tumors are often highly linearized and aligned [9, 97], and this physical restructuring has been shown to progressively stiffen the ECM [9, 41]. This process is driven, in part, by increased collagen crosslinking by enzymes such as lysyl oxidase (LOX). Interestingly, treatment

with LOX inhibitors prior to tumor formation can decrease ECM crosslinking and tumor stiffening, which inhibits focal adhesion maturation, decreases growth factor receptor signaling and ultimately reduces tumor incidence and size [9]. Furthermore, transgenic mice that misexpress the ECM degrading enzyme stromelysin-1 (MMP3) develop mammary tumors within 3-4 months of age [98, 99]. Which is consistent with the fact that increased expression of LOX and MMPs correlate clinically with tumor progression and elevated metastatic risk [100, 101].

1.3.2 Breast cancer model

In order to study the complex interactions of epithelial-stromal interactions and ECM dynamics during tumor progression culture models and animal models have been developed. In this thesis I use tumor cells isolated from C3(1) SV40 Lage T-Antigen transgenic mice that develop mammary carcinomas in 100% of female mice [102]. The mammary lesions develop over a predictable time course without the need for pregnancy or hormone stimulation to drive transgene expression. Histologically, mammary tumors pass through several distinct stages. At eight weeks of age the glands appear histologically normal. Hyperplastic lesions appear at 12 weeks of age and progress through an intermediate stage that resembles human ductal carcinoma in situ (DCIS) by 16 weeks of age. The tumors then progress to an invasive carcinoma similar to a poorly or moderately differentiated human infiltrating ductal carcinoma [103, 104]. Further, estrogen receptor α (ERα) expression is progressively lost during mammary tumor progression, as often occurs in human breast cancer [105]. ERα status is an important factor in assessing prognosis and in determining therapeutic strategies for treating breast cancer. ERα expression is associated with more differentiated and less aggressive tumors, while tumors lacking ERα are associated with a more aggressive disease course and poor clinical outcome [106, 107]. These features

make this an interesting model system to study mammary cancers.

1.4 Cancer Normalization by Embryonic Microenvironment

While transformed stroma has been shown to promote tumor formation, provocative experiments from over 40 years ago have shown that healthy stroma can have a tumor suppressing effect. In particular it has been shown that tumor cells placed in the early embryo can be instructed to 'reboot' and take part in normal development. Embryonal carcinoma cells from a spontaneous testicular teratocarcinoma contribute to the development of chimeric mice if injected into the blastocyst [108], and further contribute to a variety of tissues in cancer-free adult mice [109] showing that malignant cells can contribute to normal healthy structures if supplied the appropriate tissue context. Rous sarcoma virus, known to transform cells in culture and cause sarcomas driven by oncogene transformation [110] upon injection into chickens [111], do not lead to malignant transformation when injected into chick embryos [112]. However, removal of infected cells from the embryonic microenvironment results in rapid transformation in culture [113]. This work suggested that genetic alterations are neither necessary nor sufficient for tumorigenesis, despite growing genetic discoveries, but rather that a sufficient embryonic microenvironment can outweigh genetic changes.

These ideas led to the hypothesis that for every tumor type there is an embryonic microenvironment that may influence its growth and differentiation; for epithelial tumors that is the stroma or mesenchyme. DeCosse *et al.* reported that mammary carcinoma cells exhibit a more orderly histodifferentiation and a lower proliferative rate when grown in association with mammary mesenchyme [1, 114] and similar results were shown for prostate [115, 116], and bladder [117]. However, there have been contradictory reports; Sakakura *et al.* showed that embryonic mesenchyme

actually accelerates the development of tumors in response to oncogenic viruses [118–120] and followup studies by DeCosse *et al.* suggested that embryonic mesenchyme has no affect on mammary tumor growth *in vivo* [114].

1.4.1 Fibroblasts, ECM and growth factors in tumor cell fate

While it is clear that the stromal tissue plays a critical role with the capacity to both promote and suppress tumor progression, the mechanism is not well understood. Early breast cancer lesions, DCIS, are maintained within the basement membrane, and this has led to the hypothesis that secreted soluble factors, which can cross the basement membrane, must drive epithelial-stromal interactions. To this effect, elevated expression of SDF-1, vascular endothelial growth factor (VEGF), hepatocyte growth factor (HGF), and TGFβ have been implicated in stromal control of tumor progression, enhancing tumor cell growth and migration, as well as promoting angiogenesis [89, 121–125]. Further, conditioned media isolated from normal ovarian fibroblasts has been shown to significantly inhibit tumor cell growth [126], suggesting that secreted soluble factors can also play a role in inhibiting tumor progression.

However, misregulation of ECM expression and dynamics can also contribute to tumor progression as discussed in section 1.3.1, and manipulating signaling from the basement membrane in order to restore polarity has been shown to suppress tumoigenicity. Specifically, restoring epithelial cell contact with a healthy basement membrane can slow tumor cell growth and induce tissue organization even after carcinomas become invasive [5, 6, 8]. However, direct cell-cell contact through gap junction coupling between stroma and leukemic lymphoblasts has also been shown to prevent proliferation, maintaining the cells in a quiescent state [127].

1.5 Unanswered Questions

Numerous mechanisms likely exist for the promotion and inhibition of tumor development by the stroma. Secretion of paracrine factors, production of ECM as well as direct cell-cell interactions have all been shown to mediate tumor cell fate, however which ones are critical for tumor normalization by embryonic mesenchyme remains unclear. This dissertation is based on the hypothesis that because ECM plays a critical role in histodifferentiation and cell fate decisions in the embryo, it also may mediate the differentiation-inducing effects of embryonic mesenchyme on cancer cells. Ultimately, it is the goal of this thesis to define critical features of the embryonic microenvironment, which are necessary for tumor cell normalization. In the long term, we hope this will allow for the development of synthetic 'biomimetic' materials capable of mimicking critical inductive features of the embryonic mesenchyme, which could be used as a scaffold to 'reboot' cancer, essentially taking a tissue engineering approach to tumor therapy.

2

Embryonic Extracellular Matrix Regulates Histodifferentiation and Cell Fate Decisions in Normal Development

2.1 Introduction

The 3D pattern of epithelial tissues in the embryo is determined by the underlying mesenchyme [66]. While epithelial-mesenchymal interactions are traditionally discussed in the context of embryogenesis, adult epithelium can undergo normal morphogenesis [2, 128–130], and tumor cells can be instructed to 'reboot' and regenerate normal epithelial organization when mixed with embryonic mesenchyme [1, 114–117]. Most past work on mesenchymal induction of epithelial morphogenesis has focused on soluble chemical factors, genes and signaling molecules. However,

analysis of the mechanism of epithelial organ development has revealed that mesenchyme sculpts epithelial tissue form by accelerating and slowing ECM turnover at selective sites [131–133] and that similar changes in matrix metabolism contribute to tumor progression [10, 11]. Therefore, in this chapter we setout to develop methods to understand how interstitial ECM, produced by the embryonic mesenchyme, controls cell organization and cell fate in the embryo using the embryonic tooth as a simple model system. These methods will be applied to understand the role of mesenchymal ECM in control of mammary epithelial tumor cell fate in Chapters 3 and 4.

In this chapter we focus on the process of mesenchymal condensation, which is critical to the determination of cell fate within the mesenchyme and is required for continued tooth development [56, 57]. Previous studies have suggested various molecules and cellular mechanisms that might contribute to mesenchymal condensation, including cell proliferation [134], patterns of diffusible morphogens [58, 135–137], and local deposition of ECM components, including fibronectin, hyaluronan, collagen VI, and tenascin C [58, 138–141]. Recent studies carried out by Dr. Tadanori Mammoto in the Ingber laboratory showed that the expression of odontogenic factors (*e.g.*, Pax9, Msx1, and BMP4) within the condensed regions are directly linked with the increased packing density. Specifically, mechanical compaction-driven changes in cell size induce the expression of these odontogenic transcription factors, and decreasing the size of isolated dental mesenchyme cells or mechanical compression of whole dental mesenchyme is alone sufficient to induce tooth-specific cell fate switching [58]. However, it remains unclear whether the native ECM is sufficient to induce changes in cell organization that regulate these cell fate decisions.

In multiple recent studies native ECM has been isolated from whole adult organs, including heart, lung, and liver, by perfusing with detergent. These isolated ECMs recapitulate normal organ function if recellularized using untargeted cell mixtures

[142–144], suggesting that adult ECM scaffolds can regulate cell organization. While this decellularization approach has shown great promise with adult organs, it is difficult to achieve in the embryo. The small and fragile nature of the developing organ as well as the newly developing vasculature make perfusion impractical. In order to isolate the ECM from the specific regions of interest while maintaining the native architecture we optimized methods to remove cells from unfixed frozen histological sections of embryonic tissue, isolating the ECM only once the tissue section was already immobilized on the slide.

In this chapter I utilize this decellularization technique to gain further insight into how and to what extent native embryonic ECM is able to instruct tissue organization and cell fate decisions. In particular, I populated isolated matrices with undifferentiated embryonic cells demonstrating the ability of the native ECM to induce cells to recapitulate normal tissue architecture within the condensed mesenchyme regions. Further, by isolating ECM from high-density cultures of mesenchymal cells, I was able to show that ECM from cultured cells was also inductive and could instruct replated cells to undergo tooth differentiation as measured by increased expression of odontogenic transcription factors.

2.2 Results

2.2.1 Native tissue-derived extracellular matrix dictates cell organization

Significant spatial differences in cell organization are critical for mesenchymal condensation. To test the idea that local variations in embryonic ECM can provide critical cues to instruct tissue architecture I prepared thin sections of embryonic ECM from the embryonic tooth and repopulated them with dental mesenchyme. Methods pre-

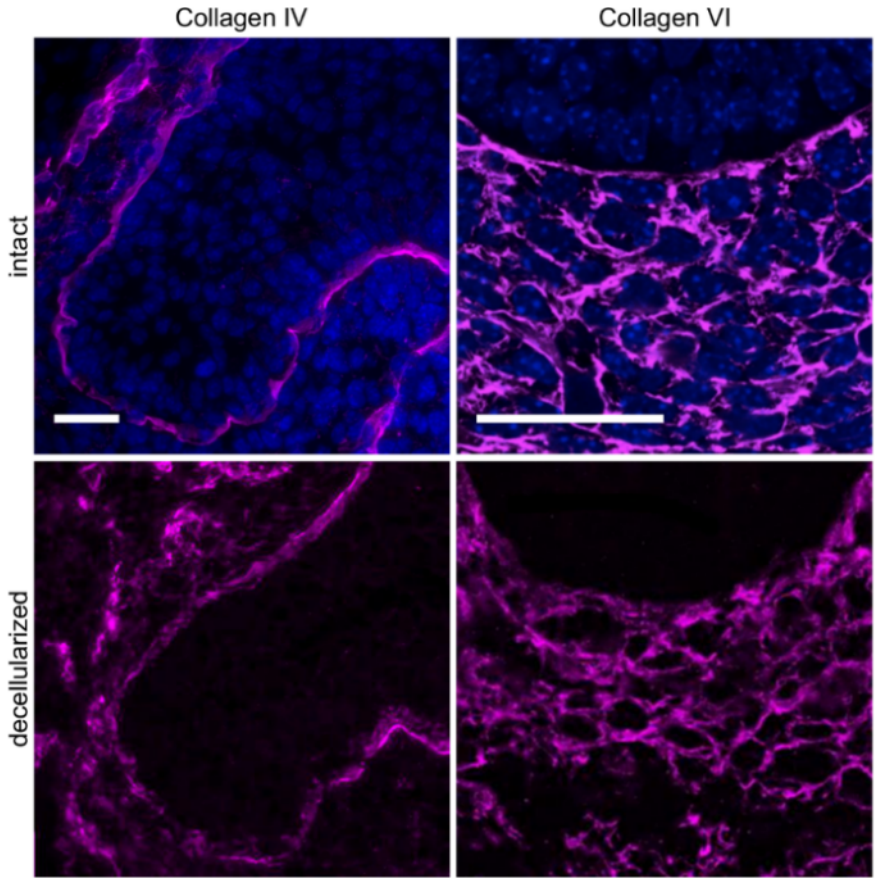

Figure 2.1: Fluorescence micrographs showing decellularization of frozen histological sections. Collagen IV and Collagen VI (purple) staining of the intact and decellularized tooth bud. Nuclei are dapi labeled in blue, showing the absence of cellular components in decellularized samples. Scale bar = 100 μm.

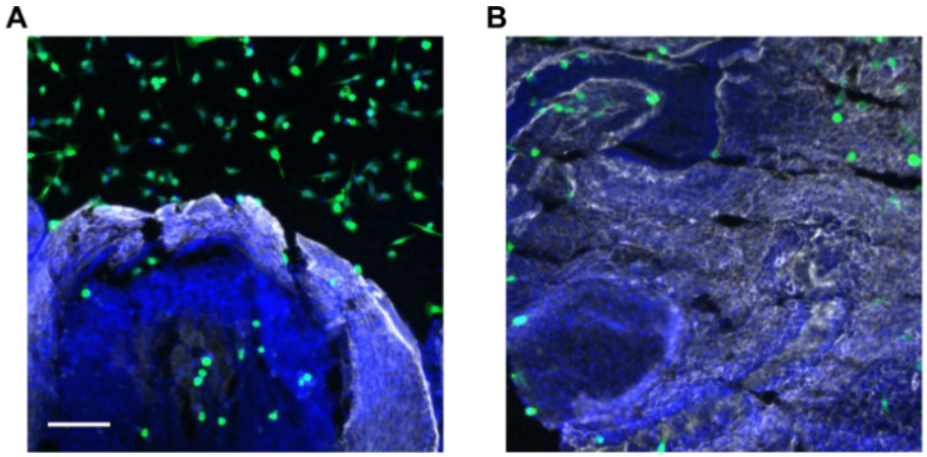

Figure 2.2: Fluorescent images showing that cells do not spread on intact histological sections. GFP dental mesenchyme cells (green) plated on intact histolotical sections (Collagen VI labeled in grey, nuclei in blue) showing representative organization at the edge of the tissue in the regions of the eye (A) and the tooth germ (B). Scale bar = 100 μm.

viously used for whole organs and ECM from cultured cells were adapted to extract cellular components from frozen histological sections of embryonic mouse tooth germs containing inductive mesenchyme (E13-E14). Cells were extracted using Ammonium Hydroxide and TritonX followed by treatment with DNase and immunohistochemical analysis was used to verify that the ECM maintained its native architecture both in the basement membrane (collagen IV) and interstitial ECM (collagen VI) (Figure 2.1). The absence of cellular components was verified by nuclear staining using DAPI (Figure 2.1). It is critical to note that released DNA could only be removed from sections that had not been refrozen, and adequate removal of DNA was necessary to achieve any cellular response.

Thin sections of isolated matrix from the embryonic tooth bud were repopulated with undifferentiated E10 dental mesenchyme cells and their localization and morphology was quantified after 16 hours in culture. The undifferentiated mesenchymal cells bound preferentially to the remaining ECM scaffolds rather than the surrounding glass. In control intact tissue sections cells bound predominately to the glass and

were unable to spread on the intact tissue sections, displaying no apparent differential patterning (Figure 2.2). To the contrary, on decellularized tissue sections, cells which were adherent to ECM in regions corresponding to the condensed mesenchyme, defined by increased collagen VI [58], exhibited a packing density nearly twice that of the surrounding non-condensed mesenchyme, a similar differential to that observed *in vivo* (Figure 2.3 a-f). Additionally, these more tightly packed cells were smaller in size (projected cell area measured as in [58]) compared to cells in the surrounding tissue, again displaying similar differentials to *in vivo* tissues (Figure 2.3 g-h). These regional differences in cell organization and morphology were not specific to ECM isolated from the region of the developing tooth, rather differential patterning of the plated dental mesenchyme could be seen throughout the section of the embryonic head, most notably in larger features, such as the brain (Figure 2.4) and eye. These results show that tissue derived ECM can act to instruct undifferentiated embryonic cells to recapitulate *in vivo* tissue patterning regardless of the tissue specificiy. Further, previous reports have shown that changes in cell size, such as those induced by the ECM within the condensed mesenchyme, are responsible for critical signaling during tooth development [58]. Thus it is possible that these changes in structure induced by the ECM may also contribute to critical cell fate decisions required for normal development.

2.2.2 Cell-derived extracellular matrix can induce cell fate decisions

To define the role of native ECM in cell fate decisions I isolated larger regions of inductive ECM from cultured dental mesenchyme using decellularization methods previously established to isolate matrix from cultured cells [145]. Inductive matrix was

Figure 2.3: Acellular ECM from histological tissue sections direct cell organization to mimic differences in normal tissue architecture. Representative images of a normal tooth bud (representative H& E image shown in A) and GFP labeled dental mesenchyme (green) repopulating decellularized tooth bud (Collagen VI labeled in grey, B), as well as high magnification images of repopulated non-condensed mesenchyme (C) and condensed mesenchyme (D) with tooth bud outlined in white. Quantification of cell density (E, F) and cell size (project cell area) (G, H) in the region of the condensed mesenchyme direclty surrounding the tooth bud (CM) and the more distal non-condensed mesenchyme (NCM) in native and repopulated tissues, respectively ($n = 3$ independent experiments; more than 30 cells counted each). Scale bar = 50 μm. * $p < 0.05$.

Figure 2.3: (continued)

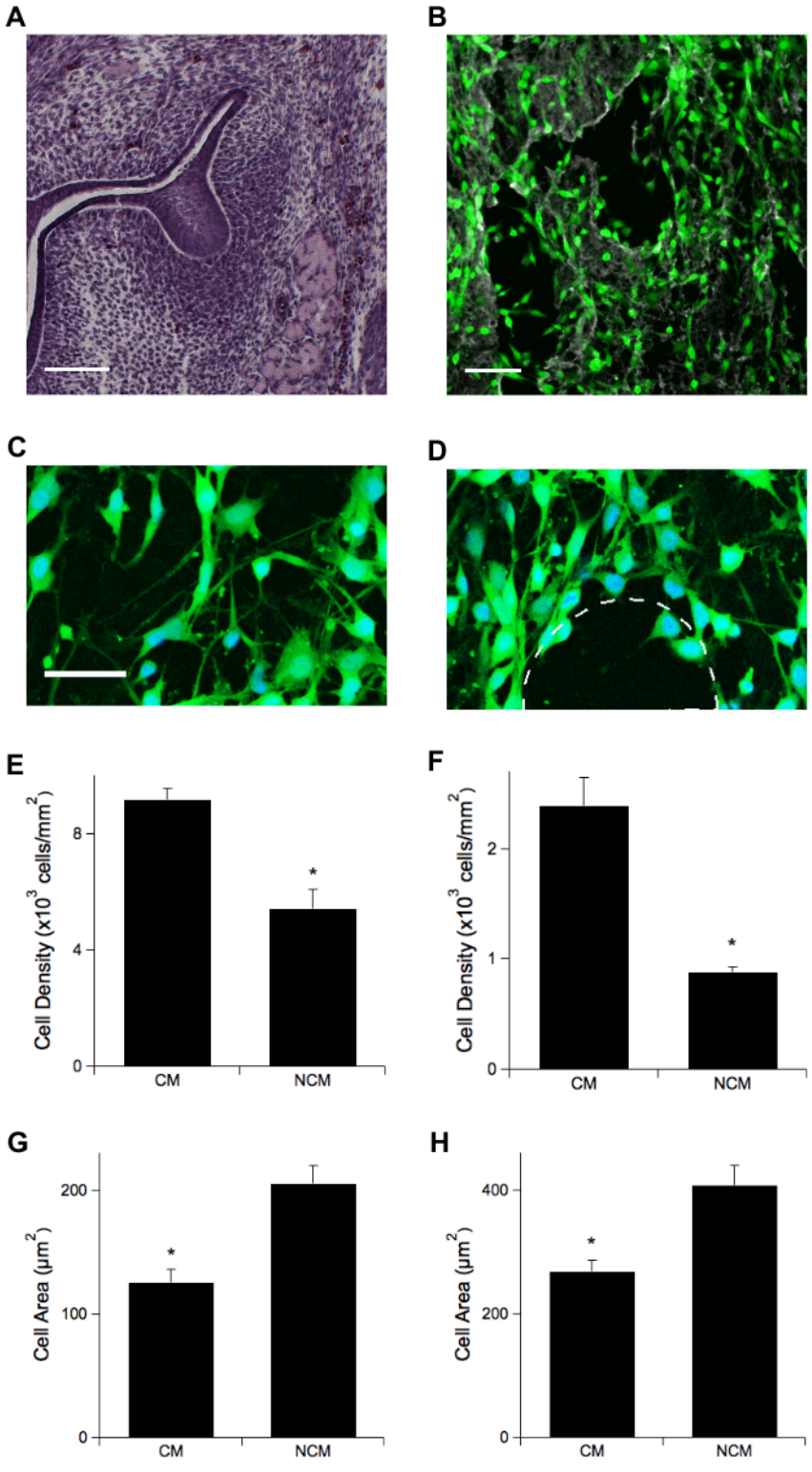

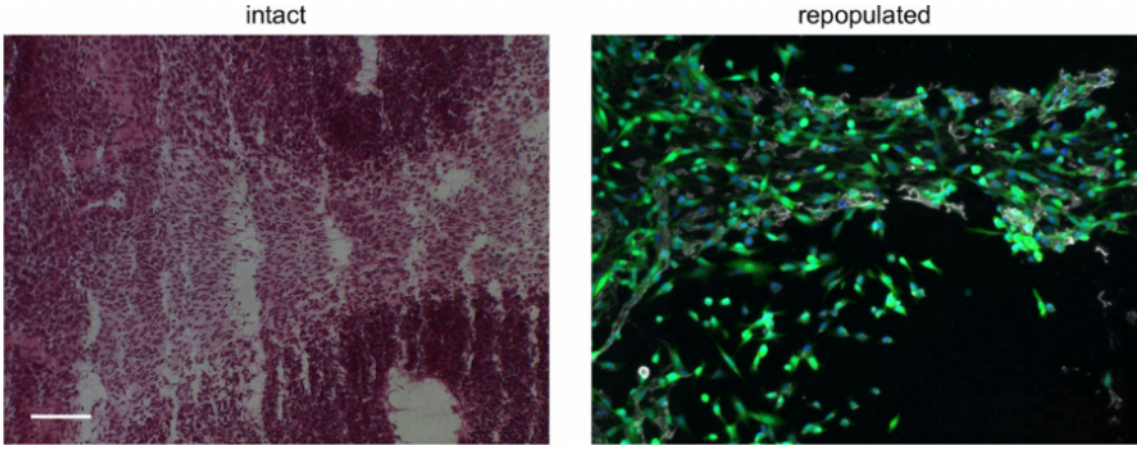

Figure 2.4: Dental mesenchyme mimics tissue architecture throughout the head. Comparison of the tissue architecture in the intact brain (H& E; left panel) and GFP labeled dental mesenchyme (green) repopulating isolated ECM (Collagen VI labeled in grey; right panel). Scale bar = 100 μm.

produced by primary dental mesenchyme cells cultured at high-density *in vitro*, previously shown to recapitulate the signaling associated with the condensed mesenchyme [58], and control ECM was isolated from low-density cultures. It is important to note that total ECM protein content was not normalized across low-density and high-density cultures and low-density cultures gave similar results to control crosslinked gelatin coated dishes. Immunhistochemical analysis was carried out to ensure that isolated matrix maintained its native structure following decellularization (Figure 2.5 a, b). Undifferentiated mesenchyme cultured on the isolated matrices were both smaller in size (Figure 2.5 c-e) and exhibited higher levels of BMP4 (Figure 2.5 f) when they were cultured on ECMs produced by high-density inductive cultures whereas ECM isolated from low density cultures had no effect. However, the change in cell size was not accompanied by a a rounded cell morphology which more precisely mimics *in vivo* condensed mesenchyme. Further, other odontogenic markers, including Pax9 and Msx1, which were previously shown to increase in high-density culture [58] were not shown to increase on ECM from high-density cultures. Still these data suggest that isolated embryonic ECM can play a role in some cell fate decisions within the embryo. However, the mechanism by which ECM is acting both in our *in situ* and *in vitro* systems remains unclear.

2.2.3 Matrix bound growth factors are maintained but do not appear to be critical

Multiple soluble factors have been shown to bind to ECM proteins [39, 58, 146], however, whether these morphogens are retained following decellularization is unknown. In order to test this we identified several growth factors which are critical for early

Figure 2.5: ECM isolated from *in vitro* culture of dental mesenchyme induces odontogenic differentiation. Collagen VI (purple) staining of ECM in intact (A) and decellularized (B) high-density cultures of E10 dental mesenchyme (nuclei in blue). Representative images showing GFP labeled mesenchymal cells plated on ECM isolated from low- (C) and high- (D) density cultures. Quantification of cell size (E) and expression of ondontogenic transcription factors by qRT-PCR (F) for cells plated on ECM from high- (■) or low-density cultures (□) (F) ($n = 4$ independent experiments; more than 50 cells counted each). Scale bar = 50 μm. *$p < 0.05$.

Figure 2.5: (continued)

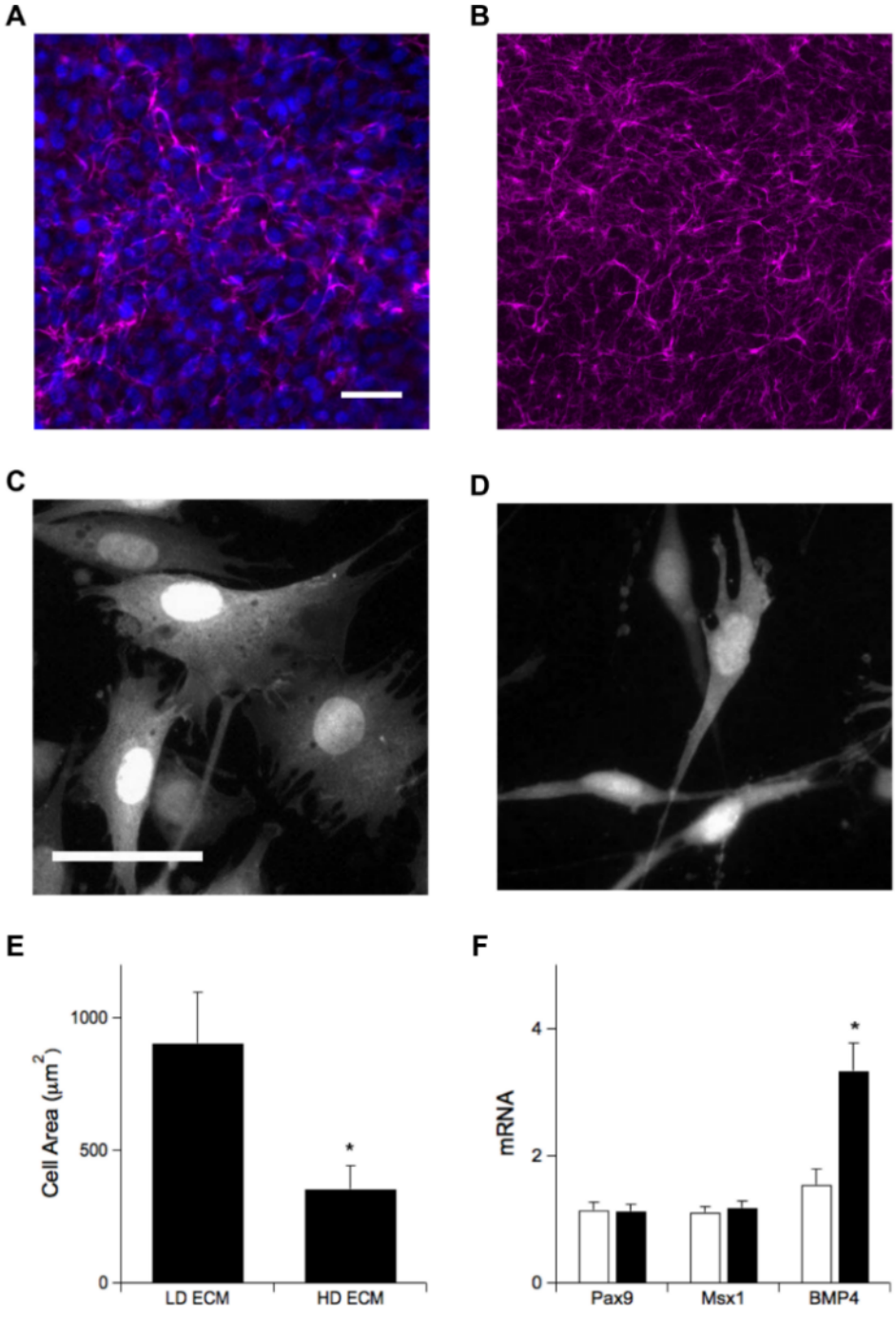

tooth development (fgf8, fgf3, BMP4, BMP2, inhibin βA, Wnt5a, and Wnt3a) [52] and tested for their presence using sing western blot analysis. I identified multiple growth factors that were maintained in our cell-derived matrices isolated from high density dental mesenchyme, specifically, fgf3, BMP4, inhibin βA, and Wnt3a, all factors which are normally produced by the embryonic tooth mesenchyme. The concentration of these growth factors was significantly decreased compared to whole cell lysates (Figure 2.6 a, normalization is by parallel cultures) and it is unclear whether these growth factors are still active following detergent treatment. To investigate the importance of these bound factors I optimized methods to remove bound growth factors using high salt washes [147, 148] verifying by western blot analysis that bound growth factors are removed to the high salt solution while matrix proteins remain bound to the dish (Figure 2.6b). Interestingly the matrix that remained following the growth factor extraction retained the ability to upregulate BMP4 to similar levels as growth factor intact matrix (Figure 2.6 c), suggesting that it is the matrix proteins rather than the bound factors that are responsible for this cell fate change. However, in order to be confident in this result a more through analysis would be required to identify any remaining growth factors.

2.2.4 Differences in mechanical properties

Matrix mechanics is known to play a critical role in cell growth, apoptosis, migration and differentiation [20, 21, 149–155], so to determine whether mechanics was playing a role here I developed methods to quantify the Young's modulus of the isolated ECM using AFM. The small tip size and precise control of tip-sample interactions make it an ideal tool to probe the elasticity of materials that are soft and exhibit inhomogeneity at microscopic scales. To extract the elastic properties the measured

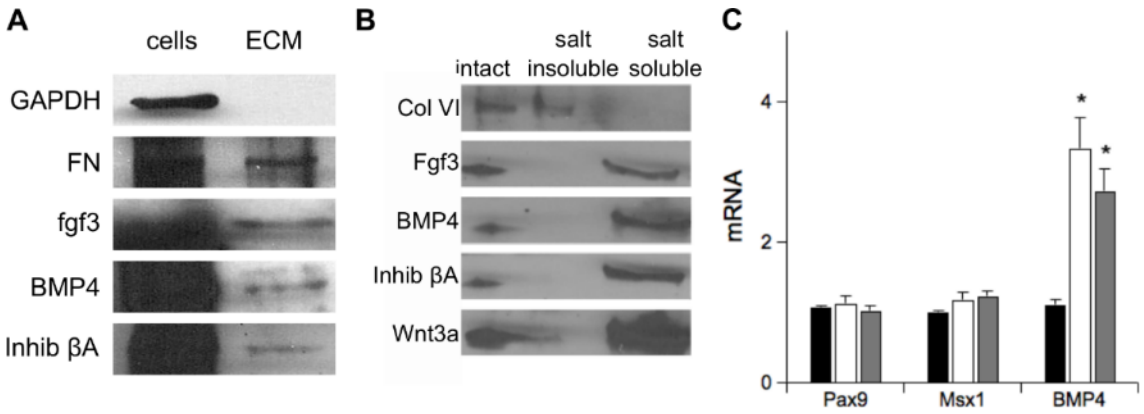

Figure 2.6: Growth factors are maintained within the decellularized matrix but are not critical for odontogenic induction. Western blot analysis showing fibronectin (FN) as well as several growth factors, fgf3, BMP4 and Inhibin $\beta\alpha$ (Inhib $\beta\alpha$), from high-density cultures of dental mesenchyme (cells) compared to decellularized ECM from parallel cultures (ECM) (A) and intact decellularized ECM (intact) compared to parallel cultures treated with high salt solutions to separate salt insoluble from salt soluble (B). (C) Quantification of the expression of odontogenic markers measured by qRT-PCR on low density ECM (■), intact high density ECM (□), and high density ECM with growth factors extracted (■) (n = 4 independent experiments). *p < 0.05.

load-displacement curve is fit using mathematical models based on classic linear elastic theory. The generalized force-indentation relation can be represented as:

$$F = \lambda d^{\beta} \tag{2.1}$$

where F is the force applied to the indenter, d is the indentation depth, and λ and β are dependent on the indenter geometry. For a spherical indenter, as was used in these experiments, the force-indentation relationship is referred to as the Hertz equation [156, 157]:

$$F = \frac{4ER^{1/2}d^{1/2}}{3(1-\upsilon^2)} \tag{2.2}$$

where R is the radius of the indenter, E is the Young's modulus, and υ is poisson's ratio, assumed to be 0.5.

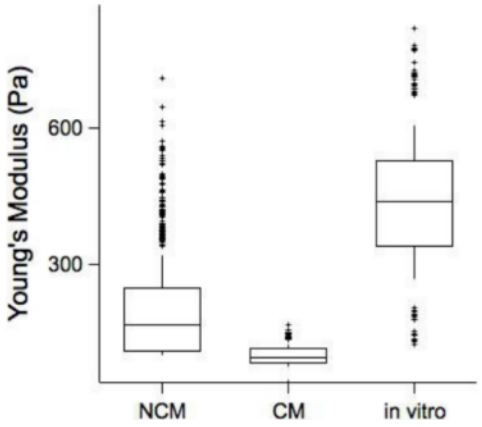

Figure 2.7: The mechanical properties of the matrix isolated from frozen histological sections and cell-derived matrix. The Young's modulus of ECM isolated from regions of non-condensed (NCM) or condensed mesenchyme (CM) of frozen histological sections and mesenchymal cells cultured at high-density (*in vitro*) displayed in a box plot. The median is displayed along with the 25th and 75th percentiles (box), and the 10th and 90th percentile (whiskers). Outliers are displayed as + (greater than 700 measurements taken on three separate days).

Using AFM I measured the mechanical compliance of ECM isolated from thin frozen tissue sections or cell-derived ECM. The ECM within the condensed region of histological sections was softer with a Young's modulus of 110 Pascals (Pa) as compared with 170 Pa for the neighboring non-condensed regions. However, the cell-derived matrix was much stiffer than either of the tissue regions, with a Young's Modulus of 450 Pa (Figure 2.7). Unfortunately, the ECM produced by low-density ECM cultures could not be measured as it was too thin and sparse. Thus the role of matrix mechanics in this system remains unclear.

2.3 Discussion

A major goal in the fields of tissue engineering and regenerative medicine is to induce whole organ regeneration. Most past approaches have focused on fabrication of tissue scaffolds that resemble ECM of the relevant adult organ and recently native

adult ECM has emerged as a tool for organ replacement. Specifically, ECM isolated from adult organs and repopulated with healthy cells has been shown to recapitulate normal organ function in multiple different organ systems [142–144]. However, this does not solve one of the major problems in organ replacement, more than 100,000 patients require organ transplantation every year in the U.S. alone and due to supply shortages close to 20 die every day waiting for replacements. In this study we took a different approach, seeking to understand how embryonic tissues use ECM throughout development to direct organ formation with the ultimate goal of fabricating biomimetic scaffolds that can induce cells within adult tissues to form new organs *in vivo*. To do this I developed a technique to isolate thin sections of ECM from histological sections of the embryonic tooth or from *in vitro* cultures of differentiated mesenchyme as a tool to define critical time points and regions which could instruct cells to differentiate along the same path used by the embryo. I was able to show that native ECM within the embryo is sufficient to induce cell organization which mimics mesenchymal condensation and further stimulates expression of some critical odontogenic markers.

The small and delicate nature of developing organs within the embryo made it nearly impossible to use perfusion decellularization techniques previously employed for adult organs [142–144]. Perfusion is difficult not only because the vascular is only beginning to develop at the stages and regions of interest, but also because it disrupts the delicate ECM structures both during decellularization and in the processing and cryosectioning. Additionally during sectioning it was extremely difficult to find the small ($\sim$50 μm across) tooth germ let alone to identify the region of the condensed mesenchyme which is present for only about 60 μm of the total depth of more than 250 μm without cells present. To overcome these difficulties it was critical to first isolate and immobilize thin section of tissue and then isolate the ECM, rather than

decellularizing the whole organ and sectioning the acellular matrix. However, having the tissue section made it more difficult to remove certain cellular components, DNA, for example, is attracted to the positively charged slides. I found that minimizing the contact time between the tissue section and the slide prior to decellularization helped to overcome this problem. Thus it was critical to remove the cells within hours after sectioning and to never refreeze the samples after sectioning. Using this technique I was able to remove cells from multiple different organs, including lung, liver, and mammary gland. This technique also proved useful for ECM characterization as removing the cells allowed for more detailed staining of the matrix facilitating the precise evaluation of structure as we did using birefringence microscopy in the 2010 paper by Kanapathipillai *et al.* [158].

It is well known that many growth factors bind to the ECM, and that these bound factors can play a critical role in tissue organization and cell fate [58, 146]. However, it has not been shown whether these bound growth factors are maintained within the acellular matrix following detergent treatment. Through immunoblotting I was able to show that multiple growth factors (*i.e.*, fgf3, msx1, BMP4, Wnt3a) are present in decellularized cell-derived ECM, but these growth factors were not important to the cellular response I observed. Still, I have not evaluated the activity of the growth factors I recovered, so the growth factors may be inactive due to the method of decellularization. Additionally I did not evaluate the growth factors present within tissue-derived matrix. Previous reports have suggested that fgf8 binds to and is released from the basement membrane within the tooth germ, acting in part to attract dental mesenchyme cells to produce the condensed mesenchyme [58]. Thus further studies would be required to completely understand the role of matrix bound growth factors within isolated matrix scaffolds.

The mechanical properties of ECM are known to play a critical role in cell fate

decisions, driving stem cells down different lineages without the addition of morphogens [22, 159], altering proliferation [160], and apoptosis [161], as well as migration [19, 162]. However, the small difference in matrix mechanics I found in the tissue derived ECM (110 versus 170 Pa), accompanied with the much stiffer cell-derived matrix (450 Pa) suggest that mechanics is not playing a large role in this case. However, questions remain about the accuracy of these mechanical measurements, particularly for the histological sections. The AFM is a very precise instrument, however because of the small surface area for measurement 100 Pa is close to the noise threshold. Additionally, cells play a large role in tissue compliance and measurements of parallel intact histological sections yield significantly different results (∼500 Pa), similar to cell-derived matrix. In order to understand the role of matrix mechanics in this process additional measurements as well as enzyme treatments to modify the mechanics would be required.

2.4 Materials and Methods

2.4.1 Animals

Embryonic mesenchyme was harvested from timed-pregnant CD1 mice (Charles River Laboratories); the morning the vaginal plug was detected was defined as E0. Using sterile technique the pharyngeal arch was dissected from E10 embryos and treated with Dispase II (2.4 U/ml; Roche) and DNase I (QIAGEN) at 37°C for 23 mins. After the epithelium and mesenchyme were separated using fine forceps, the dental mesenchyme was dissected out and cultured on fibronectin (Becton Dickinson)-coated glass bottom dishes (MatTek Corporation) in Dulbeccos' modified Eagle's medium (DMEM) supplemented with 10% fetal calf serum (FCS). All animal studies were reviewed and approved by Animal Care and Use Committee of Boston Children's

Hospital.

2.4.2 Cell Culture

Cells isolated from microdissected mesenchyme were maintained in DMEM with high glucose supplemented with 10% fetal bovine serum (FBS), 100 units/ml penicillin and streptomycin, and 2 mM GlutaMAX (Invitrogen). Mesenchymal cells were labeled with green fluorescent protein (GFP) by retroviral transduction [163] and were provided by Tadanori Mammoto.

2.4.3 Decellularization of frozen tissue sections

Embryos were harvested from 13-14 day pregnant mice, embedded in Tissue-Tek O.C.T. freezing medium (Sakura Finetek) and sectioned using a crostatic microtome (Leica). The 20 μm thick sections were collected on superfrost/plus microscope slides (Fisher Scientific) and immediately washed in phosphate buffer saline (PBS) to remove O.C.T. prior to decellularization; tissue sections were never refrozen after sectioning. The cells were then removed with sterilized extraction buffer containing 20mM Ammonium Hydroxide (Sigma) and 0.5% (v/v) Triton X-100 (Sigma) in water for 10-15 mins. Cell debris was diluted in PBS and the ECM was stored at 4°C overnight. The following day ECM was treated with DNase (10 Kunitz units/ml; Qiagen) for 2 hrs at 37°C and washed several times with PBS. Decellularized histological sections were isolated using 10 mm cloning rings (sigma) and the matrix was blocked using 2% BSA at 37°C for 1 hour. GFP labeled dental mesenchyme was plated ($1x10^3$ cells/cloning ring) and incubated at 37°C for 16 hours and then fixed in pre-warmed 4% paraformaldehyde (PFA).

2.4.4 Decellularization of cultured mesenchymal cells

To produce ECMs that can be isolated from mesenchymal cell cultures, round glass cover slips (12 mm) were coated with crosslinked gelatin by treating with 0.1% gelatin (Sigma) for 1 hr at 37°C, followed by 1% gluteraldehyde (Electron Microscopy Sciences) for 30 min at room temperature, washed with PBS, treated with 1M Ethanolamine (Sigma) for 30 min and washed with PBS again before plating of mesenchymal cells, as previously described [145]. The cells were plated near confluence on the gelatin-coated coverslips in 24 well plates and grown in medium supplemented with 50 μg/ml ascorbic acid (Sigma) changed every other day for 1 to 2 weeks before the cells were removed with pre-warmed (37°C) extraction buffer containing 20mM Ammonium Hydroxide (Sigma) and 0.5% (v/v) Triton X-100 (Sigma) in PBS for 10-15 mins. Cell debris was diluted in PBS and the ECM was stored at 4°C overnight. The following day ECM was washed with PBS and treated with DNase (10 Kunitz units/ml; Qiagen) for 2 hrs at 37°C. Undifferentiated dental mesenchyme was plated on isolated ECM and maintained in culture for 16 hours at 37°C and then fixed in pre-warmed 4% PFA.

2.4.5 Growth factor extraction

Acellular matrix isolated from cultured cells was washed several times with PBS, then incubated with 2 M Sodium Chloride (sigma) in 20 mM HEPES buffer (sigma) at 37°C for 1 hour [147, 148]. Isolated matrix was washed several times in PBS to remove excess salt while extracted growth factors were spun in desalting columns dialyzed against 10mM PBS for 48 hours, and lyophilized. Extraction of growth factors was confirmed by immunoblotting. Cells were plated on growth factor extracted ECM or on crosslinked gelatin as previously described. Salt extracted growth factors were

dissolved in fresh DMEM and added to each well.

2.4.6 Molecular analysis

Protein was isolated from cells in culture by adding RIPA buffer (Boston BioProducts) on ice, scrapping the cells from the bottom of the dish and passing them through a 23-gauge needle 5 times. Isolated matrix was scrapped from the bottom of the dish suspended in RIPA buffer, but was not passed through a needle. Samples were spun at 8,000 rpm for 5 minutes at 4°C and soluble material was treated with Laemmli SDS reducing sample buffer at a 1x final concentration (Boston BioProducts), boiled for 5 mins at 95°C, and resolved on a 4-15% Tris-Glycine Mini-Protean TGX gel (Bio-Rad). Proteins separated on the gel are transferred to nitrocellulose membranes (Bio-Rad) using a Mini-Protean Tetra System (Bio-Rad) following manufacturer's instructions. Membranes were then blocked for 1 hour (5% nonfat milk, 0.1% Tween-20, 150 mM NaCl, and 50 mM Tris HCl, pH 7.4). Primary antibodies were probed at 4°C overnight using primary antibodies followed by the appropriate peroxidase labeled secondary antibody (Vector Labs) for 1 hour at room temperature. Immunoblots were washed and developed using SuperSignal West Dura Extended Duration (Fisher Scientific) and exposed to film (X-omat; HyBlot CL, Denville Scientific). Samples prepared in parallel were loaded based on sample weight because an appropriate loading control was not available due to the absence of cellular components. Digital image analysis of immunoblots was performed with ImageJ software (http://rsbweb.nih.gov/ij/) (National Institute of Health, USA).

Total RNA was isolated using RNeasy Plus Mini Kit (QIAGEN) and RNA expression was detected by qRT-PCR. RNA was reverse transcribed into cDNA using a iScript cDNA Synthesis Kit (Bio-Rad) and cDNA was amplified with iTaq SYBR Green Supermix with ROX (Bio-Rad) using the CFX96 real-time PCR system (Bio-

Rad). Amplification was carried out using primers shown in Table 2.1.

Table 2.1: Chapter 2 qRT-PCR primers

gene		sequence (5′->3′)
BMP4	F:	TTCCTGGTAACCGAATGCTGA
	R:	CCTGAATCTCGGCGACTTTTT
Msx1	F:	TGCTGCTATGACTTCTTTGCC
	R:	GCTTCCTGTGATCGGCCAT
Pax9	F:	CATTCGGCTTCGCATCGTG
	R:	CTCCCGGCAAAATCGAACC
cyclophilin	F:	CAGACGCCACTGTCGCTTT
	R:	TGTCTTTGGAACTTTGTCTGCAA

2.4.7 Immunohistochemistry

Antibodies directed against collagen IV, collagen VI, fibronectin, fgf3, BMP4, Wnt 3a and Inhibin βA were from Abcam; Fluoromount G was from Southern Biotech. Images were captured using a Zeiss Axioscope 2 and a Leica SP5 X MP Inverted Confocal Microscope. Morphometric analysis was performed using Image J software (http://rsbweb.nih.gov/ij/) (National Institute of Health, USA).

2.4.8 Atomic force microscopy

Unfixed frozen sections of E13-14 tooth rudiments were decellularized and the stiffness of the ECM deposited between cells within the condensed mesenchyme was measured using an MFP-3D-Bio atomic force microscope (Asylum Research). Silicon nitride AFM cantilevers with a 60 pN/nm spring constant with either a 5 μm or a 10 μm borosilicate spherical bead on the tip (Novascan) were calibrated thermally according to the Sader method. The tissues were imaged following immunohistochemical staining for Collagen VI using an Olympusx81 inverted fluorescence microscope. The

AFM applied a maximum prescribed force of 1-10nN with an indenter velocity of 2 μm/s and the Hertz Model was used to determine the elastic properties of the tissue.

2.4.9 Statistical Analysis

Independent samples t-tests were used to compare results, which were considered significant at $p < 0.05$. All results are presented as mean ± standard error of the mean (SEM). Box plots were produced using IgorPro and the center line represents the median while the box represents the 25th and 75th percentiles, the whiskers are the 10th and 90th percentile, and all points outside this range are considered outliers.

2.5 Acknowledgements

This work is supported by the National Institute of Health. AFM studies were performed at the Center for Nanoscale Systems (CNS), a member of the National Nanotechnology Infrastructure Network (NNIN), which is supported by the National Science Foundation under NSF award no. ECS-0335765. CNS is part of the Faculty of Arts and Sciences at Harvard University.

3

Embryonic Extracellular Matrix as Key Mediator in Tumor Normalization by Embryonic Mesenchyme

3.1 Introduction

Nearly 40 years ago it was reported that co-culturing breast cancer cells with embryonic mammary mesenchyme can induce cancer normalization, as indicated by suppression of growth and enhanced histodifferentiation [1]. Similar results were later obtained in *in vitro* and *in vivo* recombination studies with prostate, kidney, colon and other cancers [2, 4, 164, 165]. These observations are also consistent with the finding that carcinogens that drive epithelial cancer formation can target mesenchymal cells [166, 167], and that recombination of normal epithelium with

carcinogen-treated stroma can lead to epithelial tumor formation [86, 87]. However, these results were largely ignored as molecular biology surged and genetics became the focus in the cancer research field, leaving the mechanism of this phenomenon unknown.

Although little is known about how embryonic mesenchyme might induce cancer normalization, ECM, which I have shown in Chapter 2 can mediate organization and cell fate during morphogenesis, could mediate these effects. Moreover, certain tumors can be induced to suppress their growth and differentiate by placing them in direct contact with intact basement membrane (i.e., epithelial ECM) isolated from normal embryonic or adult tissues [5, 6, 8]. However, changes in stromal cell production of soluble factors [126] or cell-cell contact formation [127, 168, 169] also can lead to suppression of cancer cell growth.

If embryonic mesenchyme or any of the factors it produces can indeed induce cancer reversion, then further understanding of this mechanism could lead to development of a new form of differentiation therapy for solid tumors, similar to those that have been found to be effective for treatment of hematopoietic cancers. However, other studies have generated conflicting results. For example, some suggest that recombination of tumors with embryonic tissue has no effect on cancer progression *in vivo* [114], whereas others show it only induces differentiation of tumors that are already highly organized [170]. Moreover, different studies suggest that embryonic tissue can actually increase tumor growth [171, 172].

Thus, here I carry out tissue recombination studies using modern culture techniques to unequivocally determine whether embryonic mesenchyme can induce cancer normalization. Specifically, 2D and 3D culture models are used to analyze growth and differentiation of tumor cells alone and in co-culture with early mammary mesenchyme (eMM) isolated from the E12.5-E13.5 embryos. Then I assess conditioned

media and cell-free ECM derived from the eMM for their capacity to differentiate mammary tumor cells. These studies reveal that cell-free ECM can induce partial cancer reversal to the same level seen by mesenchymal cells while neither CAF cells nor ECM derived from CAFs had any affect on tumor cell behavior. Further I showed that embryonic ECM could suppress cancer growth *in vivo* using a xenograft tumor model.

3.2 Results

3.2.1 Suppression of breast cancer cell growth by embryonic mesenchyme

To verify past studies which suggested that embryonic mesenchyme can induce breast cancer normalization [1], I used tumor cells previously isolated from different stage mammary glands in C3(1)SV40 T-antigen transgenic mice that undergo breast cancer progression in a robust and reliable manner [102, 103]. In our initial studies, mammary cancer M6 cells isolated from late stage solid tumors were co-cultured with an equal number of eMM or CAF cells isolated from tumor stroma in the same transgenic mouse model (Figure 3.1 a). I found that the presence of eMM cells produced a significant decrease in mammary epithelial tumor cell growth, whereas addition of CAFs had no effect, when analyzed by quantitating nuclear incorporation of EdU (Figure 3.1 b, c).

To separate the contributions of soluble versus insoluble products of the embryonic mesenchyme, as well as cell-cell interactions, I isolated insoluble matrix that was deposited by inductive eMM cells or CAFs cultured on dishes coated with cross-linked gelatin. Insoluble matrix was isolated by treating cultures with detergent to extract cells as described in Chapter 2; it is important to note that this isolated insoluble

Figure 3.1: Mammary tumor cells decrease their proliferation when combined with embryonic mesenchyme or cell-free embryonic mesenchymal ECM. (A) Schematic showing culture conditions for co-culture of epithelial tumor cells (Epi) with MM or CAF, as well as for isolation of stroma-derived ECM or conditioned medium (CM), in studies designed to detect induction of tumor cell normalization. (B) Representative images showing nuclear incorporation of EdU into DNA (green; DAPI-labeled nuclei are blue) in tumor epithelial cells co-cultured with mesenchymal cells (top) or cultured on cell-free ECM (bottom). (C) Quantification of growth (incorporation of EdU into DNA) within epithelial tumor cells grown in co-culture with eMM cells or CAFs, or on cell-free ECM isolated from eMM or CAF cultures. (D) Cell growth of early (M28) and metastatic (M6C) tumor cells on eMM ECM versus CAF ECM compared to control gelatin substrates (n=3 indepedent experiments; greater than 500 cells counted per experiment) (scale bar = 50 μm; * $p < 0.05$, ***$p < 0.001$).

Figure 3.1: (continued)

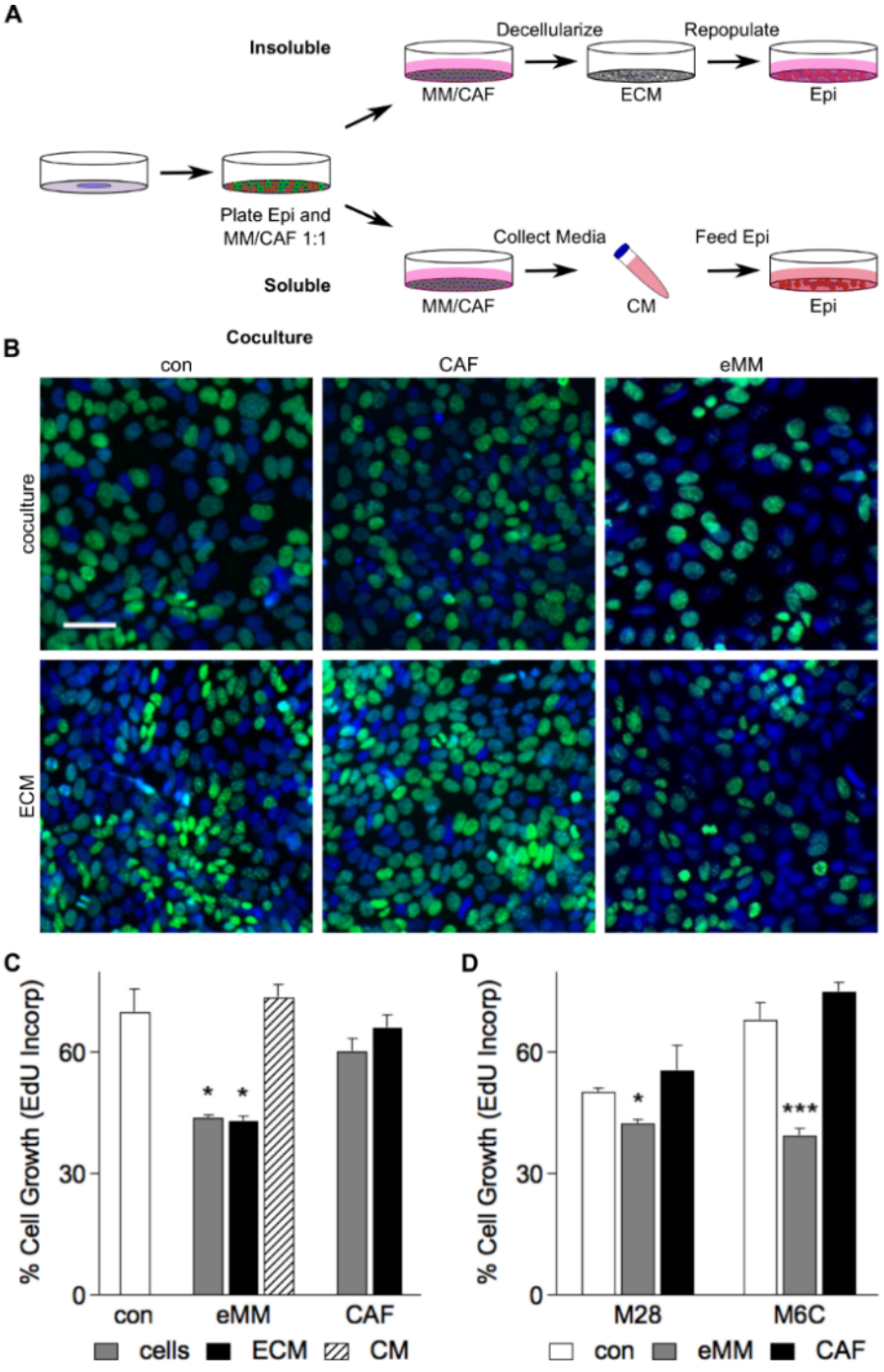

material is referred to as ECM throughout the chapter, however there are additional components present which will be further defined in Chapter 4. The isolated ECM was then repopulated with mammary tumor cells (Figure 3.1 a). These studies revealed that tumor cell contact with eMM ECM was sufficient to suppress the growth of the M6 breast cancer cells to the same level ($\sim$ 38% inhibition) as co-culturing them with living eMM cells, whereas ECM isolated from cultured CAF cells had no suppressive effect (Figure 3.1 b, c). Importantly, similar growth suppression was seen for M28 breast epithelial cells isolated from premalignant transgenic mammary glands and for M6C cells isolated from late stage metastatic lesions (summary of cell types can be seen in Table 3.1); eMM ECM decreased growth of all three tumor cell lines to nearly the same level (Figure 3.1 d).

Table 3.1: Summary of cell types

Cell	Type	Origin	Description
M28	Epi	FVB - C3(1) Tag mice	histologically normal gland
M6	Epi	FVB - C3(1) Tag mice	solid tumor
M6C	Epi	FVB - C3(1) Tag mice	lung metastasis
4T1	Epi	BALB/C mouse	aggressive tumor cell line
MCF7	Epi	human breast cancer	ERα tumor cell line
MM	Fib	FVB mouse embryo	staged mammary mesenchyme
DM	Fib	CD1 mouse embryo	staged dental mesenchyme
CAF	Fib	FVB - C(3)1 Tag mice	isolated and cloned from solid tumor

Examination of growth curves analyzed over 9 days confirmed that tumor cell proliferation was significantly slower when they were cultured on ECM isolated from eMM compared to either CAF ECM or control cross-linked gelatin substrates alone (Figure 3.2). In fact, the growth rates of tumor cells grown on the embryonic ECM (1.2 x 10^6 cells/day) was about half that exhibited by tumor cells grown on control gelatin substrates or CAF ECM (2.3 and 1.9 x 10^6 cells/day, respectively). These

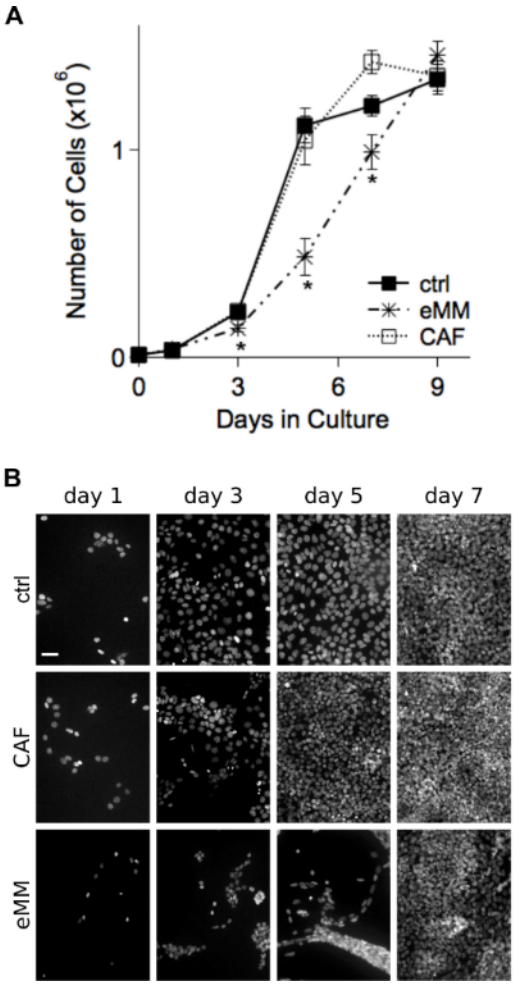

Figure 3.2: Growth of tumor cells is decreased only on ECM from eMM cells. (A) Growth curves of M6 breast tumor cells on control cross-linked gelatin substrates versus similar substrates coated with cell-free ECM isolated from cultured eMM cells or CAF. Significant differences in cell number between eMM ECM versus both control and CAF ECM were detected at days 3, 5 and 7. (B) Representative images of dapi stained nuclei on each substrate ($n = 3$ independent experiments; 2 or 3 repeats each) (scalebar $= 50$ μm * $p < 0.05$).

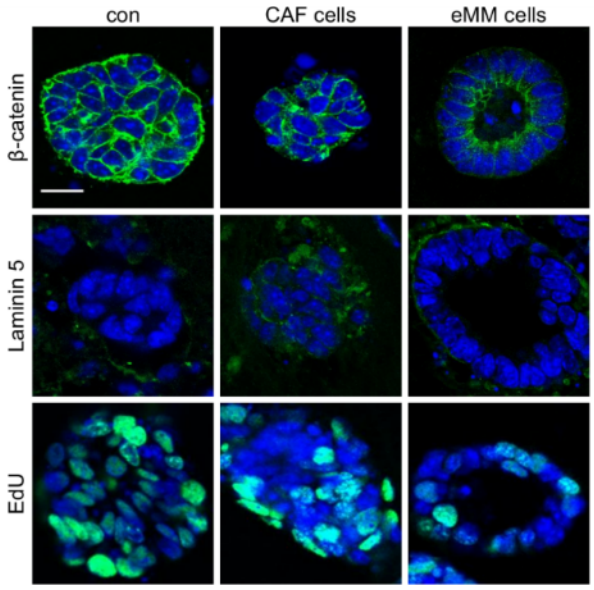

Figure 3.3: Tumor cells in 3D culture show increased lumen formation only in coculture with eMM cells. Fluorescence views of co-cultures of M6 epithelial tumor cells with eMM cells or CAF cells in 3D gels stained with antibodies against β-catenin, laminin 5, and EdU (all in green) and DAPI (blue) (scalebar = 20 μm).

results, along with the finding that conditioned medium from eMM cells had no effect on tumor cell proliferation in 2D cultures (Figure 3.1 c), suggest that the insoluble ECM is the primary component of the embryonic mesenchyme that is responsible for inducing mammary tumor cell growth suppression.

3.2.2 Mesenchymal induction of breast cancer differentiation

To explore the effects of mesenchymal cells on tumor differentiation, I carried out similar studies by placing the cells in 3D gels composed of laminin-rich Matrigel and collagen I that support formation of hollow mammary acini by normal breast epithelial cells [173]. When M6 mammary tumor cells were embedded in the gels, they grew predominantly as disorganized cell spheroids with a lack of epithelial cell polarity (Figure 3.3). In contrast, when eMM cells were co-cultured with tumor cells in the gels the tumor cells formed more than 3 times as many hollow spheroids with normal

acinar forms lined by a single layer of polarized epithelial cells (Figure 3.3 and 3.4b). Additionally coculture with eMM cells decreases the growth of tumor cells (Figure 3.3 and 3.4b). These results demonstrate that embryonic mammary mesenchyme retains the ability to suppress growth and induce differentiation of transgenic mouse breast cancer cells *in vitro*, even though their proliferation is driven by the SV40 oncogene.

3.2.3 Mesenchymal extracellular matrix is sufficient to induce tumor normalization

Next, I assessed the effects of mesenchymal ECM on tumor differentiation in a 3D culture model. Tumor cells were embedded in gels, with or without insoluble ECM that was isolated and scraped free from cultures of either inductive eMM or CAF cells (as described in Figure 3.1 a). When eMM ECM (20 mg/ml) was included during gel formation, M6 cells formed more than three times as many hollow spheroids lined by polarized epithelium, which was equal to that observed when these cancer cells were co-cultured with living eMM cells (Figure 3.4 a, b). Interestingly, the CAF ECM had no effect on lumen formation (Figure 3.4 a,b), and tumor cells only decreased their proliferation in the presence of eMM cells or ECM (Figure 3.3 and 3.4 a,d). In contrast, when tumor cells embedded in ECM gels were exposed to conditioned medium collected from eMM cells, there was no effect on lumen formation or tumor cell growth (Figure 3.4 a,b,d). Importantly, the embryonic ECM also induced tumor normalization when added to gels containing metastatic M6C breast cancer cells, as well as highly aggressive metastatic 4T1 mammary cancer cells isolated from BALB/C mice and human ERα-positive MCF7 breast cancer cells, although it had no effect on pre-metastatic M28 cells (cell lines summarized in Table 3.1 and Figure 3.4 c). Thus, the tumor reversing capacity of eMM ECM appears to function across multiple

Figure 3.4: Embryonic ECM is the primary mediator of tumor cell normalization in 3D culture. (A) Representative images of M6 tumor spheroids in control cultures and cultures supplemented with ECM or conditioned medium (CM) collected from eMM or CAFs. Apical cell-cell junctions, basement membrane and DNA synthesis were visualized by staining with antibodies to β-catenin, laminin 5, and EdU respectively (all in green); blue indicates DAPI-stained nuclei. Quantification of the effects on lumen formation in M6 cells are shown in B, and results for M6C, 4T1 and MCF7 cells are shown in C; effects of eMM ECM on M6 tumor cell growth and ERα expression measured by qRT-PCR are shown in D and E, respectively (n $>$ 4 independent experiments; more than 75 lumen counted each experiment) (scalebar = 20 μm; * $p < 0.05$, **$p < 0.01$, ***$p < 0.001$).

Figure 3.4: (continued)

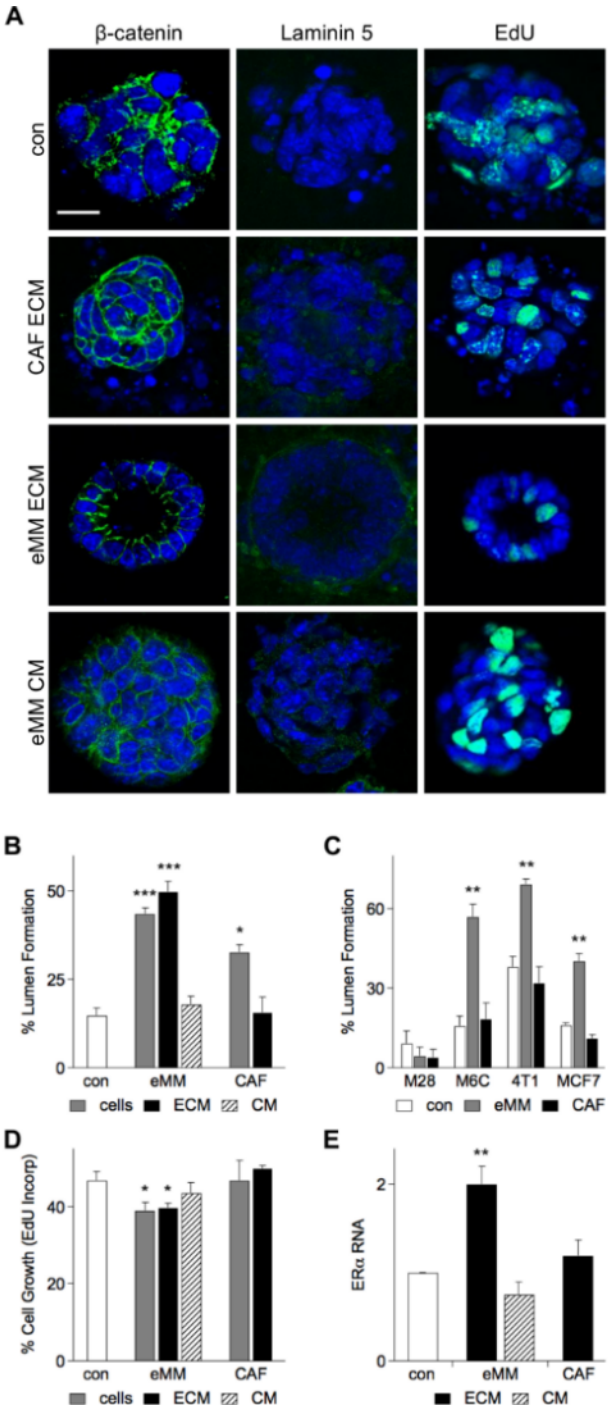

aggressive cancer cell types and species.

Another marker of differentiation that is progressively lost during breast cancer progression in humans is expression of ERα [174], and ERα expression levels similarly decrease over time in C3(1)SV40 Tag transgenic mice [103]. Interestingly, when the M6 cells were cultured in gels containing inductive eMM ECM, the tumor cells nearly doubled their levels of ERα expression as measured by qRT-PCR, while CAF ECM and eMM-conditioned medium did not produce any significant change (Figure 3.4 e).

In addition, I found that 7% of tumor cell spheroids appeared to undergo duct morphogenesis, as indicated by the formation of elongated, hollow structures lined by a single layer of polarized epithelial cells when grown in gels supplemented with inductive eMM ECM (Figure 3.5 a-c). In contrast, less than 0.4% of spheroids without cell-derived ECM exhibited ductal morphology, and no ductal structures were observed in the presence of CAF ECM (Figure 3.5 c).

As ECM dissolution and formation of physical breaks in the basement membrane are hallmarks of malignant transformation [5, 175], I next explored whether induction of tumor differentiation by embryonic ECM influences basement membrane structure. Immunofluorescence staining for the basement membrane protein laminin 5 showed that tumor spheroids either lack a basement membrane or exhibit one with many breaks as indicated by the presence of gaps in the linear pattern of laminin 5 staining, just as they do *in vivo* (Figure 3.3 and 3.4 a). In contrast, most hollow spheroids within gels supplemented with eMM ECM displayed an intact basement membrane (Figure 3.4 a), and hence, they restored normal tissue boundaries.

Tumor progression, particularly as it becomes more invasive and metastatic, is often accompanied by an epithelial-to-mesenchymal (EMT) transition. In order to

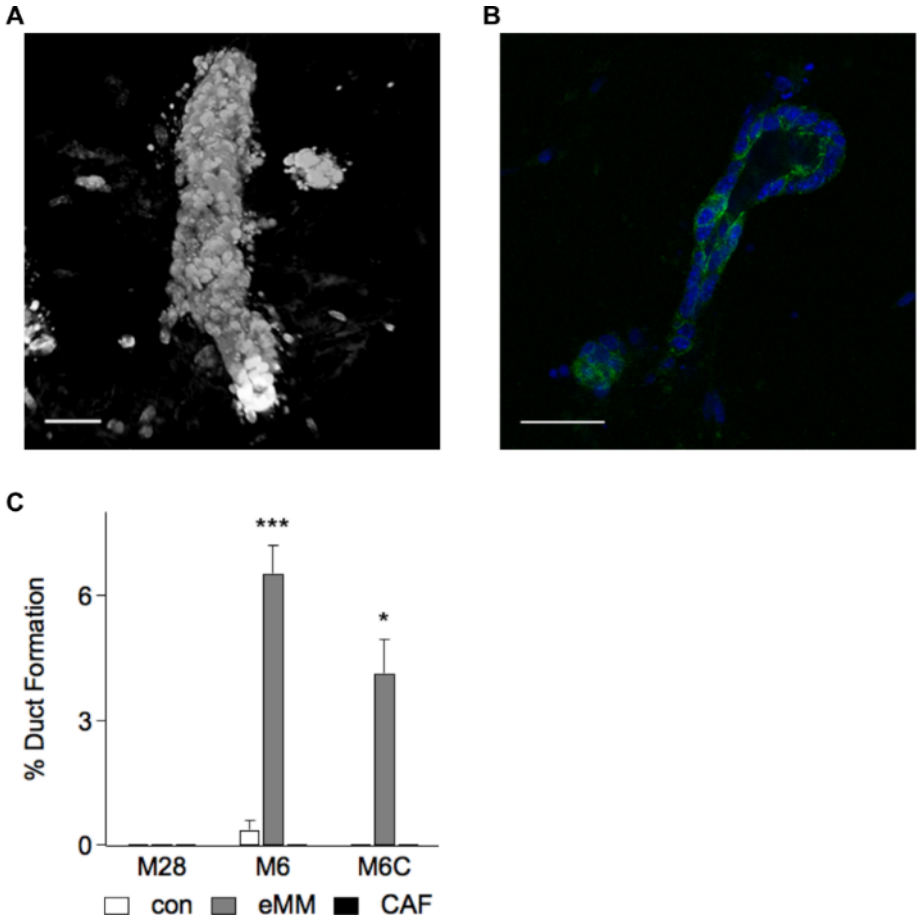

Figure 3.5: ECM from eMM cells induces ductal morphogenesis in 3D culture. (A) A 3D reconstruction of an elongated ductal structure that formed in 3D co-culture of M6 tumor cells with eMM ECM; a small spheroid at the right for reference (nuclei are labeled with DAPI). (B) β-catenin staining (green) in the elongated ductal structure. (C) Quantitation of results showing that elongated ductal structures were essentially only observed in gels supplemented with eMM ECM (n = 3 independent experiments) (scale bar = 50μm; *p $<$ 0.05, ***p $<$ 0.001).

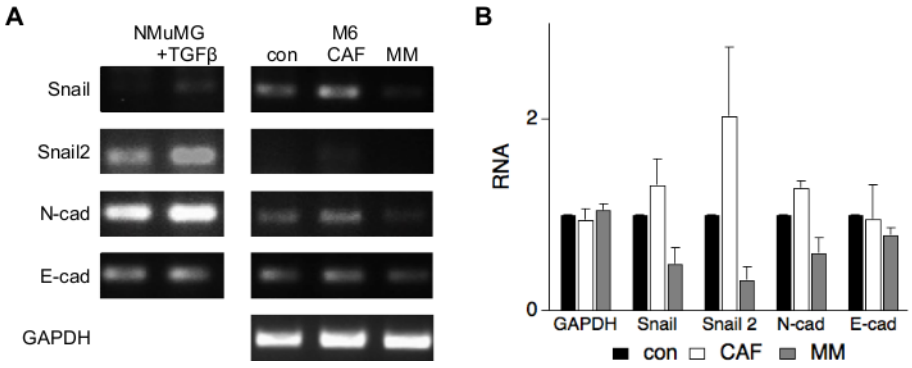

Figure 3.6: Normalization of mammary tumor cells by embryonic ECM is associated with increased epithelial signaling. (A) Representative images of RNA expression of EMT markers, Snail, Snail 2, N-cadherin (N-cad) and E-cadherin (E-cad), in control cultures (con) or cultures supplemented with MM or CAF ECM quantified in (B) (n = 3 independent experiments).

understand whether the tumor normalization I observed was further accompanied by a restoration of a more epithelial phenotype we looked into the multiple markers involved in EMT to see if they too reversed. We quantified Snail1, Snail2, N-cadherin and E-cadherin using RT-PCR and found that all three mesenchymal markers (Snail1, Snail2, and N-cadherin) decreased to nearly half when embryonic ECM was present in the cultures (Figure 3.6). While E-cadherin expression did not change, the morphological organization seen by IHC showed a polarized epithelial structure (Figure 3.4 a). Thus, embryonic mesenchyme may induce the tumor cells to take on a more a epithelial phenotype.

Finally, while the results of some past studies support the idea that mesenchymal cells can induce epithelial tumor cell normalization, other reports claim that mesenchymal cells actually stimulate tumor cell migration, and hence increase metastatic potential [176]. To explore this further, I cultured eMM or CAF cells in Transwell migration chambers, and then treated the cells with detergent to produce cell-free, ECM-coated Transwell membranes. When mammary tumor cells were plated on these

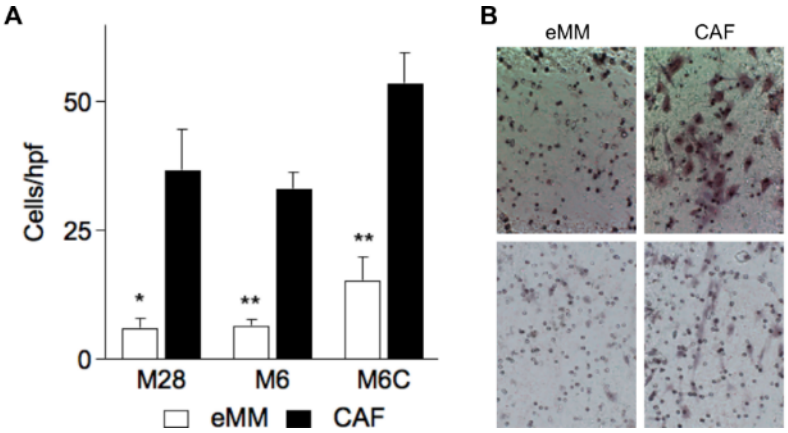

Figure 3.7: ECM from eMM cells reduces migratory potential. (A) Migration of M28, M6 and M6C mammary tumor epithelial cells decreased on eMM ECM compared to CAF ECM when analyzed in a Transwell migration assay measured by cells per high power field (hpf), representative images of hpf shown in B ($n \geq 4$ independent experiments, 8 hpf each) (*$p < 0.05$, **$p < 0.01$).

ECMs for 6 hours, I found that the eMM ECM produced a decrease in cell migration compared to the CAF ECM (Figure 3.7).

3.2.4 Molecular signaling associated with tumor normalization

The Rho/ROCK pathway is a key pathway in regulation of ECM signaling [43, 177]. Thus, I investigated the role of the small GTPases using a panel of activator and inhibitors (CN02 - rac activator, NSC 23766 - rac inhibitor, CT04 - Rho inhibitor, Y27632 - ROCK inhibitor). By treating with each of these small molecules I was able to show that rac activation is required for the tumor epithelial cells to form lumens in the presence of eMM ECM (figure 3.8).

3.2.5 Suppression of breast cancer growth *in vivo*

To explore whether the effects I observed *in vitro* might potentially be clinically relevant, I injected cell-free eMM ECM directly into tumors that were created by

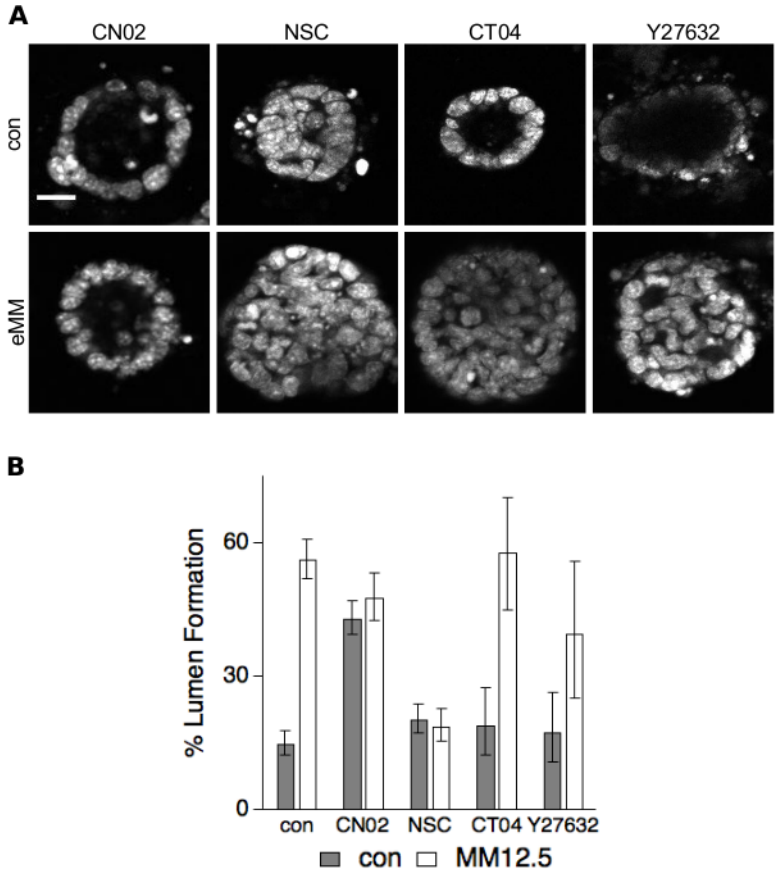

Figure 3.8: Rac1 activation required for tumor cell normalization by embryonic ECM. (A) Representative images of M6 tumor spheroids in control and eMM ECM containing cultures treated with inhibitors and activators of the Rho/ROCK pathway (CN02: rac activator; NSC: rac inhibitor; CT04: Rho inhibitor; Y27632: ROCK inhibitor;) and quantification of lumen formation (B). Error bars are 95% exact confidence intervals (binomial distribution) (con, CN02, NSC: $n \geq 3$ independent experiments; CT04, Y27632: $n = 2$ independent experiments; scale bar = 20μm).

implanting highly malignant 4T1 mouse mammary cancer cells in the left thoracic mammary fat pad of a syngeneic mouse. Tumors treated with inductive eMM ECM (50 mg/ml in PBS once every other day) displayed a significant reduction in tumor growth and expansion: eMM ECM-treated tumors displayed volumes 44% smaller than controls and 37% smaller than tumors treated with CAF ECM (Figure 3.9 a and Table 3.2). The growth rate (computed as the slope of growth curve from day 4 to day 10) of control and CAF ECM treated tumors (114 and 133 mm^3/day) is more than one and half times that of eMM ECM treated tumors (75 mm^3/day). Moreover, this suppressive effect was dependent on the ECM concentration injected, as less inhibition was produced at 10 versus 50 mg/ml (95 vs 75 mm^3/day) and a dose of 100mg/ml suppressed tumor growth most effectively (65 mm^3/day) (Figure 3.9 a).

Table 3.2: Statistical test (p-value) for *in vivo* data presented in Figure 3.9 a

	con vs. MM	con vs CAF	CAF vs MM
day 3	0.70	0.65	0.91
day 4	1.6×10^{-4}	0.19	7.7×10^{-3}
day 5	8.5×10^{-5}	0.03	0.14
day 6	1.3×10^{-4}	0.49	0.036
day 7	3.2×10^{-4}	0.08	7.9×10^{-3}
day 8	4.9×10^{-6}	0.78	0.024
day 9	1.2×10^{-4}	0.02	0.066
day 10	9.6×10^{-4}	0.12	8.6×10^{-3}

Immunohistochemical analysis of tumors treated with eMM ECM compared to controls confirmed that the eMM ECM I injected, which is highly enriched for collagen type VI (Figure 3.10), was retained within the tumor matrix (Figure 3.9 b,c). Additionally, quantification of ki67 and TUNEL revealed that the tumors treated with eMM ECM were less proliferative while very few cells underwent apoptosis (Figure

Figure 3.9: Effects of intratumoral injection of ECM isolated from cultured eMM or CAFs on mammary 4T1 breast cancer tumor growth *in vivo*. Tumors were injected into the left thoracic fat pad of female BALB/C mice and grown for 10 days. eMM ECM was injected intratumorally every other day starting on the 3rd day after implantation. (A) Significant (p-values shown in Table 3.2) concentration-dependent differences in tumor volume were detected from day 4 through 10 when injected with eMM at 10 mg/ml (n=5) (x), 50 mg/ml (n=10) (□) or 100 mg/ml (n=5) (•) compared with PBS control (n=10) (■) or 50 mg/ml CAF ECM (n=5) (+). (B) Immunofluorescence views of histological tumor sections showing staining for collagen VI, ki67 and TUNEL (green), as well as DAPI-labeled nuclei (blue). Computerized morphometric quantification of collagen VI (C) and ki67 (D) staining are shown below (scale-bar = 50 μm; ** $p < 0.01$, *** $p < 0.001$).

Figure 3.9: (continued)

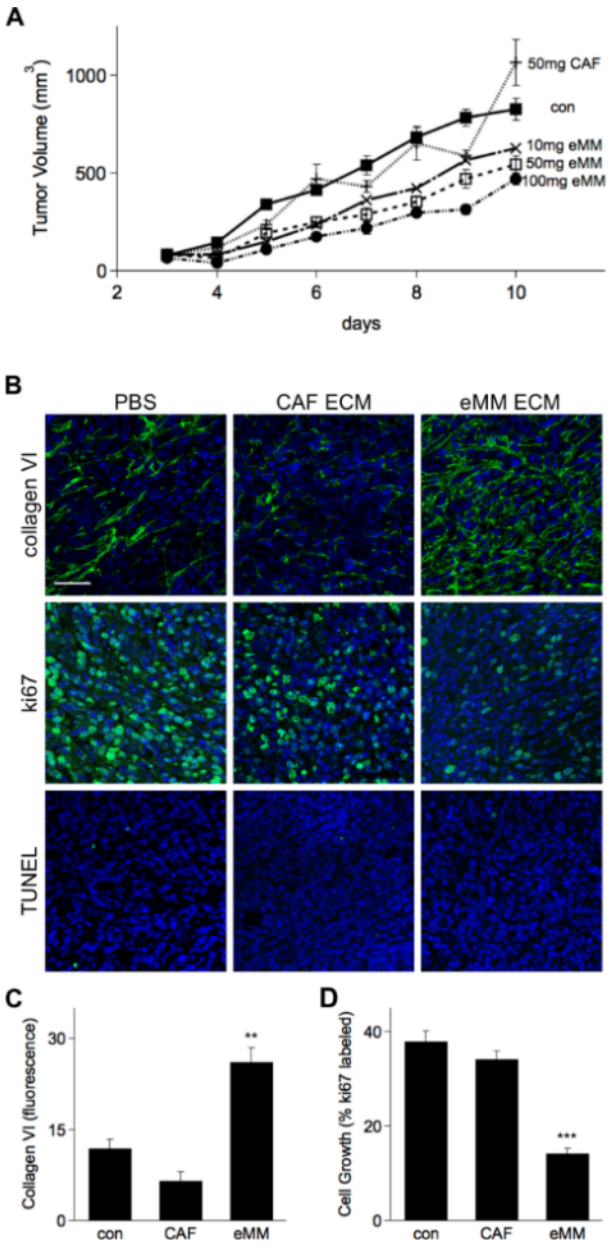

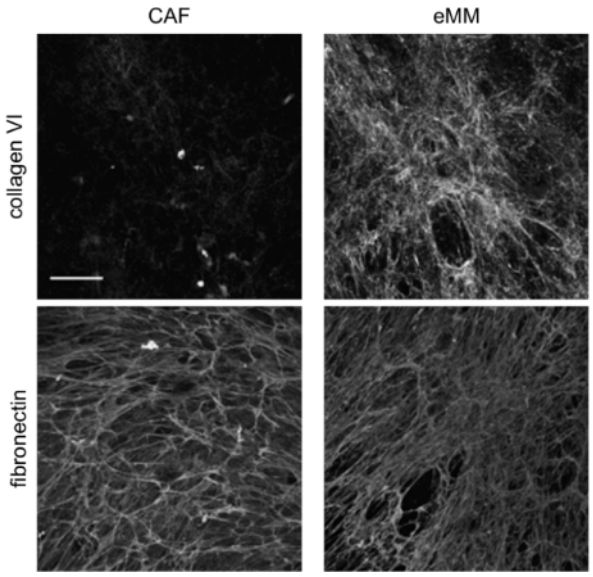

Figure 3.10: Collagen VI is more highly expressed in eMM ECM. Immunfluorescence images showing differential expression of collagen VI and fibronectin in ECM isolated from cultured CAF and eMM cells (scalebar = 50 μm).

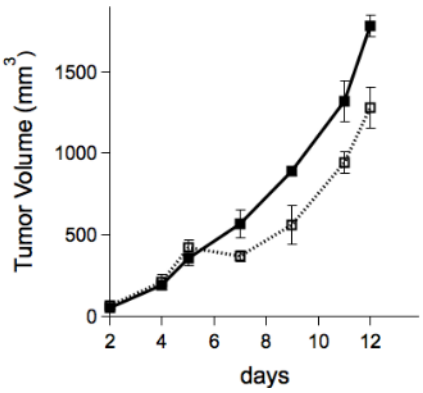

Figure 3.11: Treatment of tumors with eMM ECM at later stages of progression is less effective. Growth curves showing control, PBS injected (■) and eMM ECM (□) treated tumor volume, treatments were started on day 5.

3.9 b,d), which is consistent with the results of our *in vitro* studies. These findings suggest that the eMM ECM treated tumors are less aggressive compared to control or CAF ECM treated tumors.

Preliminary studies suggest that early treatment of tumor is critical for tumor suppression. By starting injections on day 5 following injection rather than day 3 we were able to see a small reduction in tumor volume compared to control, however it appeared to simply delay tumor progression rather than slow tumor growth (Figure 3.11). Tumor growth appeared to quickly resume a rate which was similar to that seen in control tumors. These results suggest that early treatment of tumors is more efficacious.

Critically, the *in vivo* model described here is highly aggressive and grows significantly more rapidly than normal tumors. While this allows for rapid analysis of different treatments *in vivo*, it also has significant limitations. Traditionally tumor growth curves would be exponential, however, likely because of the large number of cells injected and rapid expansion of this tumor model we see a linear tumor expansion. Additionally, the intratumoral injections of ECM material likely leads to only

portions of the tumor seeing the treatment which could be limiting the effectiveness of the treatment. In order to better understand the physiological relevance of this treatment additional *in vivo* tumor models would be necessary, including human tumor xenograft models.

3.3 Discussion

Studies carried out almost forty years ago suggest that some cancers can differentiate and normalize their growth when combined with normal embryonic mesenchyme or with ECMs that are deposited at the epithelial-mesenchymal interface [1, 2, 4–6, 8, 114, 165]. Embryonal carcinoma cells also were shown to 'reboot' and contribute to the development of various tissues as well as to the formation of living, cancer-free, chimeric mice when injected into the blastocyst [108]. Rous Sarcoma Virus, which is known to cause sarcomas through oncogenic transformation [111], similarly does not lead to malignant transformation when injected into chick embryos in the absence of additional microenvironmental cues (e.g., wounding) [112]. Thus, again suggesting that while genetic alterations might be necessary for cancer formation, they are not sufficient alone to induce tumor formation, and cues from the normal embryonic microenvironment appear to be able to suppress this transformation or induce cancer normalization. However, interest in developmental contributions and non-genetic causes of cancer faded as molecular biology surged and genetics became the focus in the cancer research field. Now, cancer is commonly thought to arise from progressive accumulation of random genetic mutations, which lead to uncontrolled cell growth and hence most treatment options focus on anti-proliferative therapies, which unfortunately produce generalized toxicity.

Our findings show that normal, early stage, embryonic mesenchyme is sufficient

to induce differentiation and suppress growth of mouse mammary tumor epithelial cells both *in vitro* and *in vivo*. Moreover, virtually all of these inductive effects are conveyed by the ECM that is deposited by these mesenchymal cells. Surprisingly ECM from CAF cells had no effect on tumor progression. It is possible that the CAF cells used in these studies have been 'normalized' due to the extensive doubling which occurred during the process of isolating and cloning the cells. The finding that embryonic ECM mediates tumor cell response is consistent with past studies which show the embryonic mesenchyme controls the form of developing epithelial tissues by accelerating and slowing ECM turnover at selective sites [131, 133], and with more recent experiments which have revealed that changes in ECM structure [99], mechanics [9], and composition [151] in the tumor microenvironment actively contribute to cancer progression. Our results suggest that embryonic ECMs that can induce normal tissue morphogenesis also have the ability to reverse this progression and 'reboot' cancers, resulting in at least partial normalization of their behavior.

While the present findings point to the insoluble ECM as the source of the inductive cues, the underlying mechanism responsible for this tumor normalization effect remains unknown. Given recent work showing that increases in ECM stiffness can promote cancer formation [9], it is possible that the cancer normalizing effects of embryonic ECMs might relate to differences in their mechanical properties. However, there are many other features of ECM that also could contribute to tumor normalization including matrix composition and nanostructure, as well as matrix-bound growth factors that may remain after decellularization.

Importantly, another group recently showed that 'embryonic-like' ECM may be used to inhibit cancer growth [178]. This work used neonatal foreskin fibroblasts cultured under hypoxic conditions in order to mimic the stem cell niche. However, the embryonic-like ECM produced by this hypoxic culture condition produced a de-

crease in tumor volume by inducing apoptosis through upregulation of Caspase 9. In contrast, our results indicate that native embryonic ECM induces tumor growth suppression in the absence of any detectable change in apoptosis. Instead, I observed induction of tumor cell differentiation and a lessening of tumor cell aggressiveness, as indicated by decreased proliferation and migration, as well as increased formation of ducts with hollow lumens plus re-expression of ERα. Thus, I believe the cancer-normalizing effects of native embryonic ECM act via a different mechanism than that previously reported with neonatal fibroblasts cultured under hypoxic conditions [178].

During the past decade, there has been an increasing focus on mesenchymal stem cells that have been shown to be attracted to both primary and metastatic tumor sites [179]. These studies have revealed that when mesenchymal stem cells or healthy fibroblasts are exposed to the tumor microenvironment, they can transform into CAFs that promote angiogenesis and tumor growth [180–183]. Thus, in light of the potential pro-tumorigenic behavior of stromal cells, care must be taken in proceeding with cell-based therapies. However, our results show that ECM rather than direct cell-cell contact is responsible for tumor cell normalization, which opens up the possibility that it might be possible to bypass this danger by designing biomimetic inductive materials that mimic critical properties of the embryonic mesenchymal ECM [184].

3.4 Materials and Methods

3.4.1 Animals

Embryonic mesenchyme was harvested from timed-pregnant FVB/N female mice (Jackson Laboratory, Bar Harbor, ME); the morning the vaginal plug was detected was defined as E0.5. Epithelium was peeled away and the underlying mesenchyme of each mammary bud was microdissected from the embryo. Dental mesenchyme was

dissected as previously described [58]. For tumor growth studies, 4T1 cells ($3x10^6$ cells/ 100 μl PBS) were injected into the mammary fat pad of 8- to 10-week old female BALB/C mice (Charles River Laboratories, Wilmington, MA). After 3 days, 100 μl PBS (with or without ECM) was injected intratumorally, and this was repeated every other day until sacrifice on day 10. All animal studies were reviewed and approved by Animal Care and Use Committee of Boston Children's Hospital.

3.4.2 Molecular Analysis

Total RNA was isolated using RNeasy Plus Mini Kit (Qiagen) and ERα expression was detected by qRT-PCR. For 3D cultures, hydrogels were solubilized using cold Cell Recovery Solution (BD Biosciences) supplemented with 1 mg/ml Collagenase A (Roche). RNA was reverse transcribed into cDNA using a iScript cDNA Synthesis Kit (Bio-Rad) and cDNA was amplified with iTaq SYBR Green Supermix with ROX (Bio-Rad) using the CFX96 real-time PCR system (Bio-Rad). Amplification was carried out using primers shown in Table 3.3 [185]. RT-PCR was used for the detection of EMT markers 0.5 μg of total RNA from each sample was reverse transcribed using the Omniscript RT Kit (Qiagen), and the cDNA was then amplified using the PCR Master Mix Kit (Qiagen). PCR conditions were: 94°C for 30 sec, 55°C for 30 sec, 72°C for 60 sec for 25 cycles with a final 72°C extension for 10 min using the primers shown in table 3.3. The sizes of the PCR products were 218 BP for Snail1, 149 bp for Snail2, 153 bp for E-cadherin, 226 bp for N-cadherin, and 305 bp for GAPDH.

3.4.3 Immunohistochemistry

Antibodies directed against collagen VI, β-catenin, laminin 5, BrdU and ki67 were from Abcam; Fluoromount G was from Southern Biotech. For detection of cell pro-

Table 3.3: Chapter 3 qRT-PCR primers

gene		sequence (5′->3′)
ERα	F:	CCTCCCGCCTTCTACAGGT
	R:	CACACGGCACAGTAGCGAG
GAPDH for ERα	F:	AGGTCGGTGTGAACGGATTTG
	R:	TGTAGACCATGTAGTTGAGGTCA
Snail1	F:	CTTCTCTAGGCCCTGGCTG
	R:	CTCTTGGTGCTTGTGGAGC
Snail2	F:	GCAAGATCTGTGGCAAGG
	R:	AGTGGGTCTGCAGATGTG
E-cadherin	F:	CTATGATGAAGAAGGAGG
	R:	CATCAGGATTGGCAGGAC
N-cadherin	F:	GGCCAGGAGCTGACCAGC
	R:	CCCATTCCAAACCTGGTG
GAPDH for EMT	F:	TGTCATCAACGGGAAGCCCA
	R:	TTGTCATGGATGACCTTGGC

liferation, cells were pulsed with 10 μM 5-ethynyl-2'-deoxyuridine (EdU) for 16 hours and then fixed and analyzed using a Click-iT Imaging Kit (Invitrogen). Images of 2D cultures were captured using a Zeiss Axioscope 2 and 3D cultures were captured using a Leica SP5 X MP Inverted Confocal Microscope with multiphoton pulsed IR laser Chameleon Vision 2. Morphometric analysis was performed using Image J software (`http://rsbweb.nih.gov/ij/`) (National Institute of Health, USA) as well as Volocity (PerkinElmer).

3.4.4 Decellularization

To produce ECMs that can be isolated from mesenchymal cell cultures, round glass cover slips (12 mm) were coated with crosslinked gelatin by treating with 0.1% gelatin (Sigma) for 1 hr at 37°C, followed by 1% gluteraldehyde (Electron Microscopy Sciences) for 30 min at room temperature, washed with PBS, treated with 1M

Ethanolamine (Sigma) for 30 min and washed with PBS again before plating of mesenchymal cells, as previously described [145]. The cells were plated near confluence on the gelatin-coated coverslips in 24 well plates and grown in medium supplemented with 50 μg/ml ascorbic acid (Sigma) changed every other day for 1 to 2 weeks before the cells were removed with pre-warmed (37°C) extraction buffer containing 20mM Ammonium Hydroxide (Sigma) and 0.5% (v/v) Triton X-100 (Sigma) in PBS for 10-15 mins. Cell debris was diluted in PBS and the ECM was stored at 4°C overnight. The following day ECM was washed with PBS and treated with DNase (10 Kunitz units/ml; Qiagen) for 2 hrs at 37°C. ECM was then removed from the bottom of the dish using a cell scraper, lyophilized and resuspended in PBS prior to use in 3D culture or *in vivo* assays.

3.4.5 Cell culture

Mammary epithelial cell lines obtained from different stages of breast cancer progression in C3(1)/SV40 T-antigen transgenic mice were kindly provided by Cheryl Jorcyk's laboratory [186]. The cells were maintained in DMEM with high glucose (GIBCO), supplemented with 5% FBS, 100 units/ml penicillin and streptomycin (Invitrogen). CAFs, which were isolated from 18 week transgenic mouse breast tumors, and cells isolated from microdissected mesenchyme were maintained in DMEM with high glucose supplemented with 10% FBS, 100 units/ml penicillin and streptomycin, and 2 mM GlutaMAX (Invitrogen).

In 2D culture studies, mammary epithelial tumor cells were plated (1 x 10^4 cells/well) alone or with mesenchymal cells (1:1 ratio) on gelatin-coated coverslips with or without overlying cell-free mesenchymal ECM. Cultures were maintained for 5 days; cells were trypsinized and counted on the T10 Automated Cell Counter (Bio-Rad) for proliferation assays. In order to estimate the growth rate the sigmoidal

growth curves were fit using the Verhulst-Pearl equation:

$$N(t) = \frac{KN_o e^{rt}}{K + N_o(e^{rt} - 1)} \tag{3.1}$$

where N is the number of cells, K is the carrying capacity, N_o is the initial population (assumed to be 10,000 based on initial seeding number), t is time, and r is the growth rate. The curve was fit by minimizing the sum or squared errors in order to identify the carrying capacity and the growth rate for each condition. Because the carrying capacity was similar across all conditions I only reported the growth rate.

3D cultures of tumor epithelial cells were prepared in gels containing Matrigel (BD Biosciences) and type I collagen (final concentration of 1 mg/ml; BD Biosciences). Epithelial cells (2.75 x 10^4) were resuspended in hydrogel (220 μl) either alone or in a 1:1 ratio with mesenchymal cells, and seeded into 35mm glass bottom dish (MatTek Corporation). Cultures were maintained for 2 weeks; culture medium was changed every two to three days. For histological analysis, the gels were fixed and frozen; lumen formation was quantified in well by staining the nuclei with Hoechst dye (Invitrogen). Lyophilized ECM solubilized at 100 mg/ml in PBS was mixed with prepared Matrigel and collagen type I hydrogel to achieve the desired final ECM concentration. Conditioned media was collected from eMM in 2D cultured alone for 2 or 3 days, spun at 1500 rpm, filtered (0.4 μm pore), and quick frozen to be stored at -20°C; prior to use the media was warmed to 37°C and supplemented 1:3 with normal media.

Activators and inhibitors for the Rho/ROCK pathway were used to supplement the media of 3D cultures starting on day 3. The small molecules were used as suggested by the manufacturer: CN02 (.1 U/mL, Cytoskeleton Inc.), NSC (50 μM, R&D Systems), CT04 (1 μg/mL, Cytoskeleton Inc.), Y27632 (10 μM, Reagents Direct).

3.4.6 Migration assay

To analyze effects on tumor cell motility, 24-well Transwell chambers (8 μm pores) were coated with mesenchymal ECM as described above. Epithelial cells (1 x 10^5) were added to the top chamber in serum-free medium while the bottom chamber contained medium supplemented with 5% FBS. After 6 hours, cultures were fixed in paraformaldehyde and stained with Mayer's Hematoxlyin; cells on top of the chamber were removed with a cotton swab prior to cell imaging.

3.4.7 Statistical Analysis

Independent samples t-tests were used to compare results, which were considered significant at $p < 0.05$. All results are presented as mean ± standard error of the mean (SEM).

3.5 Acknowledgements

This chapter is primarily compromised of a manuscript currently under review. Contributing authors for publication: Ashley G. Bischof, Deniz Yüksel, Tada Mammoto, Akiko Mammoto, Silva Krause, and Donald E. Ingber. Ashley G. Bischof designed the study, performed experiments, analyzed data, and drafted the manuscript. Deniz Yuksel assisted in performing the three dimensional culture experiments. Tada and Akiko Mammoto assisted with *in vivo* studies. Silva Krause performed further three dimensional culture experiments not included in this thesis. Mariko Kobayashi performed the analysis for EMT, not included in the paper. Donald E. Ingber supervised the work and revised the manuscript. This work was supported by a Department of Defense Breast Cancer Innovator Award (BC074986 to DEI).

4

Defining Critical Extracellular Matrix Features for Tumor Cell Differentiation

4.1 Introduction

PREVIOUS studies have shown that tumor cells can be induced to slow their growth and organize in the embryonic microenvironment [1–4, 108, 109, 114–117], and in Chapter 3 we confirm that early embryonic mesenchyme can normalize mammary epithelial tumor cell behavior. More importantly, we found that detergent extracted ECM produced by embryonic mesenchyme mediates this process. As described in detail in Chapter 1 the ECM is a complex meshwork of cross-linked proteins providing both biophysical and biochemical cues which regulate many cellular processes, including cell proliferation, survival, differentiation, and migration [20, 21, 149, 151, 152]. In this chapter I set out to identify critical features within the embryonic ECM that

regulate tumor cell normalization.

The deposition of additional ECM and its cross-linking creates an environment that is stiffer surrounding tumors [187–189]. In a recent study it was shown that increasing mammary ECM stiffness by varying collagen cross-linking promotes tumor progression and cell invasion, while reduction of LOX-mediated cross-linking lowered tumor incidence [9]. Suggesting that preventing or reversing matrix stiffness could impede tumor progression. Further, one way mammary epithelial cells respond to matrix stiffness is through Rho-mediated contractility [43]. Thus the activation of the Rho GTPase, rac1, shown in Chapter 3 to be required for tumor normalization by embryonic ECM, suggests that matrix mechanics may be playing a role.

Both the composition and biophysical properties of the ECM have been shown to contribute to normal development as well as tumor progression. Each developmental state has a unique ECM protein content, which regulates mammary gland organization and differentiation [60, 190–192]. These include a diverse array of ECM proteins: laminins, fibrillar collagens type I, III, and V, bead-filament collagen VI and IX as well as basal lamina collagen IV and collagen-associated proteins known to effect crosslinking such as elastin, fibrillin 1, decorin, lumican, and biglycan [60]. Precise control of the expression and remodeling of these proteins is critical for normal development as well as tissue homeostasis in the adult [99, 193]. However, attempts to characterize ECM composition by proteomics analysis both *in vitro* and *in vivo* has been limited because of the insolubility, high molecular weight glycans, and covalent protein crosslinks [194–196] which make full digestion of the proteins difficult. This is further complicated within the embryonic microenvironment by the small sample size. To overcome these difficulties we performed multi-stage digestions on our detergent extracted ECM samples from cultured embryonic cells.

In Chapter 4 I set out to identify critical features of the inductive ECM that are

responsible for tumor normalization. Specifically, I tested the inductive capacity of five cell-derived ECMs (MM12.5, 13.5 and 14.5, DM10, and CAF) finding three inductive, one weakly inductive, and one which is not inductive. On this panel of ECMs I performed immunoblotting, AFM, and proteomics analysis to identify key biochemical and mechanical features of the inductive matrices. I then went on to test these features *in vitro*, identifying three proteins that contribute to tumor normalization.

4.2 Results

4.2.1 Specificity of the tumor normalization capacity of embryonic mesenchyme

We previously showed that ECM isolated from early stage MM (eMM: E12.5-E13.5) but not adult CAFs could induce mammary tumor cell normalization, as seen by decreased growth and migration, as well as increased ERα expression and lumen formation in 3D culture. Embryonic ECM was sufficient to increase lumen formation by more than 3-fold, representing the largest and most consistent readout for tumor cell normalization, thus lumen formation in 3D culture was used as the primary readout moving forward.

In order to identify critical ECM features involved in tumor cell normalization from cell-derived ECM I first set out to define a panel of inductive and non-inductive matrices. For these studies I focused on embryonic matrices from different embryonic stages of the mammary gland (E12.5, 13.5 and 14.5) as well as from a different organ, embryonic day 10 dental mesenchyme (DM10). Interestingly, only ECM isolated from mesenchyme at the earlier stages (MM12.5, MM13.5, and DM10) that are also inductive during embryological development produced a significant increase

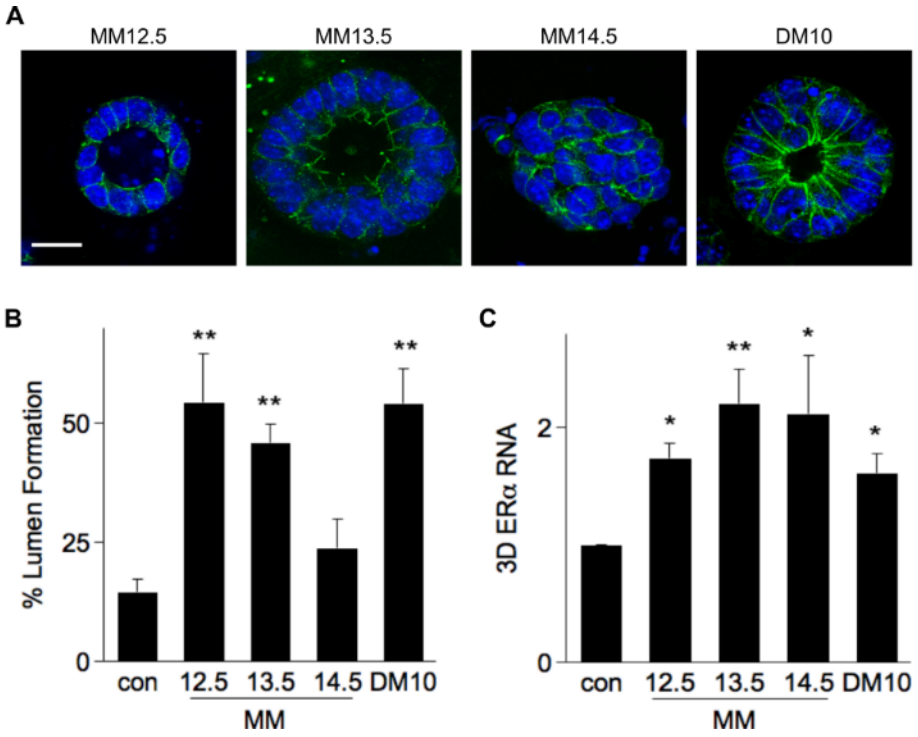

Figure 4.1: Tumor cell differentiation in 3D culture is most effective with early stage embryonic mesenchyme. (A) Fluorescent images showing M6 epithelial tumor spheroids cultured with ECM isolated from E12.5, 13.5 or 14.5 embryonic mammary mesenchyme (MM) or E10 dental mesenchyme (DM) and stained with DAPI and anti-β-catenin (green) to visualize epithelial polarization (nuclei are in blue). Quantification of lumen formation (B) and ERα induction (C) in these cultures ($n \geq 3$ independent experiments) (scalebar = 50 μm; * $p < 0.05$, ** $p < 0.01$).

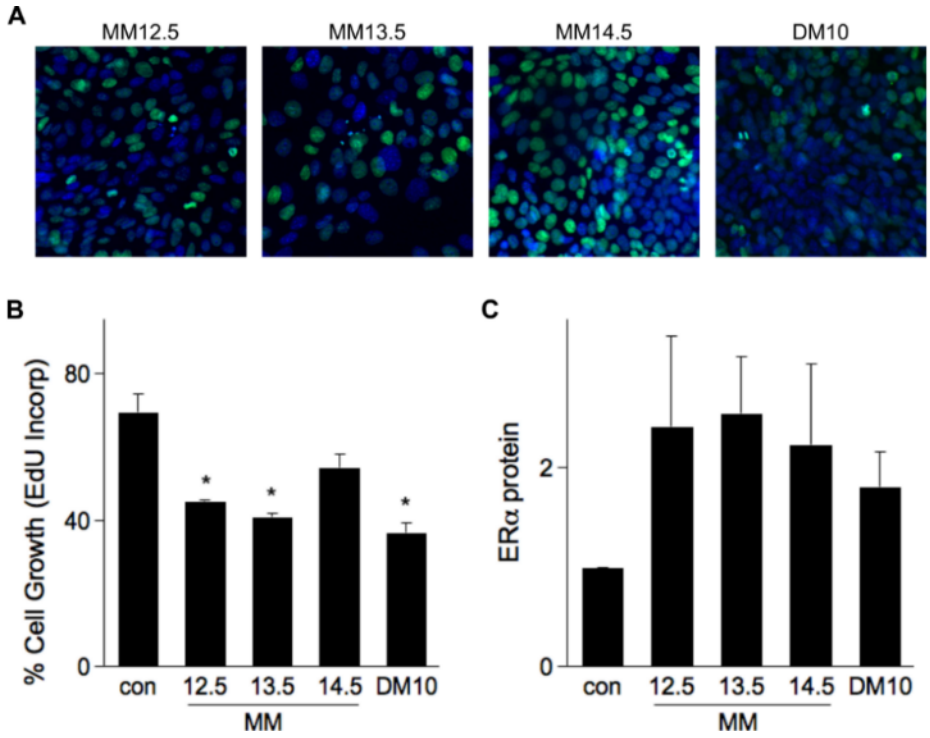

Figure 4.2: Tumor cell differentiation in 2D culture is most effective with early stage embryonic mesenchyme. (A) Fluorescent images showing M6 epithelial tumor spheroids cultured with ECM isolated from E12.5, 13.5 or 14.5 embryonic mammary mesenchyme (MM) or E10 dental mesenchyme (DM) and stained with DAPI (blue) and EdU (green) to visualize cells which have undergone division. Quantification of the percentage of cells which are stained for EdU, representing cell growth (B) and ERα induction (C) in these cultures (n = 3 independent experiments) (scalebar = 50 μm; * $p < 0.05$).

in lumen formation in 3D culture (50.1%, 46%, and 54% lumen, respectively), while ECM isolated from later stage (MM14.5) mammary mesenchyme failed to produce a significant effect in 3D culture (Figure 4.1 a,b). Further, the same trend could be seen in 2D culture where only ECM from earlier stages was sufficient to decrease tumor cell growth (Figure 4.2 a,b). However, day 14.5 MM still retained its ability to re-induce ERα expression in M6 cells (Figure 4.1 c and 4.2 c), suggesting that histodifferentiation and cytodifferentiation might be controlled through independent mechanisms, as previously described [66].

4.2.2 Analysis of matrix bound growth factors

It is known that some growth factors bind to ECM [147, 197, 198] however, little is known about what role these growth factors play in cellular response to acellular matrix. I used western blot analysis to analyze which growth factors remained following decellularization, testing multiple factors known to be critical for embryonic mammary gland development (InhibinβA, BMP4, Msx1, Fgf8, Fgf3, Wnt5a and Wnt3a) [62]. I was able to identify several growth factors that are maintained in cell-derived ECM, specifically, Msx1, Fgf8 and Wnt3a (Figure 4.3 a). To determine whether these bound growth factors are critical for the cell-derived induction of mammary tumor cell normalization I optimized methods to remove the growth factors using high salt washes as has been previously described in Chapter 2 [147, 198]. Isolated ECM was treated with high salt solutions, which released bound factors, leaving matrix proteins adherent to the tissue culture dish. The growth factors present within the salt wash was then concentrated, reducing the salt concentration using desalting columns. Then both fractions (salt soluble and insoluble, scrapped from the bottom of the dish) were dialyzed for 48 hours in PBS in order to remove any remaining salt. The extracted growth factors (salt soluble) and ECM proteins (salt insoluble) were then incorporated in 3D culture with mammary tumor cells to separately test their inductive capacity. Interestingly, the salt insoluble fraction could increase lumen formation to the same extent as control ECM while the salt soluble fraction had no effect, suggesting that the matrix proteins may be responsible for the tumor cell normalization (figure 4.3 b), just as they were in the embryonic tooth (Figure 2.6). However, in order to be confident in this result further analysis would be required to assure the absence of all growth factors. Specifically, additional growth factors should be tested and more quantitative measures of growth factor concentration in

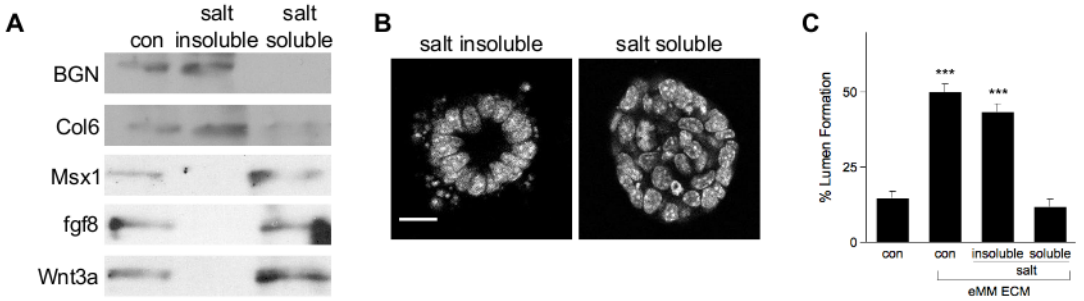

Figure 4.3: Salt insouble matrix proteins sufficient to normalize tumor cells. (A) Western blot analysis showing ECM proteins as well as bound growth factors in intact aceullar matrix (con), and fractions of the insoluble matrix following salt washes. (B) Representative images showing M6 tumor spheroids in 3D culture with salt soluble and salt insoluble fractions, quantification of the effects of each of these fractions are shown in C (scale bar = 20 μm; ***p < 0.001).

each fraction should be carried out.

4.2.3 Differences in matrix stiffness suggest a role for mechanics

Cancer progression is commonly accompanied by a concomitant increase in tissue rigidity, and past studies have shown that breast cancer development can be stimulated by experimentally increasing ECM stiffness [9]. I used AFM to confirm that mammary tumor progression in the C3(1)-Large T transgenic mice is accompanied by an increase in tissue stiffness. I showed that the Young's modulus increased approximately 4-fold in 16 week transgenic glands which contain ducts displaying a DCIS phenotype (1,770 ± 1,150 Pascals; median ± median absolute deviation) relative to 8 week wild type glands (460 ± 110 Pa) (figure 4.4 a). Interestingly, as the mammary tumors progressed and their stiffness increased, so did the heterogeneity of their compliance (figure 4.4 a,b).

To explore the origin of this heterogeneity in greater detail, I took advantage of the observation that 16 week transgenic glands display multiple morphological stages

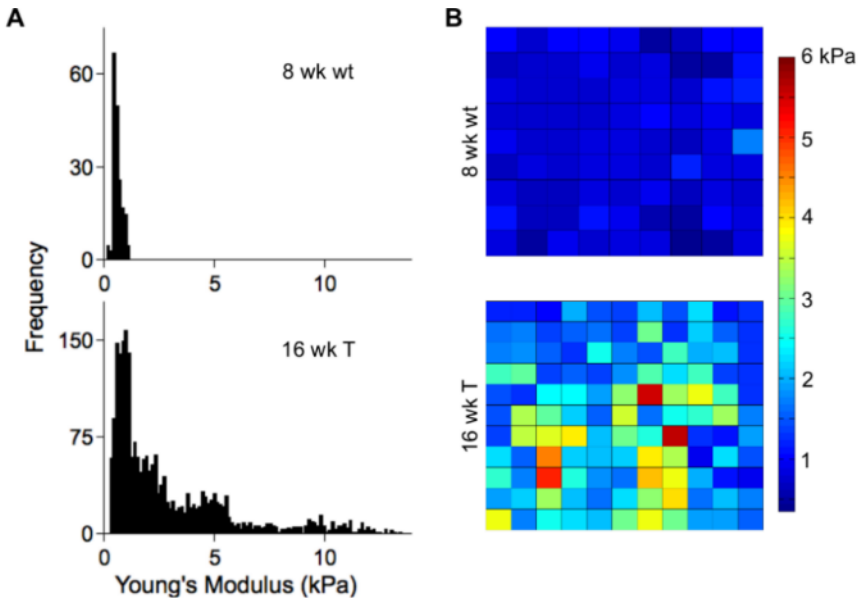

Figure 4.4: Tumor progression in transgenic mice is accompanied by a increase in tissue stiffness and heterogeneity in mechanical properties. (A) Histograms of Young's modulus measured by AFM from 8 week wildtype glands (8 wk wt) and 16 week transgnic glands (16 wk T). (B) Representative maps of Young's modulus resulting from AFM measurements of a single gland in each stage (8 wk wt on top, 16 wk T on bottom) (Measurement for each group take on five separate days).

of breast cancer progression (i.e., normal and DCIS) at different sites within a single gland. So, I used AFM, which allows for precise spatial control, to analyze the mechanics of the epithelial and stroma compartments individually within these morphologically distinct regions. These studies revealed that the Young's modulus of the epithelium in histologically normal 16 week transgenic ducts was double that of 8 week wild type glands (1,010 ± 600 vs 460 ± 110 Pa) and there was also a much greater heterogeneity of mechanical stiffness values (median absolute deviation of 600 Pa vs 110 Pa), while the surrounding periductal stroma of both types of normal appearing ducts remained relatively soft and uniform (660 ± 220 Pa) (figure 4.5 a,b). In contrast, the epithelium and periductal stroma of 16 week transgenic ducts that exhibited a DCIS morphology both showed significant increases in their compliance (2470 ± 1,280 Pa and 5,950 ± 2,520 Pa, respectively) compared to histologically normal ducts from 16 week transgenic tissues (690 ± 270 Pa) or wild type glands (460 ± 110 Pa) (figure 4.5 a,b). While these observations show that a dramatic increase in mechanical stiffness accompanies tumor progression, and that changes in epithelial stiffness may even precede histological duct filling, it is unclear what role this stiffness is playing.

To understand whether differences in mechanical compliance are contributing to the tumor normalization observed with embryonic ECM I used AFM to quantify the five cell-derived matrices. I was able to show that early stage inductive scaffolds (MM12.5, MM13.5 and DM10) were relatively soft (1,100 ± 300 Pascals (Pa), 800 ± 200 Pa, 450 ± 100 Pa, respectively) while later stage MM14.5 had a significantly higher Young's Modulus (3,100 ± 900 Pa), and CAF ECM was even stiffer (6,300 ± 2600 Pa) (figure 4.6 a). These results were suggestive that matrix mechanics may be contributing to tumor cell normalization.

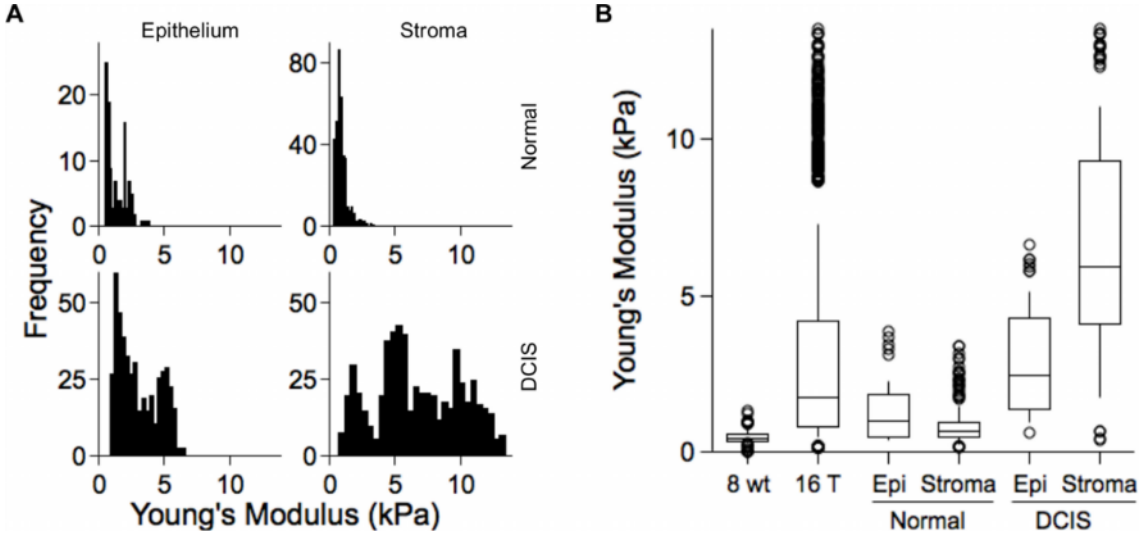

Figure 4.5: Mechanical properties of both epithelial and stromal compartments correlate with histological stage in adjacent glands within transgenic mice. (A) Histograms of AFM measurements from epithelium and stroma of ducts which were histologically normal or DCIS in 16 week transgenic mice. (B) Box plot showing 8 week wildtype (8 wt), 16 week transgenic (16 T) and separation of epithelium (Epi) and stroma from histological distinct ducts in 16 week transgenic animals. The median is displayed along with the 25th and 75th percentiles (box), and the 10th and 90th percentile (whiskers). Outliers are displayed as o (Measurement for each group take on five separate days).

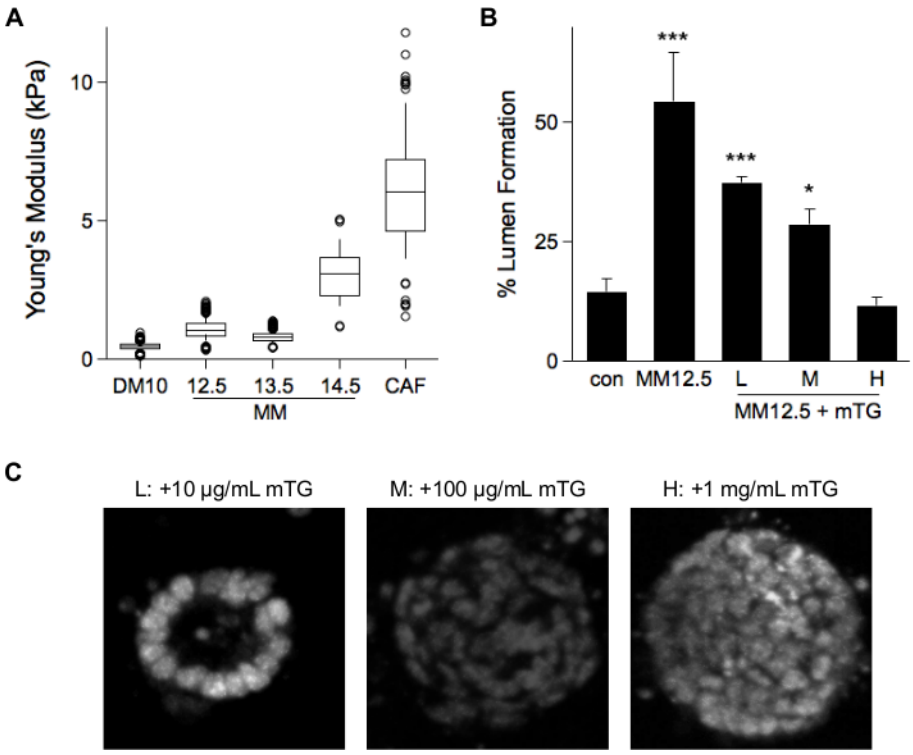

Figure 4.6: Mechanical and structural properties may play a critical role in inductive capacity of tumor normalization. Box plots showing Young's modulus of *in vitro* matrix (A). (B) Quantification of lumen formation with 0.01 mg/mL (L), 0.1 mg/mL (M), or 1 mg/mL (H) transglutaminase (mTG) added to MM12.5 cells during ECM production, representative images of M6 tumor spheroids in each condition shown in C (AFM measurements taken on two separate days; Lumen formation: n = 3 independent experiments; scale bar = 20 µm; * $<$ 0.05, ***p $<$ 0.001). .

In order to alter matrix mechanics I chose to use the native tissue crosslinker, transglutaminase. During ECM production, the growth media was supplemented with increasing concentrations of transglutaminase, producing a clear cellular response. MM12.5 cells, which were supplemented with 1 mg/mL transglutaminase, had a more spread morphology indicative of a stiffer substrate. Surprisingly, AFM measurements of the resulting matrix showed that adding this tissue crosslinker did not increase matrix mechanics. However, treatment of the ECM with transglutaminase did significantly decrease the ability of the matrix to induce lumen formation in 3D culture, in a concentration dependent manner (figure 4.6 b, c). Thus it remains unclear whether matrix mechanics contributes to tumor cell normalization. Previous reports have shown that crosslinking native matrix can prevent exposure of mechanically unfolded cryptic sites [199], alternatively crosslinking may induce changes in mechanical properties at a larger scale, which could not be detected by the small probe used for AFM.

4.2.4 Proteomics analysis to define matrix composition

The biochemical makeup of the ECM is known to play a large role in the control of cell behavior, thus I setout to identify the proteins that remained following detergent extraction using proteomics analysis. ECM proteins are difficult to identify using proteomics analysis because of their wide range of expression, high molecular weight glycans, and the presence of covalently cross-linked proteins that can be difficult to digest. In order to overcome these issues I used a multi-stage digestion protocol involving PNGase, Lys-C, and trypsin in order to completely digest the samples [200]. Further, because of the large number of proteins present in the mixture with wide range of concentrations and sizes, the LC-MS/MS was run at a shallow gradient in order to detect more of the smaller peaks. Each sample was run in triplicate in

order to assure that any sample to sample variability was accounted for. Our analysis across replicates showed striking similarity between independent sample preparations, suggesting that our method of ECM preparation is consistent.

Using this proteomics analysis I was able to identify a large number of proteins (a complete list of proteins can be found at the end of the chapter in Table 4.4). In addition to ECM proteins multiple cellular components also remained in our detergent insoluble material. A number of cytoskeletal proteins (e.g. actin, tubulin, intermediate filaments, myosin), DNA associated proteins (e.g. topoisomerase, replication and repair protein), histones, and transmembrane proteins (e.g. aquaporin, lipid A export ATP-binding) among other components were found in the protein mixtures. However, these proteins were largely found in all five matrices studied suggesting they do not play a critical role in the biological activity. Interestingly, neither integrins nor growth factors appeared in the proteomics results. It is possible that the alternative digestion carried out to completely digest the ECM samples somehow selected for ECM proteins.

Proteomics analysis also identified multiple ECM proteins across all five samples some of which were expressed only in embryonic ECMs (Table 4.1 and Figure 4.7). However, from proteomics analysis alone I cannot be sure about the expression level of these proteins. So, in order to validate and better understand the differences in expression I used Western blot analysis showing that SPARC, Collagen VI and Collagen III are expressed only in embryonic ECMs and that biglycan is much more highly expressed in embryonic matrices compared to CAFs (figure 4.8 a) (using total protein to normalize). Further, western blot analysis revealed that most of these proteins have a lower expression in ECM isolated from MM14.5, which has been shown to be less inductive then other embryonic matrices.

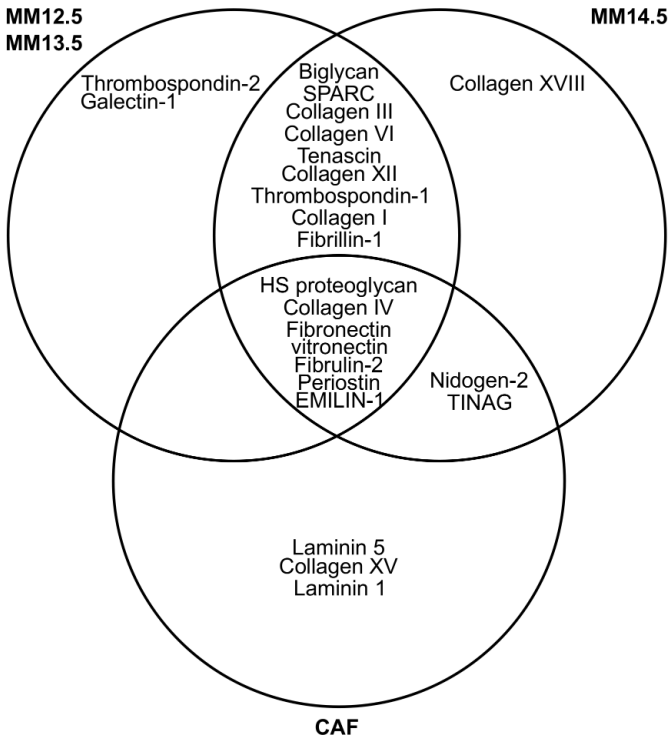

Figure 4.7: Multiple ECM proteins were identified in each of the cell-derived matrices by proteomics analysis. A venn diagram illustrating matrix proteins shared and specific to each of the matrix protein mixtures (Data pooled from at least two independent samples for each cell type).

Table 4.1: Summary of ECM proteins identified in proteomics analysis and microarray

Protein	Proteomics				20 wk T microarray	
	MM12.5	MM13.5	MM14.5	CAF	storma	Epi
biglycan	x	x	x			
SPARC	x	x	x		-	-
Collagen III	x	x	x		-	-
Collagen VI	x	x	x		-	-
Tenascin	x	x	x			+
Collagen XII	x	x	x			+
Collagen I	x	x	x			-
Fibrillin-1	x	x	x			-
Thrombospondin-2	x	x				-
Thrombospondin-1	x	x	x			+
Galectin-1	x	x				-
Collagen XVIII			x			
Tin-ag			x	x		
Nidogen-2			x	x		-
Fibronectin	x	x	x	x		
HS proteoglycan	x	x	x	x		
Fibrulin-2	x	x	x	x		-
Vitronectin	x	x	x	x		-
Periostin	x	x	x	x		
EMILIN-1	x	x	x	x		
Collagen IV	x	x	x	x		-
Laminin 5				x		+
Laminin 1				x		-
Collagen XV				x		-

In order to understand which of these proteins might be active during tumor progression within C3(1) SV40 Tag transgenic mice I utilized microarray data previously collected by Amy Brock and Silva Krause in the Ingber laboratory. RNA levels from whole tissue lysates from normal 8 week mammary glands (both epithelial and stromal compartments) as well as tumors from 20 week transgenic glands, where the bulk tumor (Epi) and the adjacent stroma were manually separated were compared. Interestingly, in late stage tumors multiple of the ECM proteins enriched in embryonic ECM had differential expression compared to 8 week wildteype glands (Table 4.1).

Of particular interest SPARC, Collagen III, and Collagen VI were the only ECM proteins examined which had altered expression within the tumor stroma and they all had decreased expression (Table 4.1).

To investigate the effect of the different ECM proteins identified through proteomics analysis on mammary tumor cell behavior I embedded individual proteins (purchased commercially) in 3D control gels composed of Matrigel and Collagen I and quantified lumen formation. Interestingly, three of the proteins tested had the capacity to induce lumen formation in 3D culture (biglycan, SPARC, and Collagen III) while the others (Fibrillin-1, Tenascin C, and Collagen VI) had no effect (figure 4.8 b, c). Biglycan and SPARC have both been shown previously to interact with collagens, particularly collagen I and collagen III [36, 201, 202], suggesting that these three proteins may be acting together to regulate tumor cell behavior.

Biglycan is a small leucine-rich proteoglycan (SLRP) characterized by a typical cluster of cysteine residues at the N terminus. The protein core consists of about 331 amino acids with two covalently linked GAG side chains containing chondroitin sulfate and/or dermatan sulfate and two oligosaccharide moieties. Previous studies on biglycan have highlighted a role in the tumor microenvironment, which can be either tumor promoting [200] or suppressing [203, 204] depending on the tissue context and attached glycans. Immunoblot analysis revealed that the biglycan present in all 5 matrices had a molecular weight of 50kDa, slightly different from the expected 42kDa, however, significantly lower than the traditional fully glycosylated protein in the range of 100-200 kDa and preliminary studies to identify carbohydrates in the protein mixtures using Periodic acid-Schiff base staining revealed no carbohydrates in the protein mixtures. Further, the biglycan protein core purchased commercially was sufficient to increase lumen formation *in vitro* (Figure 4.8 b), suggesting that

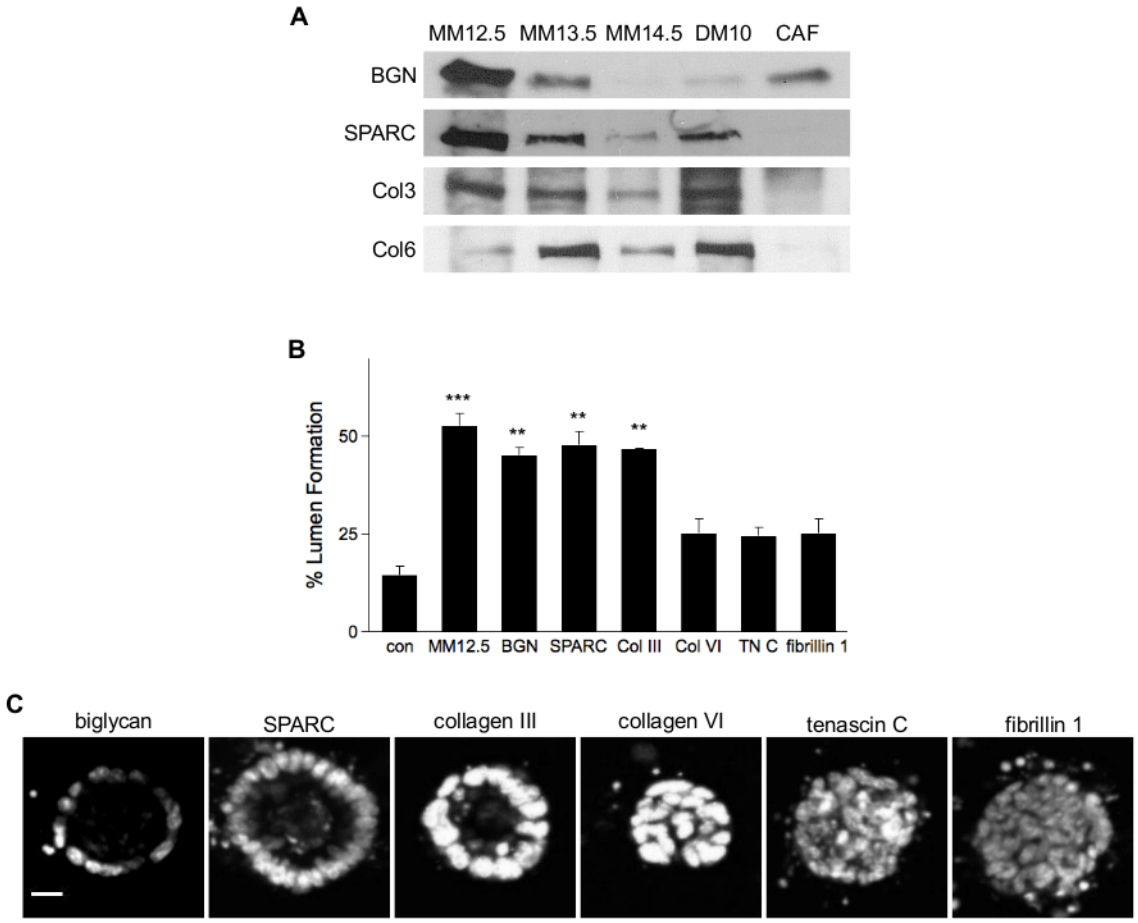

Figure 4.8: Three ECM proteins identified by proteomics were shown to reproduce the mammary tumor normalization in 3D. (A) Western blot analysis of multiple ECM proteins showing expression in different stages of MM and DM as well as CAF. (B) Quantification of lumen formation in 3D cultures which contain matrix proteins identified to be expressed in inductive matrices, reprentative images of M6 cell spheroids shown in C (biglycan (BGN), SPARC, Tenascin C (TN C), fibrillin 1: $n = 3$; Collagen III (Col III), Collagen VI (Col VI): $n = 2$ independent experiments) (**$p < 0.01$, ***$p < 0.001$; scale bar = 20 μm).

GAG chains are not playing a role in this case. In order to better understand the role of biglycan in the embryonic ECM I used siRNA to knockdown biglycan in MM12.5 cells [205] resulting in a nearly 8-fold decrease in biglycan expression as shown by qRT-PCR and immunoblot (Figure 4.9 a,b). ECM isolated from MM12.5 cells with decreased biglycan failed to induce tumor cell normalization in 3D culture (figure 4.9 c, d). However, the effect of biglycan knockdown on Collagen III or SPARC expression or fibrillogenesis has not been evaluated in these matrices.

4.3 Discussion

While it has been nearly forty years since it was first shown that certain epithelial cancers can normalize their growth and show signs of histodifferentiation when combined with normal embryonic mesenchyme or basement membrane [1, 2, 4–6, 8, 114, 165], the mechanism has remained illusive. Our work in Chapter 3 showed that ECM produced by mesenchymal cells alone is sufficient to induce tumor cell normalization both *in vitro* and *in vivo*, and this is supported by a number of recent findings showing that changes in ECM structure [99], mechanics [9], and composition [151] in the tumor microenvironment actively contribute to cancer progression. These findings open up the possibility of taking a tissue engineering approach to cancer therapy by designing a biomimetic material that mimics critical properties of the embryonic mesenchymal ECM [184]. However, to design such a material would require an understanding of the mechanism underlying tumor normalization by embryonic mesenchymal ECM.

Our work shows that early mammary mesenchyme (E12.5-13.5) can normalize tumor cell behavior, while mesenchyme from E14.5 is less effective both in 2D and 3D culture. Interestingly, the embryonic mammary gland undergoes significant changes between E13.5 and E14.5. During E12.5-E13.5 the embryonic mammary epithelium

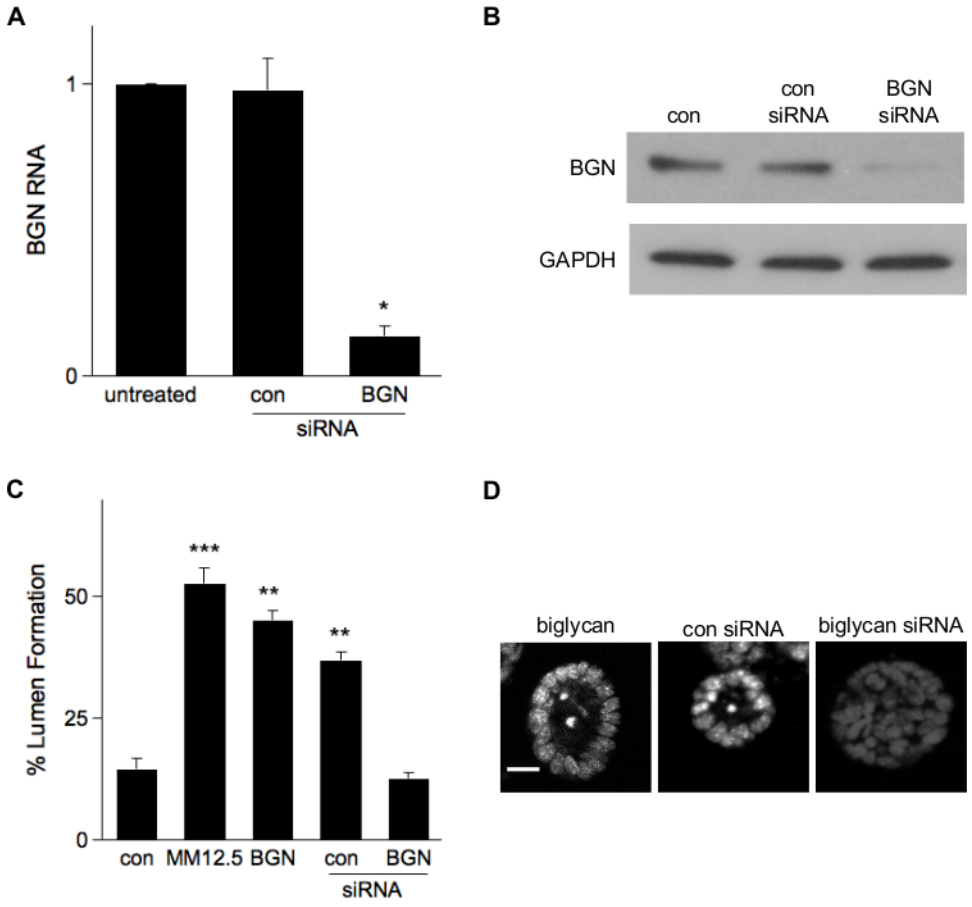

Figure 4.9: Biglycan expression in necessary for induction of tumor normalization. Biglycan (BGN) expression in control MM12.5 ECM (untreated), nonsense siRNA (con siRNA) and BGN siRNA shown by qRT-PCR (A) and western blot (B). (C) Quantification of lumen formation in 3D culture in control cultures or with added MM12.5 ECM, biglycan protein, or MM12.5 ECM treated with control siRNA or biglycan siRNA, representative images of M6 cell spheroids shown in D ($n \geq 3$ independent experiments). (**$p < 0.01$, ***$p < 0.001$; scale bar = 20 μm).

is in a rest phase, it does not undergo significant cell growth [206]. However, by E15 DNA synthesis resumes within the mammary epithelium of female mice, and the mammary mesenchyme differentiates into two separate lineages, the fibroblastic mesenchyme directly surrounding the epithelial bud and the fat pad precursor [68]. Recombination studies have shown that the fibroblastic mesenchyme induces atypical ductal branching with hyperplastic ducts, while the fat pad mesenchyme induces epithelial cell elongation and branching [68]. Thus it is clear that mesenchyme from different differentiation statuses can play a large role in controlling epithelial cell fate during embryonic development, and it is possible that the cell growth arrest observed in tumor cells is carried out by the same mechanism as used during embryonic development.

Our AFM studies demonstrate that the ductal mammary epithelium exhibits local micromechanical changes prior to undergoing morphological transformation, as evidenced by the increased stiffness of histologically normal ductal epithelium in 16 week transgenic glands. Further it has been shown previously that preventing matrix crosslinking and increased tissue stiffness can actually slow tumor progression [9]. It is still unclear what role matrix mechanics is playing in tumor normalization by embryonic ECM. Our results show that crosslinking the matrix using transglutaminase does decrease tumor cell response, however, I was unable to detect a change in the matrix mechanics using AFM. Thus more studies are necessary to clearly understand what changes were induced by transgluatminase. It is still possible that the mechanical properties are changed but that it is the tensile properties which change or that these changes can only be detected at a larger length scale. Additionally, it is possible that alterations of the matrix composition, such as biglycan knockdown, which decreased the inductive capacity of the matrix, also affects the matrix mechanics.

Type III collagen is a fibrillar collagen which frequently associates with type I colla-

gen and is found extensible in connective tissues, skin, lung, and the vascular system. During development collagen III accumulates specifically at the clefts of branching organs where it is thought to provide a rigid support to stabilize the cleft and prevent further growth and invasion [207]. Our studies suggest that collagen III may be taking on a similar role for tumor cells, acting to slow growth and stabilize the cells in differentiated states. Interestingly, the other two matrix proteins identified as playing a role in tumor normalization by embryonic ECM, biglycan and SPARC, have both been shown to bind to Collagen III and regulate fibrillogenesis and matrix remodeling [202, 208, 209]. Further while any of these three components can increase tumor cell differentiation in 3D culture, knocking down biglycan alone is sufficient to disrupt the inductive capacity of the embryonic matrix. These data suggest that all three matrix components may be working together to regulate tumor cell behavior. However, to fully understand this it will be critical to determine how decreased biglycan affects collagen III and SPARC expression.

4.4 Materials and Methods

4.4.1 Decellularization of cultured mesenchymal cells

To produce ECMs that can be isolated from mesenchymal cell cultures, round glass cover slips (12 mm) were coated with crosslinked gelatin by treating with 0.1% gelatin (Sigma) for 1 hr at 37°C, followed by 1% gluteraldehyde (Electron Microscopy Sciences) for 30 min at room temperature, washed with PBS, treated with 1M Ethanolamine (Sigma) for 30 min and washed with PBS again before plating of mesenchymal cells, as previously described [145]. The cells were plated near confluence on the gelatin-coated coverslips in 24 well plates and grown in medium supplemented with 50 μg/ml ascorbic acid (Sigma) changed every other day for 1 to 2 weeks before

the cells were removed with pre-warmed (37°C) extraction buffer containing 20mM Ammonium Hydroxide (Sigma) and 0.5% (v/v) Triton X-100 (Sigma) in PBS for 10-15 mins. Cell debris was diluted in PBS and the ECM was stored at 4°C overnight. The following day ECM was washed with PBS and treated with DNase (10 Kunitz units/ml; Qiagen) for 2 hrs at 37°C. Undifferentiated dental mesenchyme was plated on isolated ECM and maintained in culture for 16 hours at 37°C and then fixed in pre-warmed 4% PFA.

4.4.2 Growth factor extraction

Acellular matrix isolated from cultured cells was washed several times with PBS, then incubated with 2 M Sodium Chloride (sigma) in 20 mM HEPES buffer (sigma) at 37°C for 1 hour [147, 148]. Isolated matrix was washed several times in PBS to remove excess salt while extracted growth factors were spun in desalting columns and then both were dialyzed against 10mM PBS for 48 hours, and lyophilized. Extraction of growth factors was confirmed by immunoblotting, where protein content was normalized by weight. Salt extracted growth factors or ECM was used as acellular matrix in 3D culture.

4.4.3 Atomic force microscopy

Unfixed intact frozen sections of mammary tissue or detergent extracted matrices from cultured cell were measured using an MFP-3D-Bio atomic force microscope (Asylum Research) in PBS. Silicon nitride AFM cantilevers with a 60 pN/nm spring constant with either a 5 μm or a 10 μm borosilicate spherical bead on the tip (Novascan) were calibrated thermally according to the Sader method. The tissues were imaged following immunohistochemical staining for Laminin5 and dapi using an Olympusx81 inverted fluorescence microscope. The AFM applied a maximum prescribed force

of 1-10nN with an indenter velocity of 2 μm/s and the Hertz Model was used to determine the elastic properties of the tissue.

4.4.4 Proteomics analysis

Detergent extracted ECM (5 mg) isolated from cultured cells was solubilized and reduced in 100 μL of 8 M urea, 100 mM ammonium bicarbonate, 10 mM dithiothreitol, pH 8 with shaking at 37°C for 30 minutes. After cooling to room temperature, cysteines were alkylated by adding iodoacetaminde to a final concentration of 25 mM for 30 minutes in the dark. The solution was then diluted to 2 M urea, 100 mM ammonium bicarbonate, pH 8.0, followed by digestion with 1000-2000 units of PNGaseF (New England BioLabs) for 2 hours at 37°C. Next the samples were digested with Lys-C (Wako Chemicals) at a ratio of 1:100 enzyme:substrate with vortexing at 37°C for 2 hours. Final digestion was done using trypsin (Sequenceing grade, Sigma), at a ratio of 1:50 enzyme:substrate, with vortexing at 37°C overnight, followed by a second aliquot of trypsin, at a ratio of 1:100 enzyme:substrate, and an additional 4 hours of incubation. Digests were acidified and desalted using 30 mg HLB Oasis Cartridges (Waters Corp) and eluted with graded acetonitrile (50%, followed by two washes in 75%) with 0.1% trifluoroacetic acid (TFA), followed by concentration in a Speed-Vac.

Tryptic digests were analyzed at the Dana-Farber Cancer Institute Molecular Biology Care Facilities (Boston, MA) on the Waters Corporation (Milford, MA) NanoAcquity UPLC system fitted with a self-packed trap and analytical column setup. They were analyzed by nanoflow HPLC microelectrospray ionization on a LTQ Orbitrap XL (Thermo Scientific, Waltham, MA). Samples are trapped on a self packed fused silica (Polymicro Technologies, Phoenix, AZ) trap-column 100umX, 50mm, packed with Poros 10R2 media (Applied Biosystems Foster City, CA) and subse-

quently eluted on the analytical column. The 75 μm ID x 10 cm self packed fused silica analytical column was slurry packed with Magic C18AQ 200 Å, 5 μm (Michrom BioResources Auburn, CA) using a 420 minute gradient at a flow rate of 200 nL/min. The elution was 1% B for 5 minutes, from 1% to 70% B in 355 minutes, then from 70% to 90% B in 10 minutes, 90% B for 30 minutes then to 1% B in 20 minutes (A is 0.1% formic Acid in water, B is 0.1%formic acid in Acetonitrile, (Burdick and Jackson)). The column outflow is ionized and sprayed into the LTQ Orbitrap by way of a 8 μm SilicaTip (New Objective) and Picoview source (New Objective). Spectra were acquired in a data dependent mode throughout the gradient, a full MS scan in the Orbi-trap analyzer followed by 7 subsequent MS/MS scans in the ion trap based on the seven most intense peaks in the previous full scan. Collision-induced dissociation (CID) fragmentation was achieved by collision energy of 35%, heated capillary was 150° C and electrospray voltage was 1.9 kV. Once an MS/MS spectra was obtained two times it was put on exclusion list for 3 minutes to allow for lower intensity peptides to be analyzed.

All MS data was analyzed using the Mascot algorithm by searching against the updated non-redundant database from NCBI containing mouse only sequences. Initial search parameters included: ESI linear ion-trap scoring parameters, trypsin enzyme specificity with a maximum of two missed cleavages, +/- 20 ppm precursor mass tolerance, +/-0.2 Da product mass tolerance, and carbamidomethylation of cysteines as fixed/mix modifications. Allowed variable modifications were oxidized methionine and pyro-glutamic acid modification at N-terminal glutamine.

4.4.5 Molecular analysis

Antibodies directed against collagens III, VI, biglycan, Msx1, fgf8, Wnt3a, laminin 5, and SPARC were from Abcam.

For silver staining and Periodic acid-Schiff base staining isoalted ECM proteins were resolved on a 4-15% Tris-Glycine Mini-Protean TGX gel (Bio-Rad). Silver staining (Invitrogen) and Periodic acid-Schiff base staining (sigma) was carried out according to the manufacturer's protocols. Fetuin (New England Biolabs) proteoglycan was used as a control, run as both intact and deglycosylated using the Deglycosylation kit (New England Biolabs).

Biglycan siRNA was transfected using Lipfectamine RNAiMAX transfection reagent (Invitrogen) according to the manufacturer's instsructions for reverse transfection. The biglycan siRNA was 5′-AAACCCUUCUGCUCAAAGGGCAAGG-3′ and the control siRNA was All Star non-targeting control (Qiagen). Total RNA was isolated using RNeasy Plus Mini Kit (QIAGEN) and biglycan expression was detected by qRT-PCR. RNA was reverse transcribed into cDNA using a iScript cDNA Synthesis Kit (Bio-Rad) and cDNA was amplified with iTaq SYBR Green Supermix with ROX (Bio-Rad) using the CFX96 real-time PCR system (Bio-Rad). Amplification was carried out using primers shown in Table 4.2.

Table 4.2: Chapter 4 qRT-PCR primers

gene		sequence (5′->3′)
biglycan	F:	GTGTTGCTTCTTCATCTGGCTATG
	R:	ACCTTCCGCTGCGTTACTG
GAPDH	F:	TCTGACGTGCCGCCTGGAG
	R:	TCGCAGGAGACAACCTGGTC

4.4.6 Cell culture

3D cultures of tumor epithelial cells were prepared in gels containing Matrigel (BD Biosciences) and type I collagen (final concentration of 1 mg/ml; BD Biosciences). Epithelial cells (2.75 x 10^4) were resuspended in hydrogel (220 µl) and seeded into

35mm glass bottom dish (MatTek Corporation) for ECM gels. Cultures were maintained for 2 weeks; culture medium was changed every two to three days. Lyophilized ECM solubilized at 100 mg/ml in PBS or commercialized ECM proteins at the concentration described in Table 4.3 was mixed with prepared Matrigel and collagen type I hydrogel to achieve the desired final ECM concentration.

Table 4.3: Protein used for 3D assay

	Supplier	Final Concentration
biglycan	Sigma	5 μ g/mL
SPARC	Abcam	1.33 μ g/mL
Collagen III	Abcam	10 μ g/mL
Collagen VI	Abcam	10 μ g/mL
Tenascin C	Abcam	5 μ g/mL
Fibrillin 1	Abcam	1.33 μ g/mL

4.4.7 Statistical Analysis

Independent samples t-tests were used to compare results, which were considered significant at $p < 0.05$. All results are presented as mean ± standard error of the mean (SEM), unless otherwise specified.

4.5 Full Proteomics Results

Table 4.4: Full Proteomics Results

protein	**MM12.5**	**MM13.5**	**MM14.5**	**CAF**
14-3-3 protein	x	x		
3-beta-hydroxysteroid-δ(8),δ(7)-isomerase				x
3-phosphoshikimate 1-carboxyvinyltransferase		x		
40S ribosomal protein	x	x	x	x

Table 4.4: (continued)

protein	MM12.5	MM13.5	MM14.5	CAF
50S ribosomal protein	x	x		
60S ribosomal protein	x	x		x
ABC transporter G family member 12	x			
acetyl-coenzyme A synthetase			x	
aconitate hydratase	x	x		x
actin	x	x	x	x
adenine deaminase				x
adenylosuccinate synthetase		x		x
ADP/ATP translocase 1	x	x	x	x
alanine racemase			x	
alanyl-tRNA synthetase		x		
aldehyde dehydrogenase				x
aliphatic amidase			x	
alpha actinin	x	x		
alpha-1-antiproteinase		x		
alpha-2-HS-glycoprotein	x	x	x	x
alpha-2-macroglobulin		x		
annexin A2	x	x		
annexin A5		x		
annexin A6				x
apolipoprotein A-I	x			
aquaporin				x
arginine repressor			x	
argininosuccinate lyase		x		
asparaginyl-tRNA synthetase			x	

Table 4.4: (continued)

protein	MM12.5	MM13.5	MM14.5	CAF
aspartate carbamoyltransferase				x
aspartyl/glutamyl-tRNA amidotransferase β			x	
ATP synthase subunit β	x	x	x	x
ATP-dependent RNA helicase		x		
ATP/ADP carrier protein			x	
barrier-to-autointegration factor				x
BM specific HS proteoglycan core protein	x	x	x	x
β-lactam-inducible penicillin-binding protein		x		x
bifuncational HS N-deacetylase/sulfotransferase			x	
bifunctional protein folD		x	x	
biglycan	x	x	x	
calnexin	x	x	x	
calreticulin	x		x	
centromere protein C1				x
centrosomal protein kizuna		x		
ceramide glucosyltransferase-A		x		
chaperonin		x	x	
chloride intracellular channel protein	x			
chorismate synthase	x		x	x
cinA-like protein			x	
clathrin heavy chain 1			x	
coagulation factor	x		x	
cofilin-1	x	x		
collagen α-1 (XV) chain				x
collagen α-1(I) chain	x	x	x	

Table 4.4: (continued)

protein	MM12.5	MM13.5	MM14.5	CAF
collagen α-1(III) chain	x	x	x	
collagen α-1(VI) chain	x	x	x	
collagen α-1(XII) chain	x	x	x	
collagen α-1(XVIII) chain			x	
collagen α-2(I) chain	x	x	x	
collagen α-2(IV) chain	x		x	x
collagen α-3(VI) chain		x		
collagen α-2(VI) chain	x	x	x	
cytoskeleton-associated protein 4	x	x		
cytosolic thyroid binding protein		x		
desmin	x	x		
dihyroorotate dehydrogenase	x	x		
DNA integrity scanning protein disA		x		
DNA polymerase			x	
DNA primase		x		
DNA replication and repair protein recF	x			x
DNA replication licensing factor				x
DNA sythesis and repair		x		
DNA topoisomerase				x
DNA-directed RNA polymerase subunit β	x			
dolichyl-diphosphooligosaccharide	x			x
elongation factor 1-α	x	x	x	x
EMILIN-1	x		x	x
endoplasmin			x	
ER lumen protein retaining recptor 2				x

Table 4.4: (continued)

protein	MM12.5	MM13.5	MM14.5	CAF
error prone DNA polymerase		x		
eukaryotic initiation factor 4A		x	x	x
exodeoxyribonuclease 7 large subunit				x
exportin-2	x	x	x	x
ezrin	x			
F420-dependent NADP reductase		x		
fibrillin-1	x	x	x	
fibronectin	x	x	x	x
fibulin-2	x	x	x	x
filamin-A	x	x	x	
filamin-B	x		x	
folding and unfolding of proteins		x		
galectin-1	x			
gelsolin	x	x		
glial fibrillary acidic protein	x	x		
glutamate racemase		x		
glyceraldehyde-3-phosphate dehydrogenase	x	x	x	x
glycine dehydrogenase		x		
GMP synthase		x	x	
golgin subfamily A member 4	x	x	x	x
GPI ethanolamine phosphate transferase		x		x
GTP-binding protein lepA		x		
guanine nucleotide-binding protein	x			x
heat shock protein	x	x	x	x
hemoglobin fetal subunit	x	x	x	x

Table 4.4: (continued)

protein	MM12.5	MM13.5	MM14.5	CAF
heterogeneous nuclear ribonucleoprotein	x	x		x
high frequency lysogenization protein			x	
high mobility group protein HMGI-C		x		
histidine biosynthesis bifunctional protein hisIE	x	x	x	x
histone	x	x	x	x
holliday junction ATP-dependent DNA helicase				x
indoethylamine N-methyltransferase				x
isocitrate dehydrogenase [NAD] subunit α	x			
ISWI one complex protein 3		x		
kunitz-type serine protease inhibitor BvKI			x	
L-fucose isomerase			x	
lamin-A/C	x	x		
laminin subumit γ-1				x
laminin subunit α-5				x
large T antigen				x
lipid A export ATP-binding protein msbA	x	x		
lipoprotein		x		
lipoyl synthase		x		
macrolide export ATP-binding protein		x		
major vault protein			x	
malate dehydrogenase		x	x	
mediator of RNA polymerase II transcription	x			x
metalloproteinase inhibitor 3		x		
mitochondrial carrier homolog				x
mitochondrial substrate carrier protein		x		

Table 4.4: (continued)

protein	MM12.5	MM13.5	MM14.5	CAF
myosin	x	x	x	x
myosin regulatory light chain 2	x	x	x	x
NAD-dependent deacetylase sirtuin-2		x		
NADH dehhydrogenase 1 α subcomplex 4				x
NADP-dependent dehydrogenase				x
NADPH oxidase organizer 1	x			
nascent polypeptide-associate complex β	x			
neprilysin				x
nidogen-2			x	x
nodulation protein nolF	x			
nucleolar transcription factor 1-A				x
nusA protein homolog			x	
oligopeptide-binding protein AmiA			x	
oligosaccharyltransferase complex OSTC	x			
pantothenate kinase		x		
peptide-N-(4-acetyl-β-D-glucosaminyl) amidase	x	x	x	x
peptidyl-prolyl cis-trans isomerase A	x	x		
periostin	x	x	x	x
peroxiredoxin-1	x			
peroxisomal Ion protease homolog 2				x
phosphate carrier protein				x
phosphoenolpyruvate carboxykinase	x			
phosphoglycerate kinase			x	
phosphoribosylaminoimidazole-succinocarboxamide			x	
plasticin				x

Table 4.4: (continued)

protein	MM12.5	MM13.5	MM14.5	CAF
plectin-1	x			
polyribonucleotide nucleotidyltransferase		x		x
pre-mRNA-splicing factor SYF1	x	x	x	
protaglandin E synthase 3				x
protease-1	x	x	x	x
protein disulfide-isomerase A3	x			
protein lava lamp	x	x	x	x
protein S100-A4 or 6	x	x	x	x
protein traJ			x	
protein translocase subunit secA		x	x	
protein-glutamine gamma-glutamyltransferase				x
protocadherin-like wing polarity protein stan			x	
putative pentatricopeptide protein	x			
pyrimidine biosynthesis		x		
pyruvate kinase muscle isozyme	x		x	
quinolinate synthase A		x		
ras-related protein Rab		x		x
ribose import ATP-binding protein RbsA 2			x	
ribose-phosphate pyrophosphokinase		x	x	
ribosomal RNA large methyltransferase				x
ribosomal RNA small methyltransferase		x		
ribosome-binding protein 1	x			
RNA exonuclease 4	x			
RNA polymerase sigma factor rpoD1			x	
serine protase HTRA1			x	

Table 4.4: (continued)

protein	MM12.5	MM13.5	MM14.5	CAF
serine protease 23	x	x	x	
serine/arginine repetitive matrix protein 2				x
serine/threonine-protein kinase Nek10	x	x	x	x
serpin H1	x	x	x	
sorbin and SH3 domain-containing protein 1			x	
SPARC	x	x	x	
splicing factor, arginine/serine-rich 3	x			
succinyl-CoA ligase				x
succinyl-CoA ligase	x	x	x	
tenascin	x	x	x	
thrombospondin-1	x	x	x	
thromobospondin-2		x		
thy-1 membrane glycoprotein		x		
thymidylate synthase	x		x	
toxin coregulated pilus biosynthesis protein E		x		
transgelin		x		
transmembrane protein 43	x			x
tRNA dimethylallyltransferase	x	x	x	
tRNA modification GTPase	x			
tRNA pseudouridine synthase D	x			
tropomodulin	x			
tropomyosin α	x	x		
trypsin	x	x	x	x
tubulin	x	x	x	x
tubulointerstitial nephritis			x	x

Table 4.4: (continued)

protein	MM12.5	MM13.5	MM14.5	CAF
ubiquitin	x	x		x
UBX domain-containing protein 3			x	
ventricular zone-express pH domain				x
versican core protein			x	
vimentin	x	x	x	x
vitronectin	x	x	x	x
voltage-dependent anion channel protein	x	x	x	x
zinc finger protein 429		x		

4.6 Acknowledgements

Ashley G. Bischof designed the study, performed experiments, analyzed data, and wrote the chapter. Deniz Yuksel assisted in performing the three dimensional culture experiments and carried out the SDS-PAGE gel analysis for carbohydrates. Silva Krause and Amy Brock supplied microarray data from the C3(1) SV40 Tag transgenic mice. Donald E. Ingber supervised the work and revised the manuscript.

This work was supported by a Department of Defense Breast Cancer Innovator Award (BC074986 to DEI). AFM studies were performed at the Center for Nanoscale Systems (CNS), a member of the National Nanotechnology Infrastructure Network (NNIN), which is supported by the National Science Foundation under NSF award no. ECS-0335765. CNS is part of the Faculty of Arts and Sciences at Harvard University. LC-MS/MS studies were carried out by James Lee at the Dana Farber Cancer Institute Molecular Biology Core Facilities.

5
Discussion

PROVOCATIVE experiments first carried out 40 years ago showed that certain cancers differentiate and normalize their growth when combined with normal mesenchyme or other embryonic tissues [1–4, 108, 109, 114–117]. Most researchers who know of the ability of embryonic tissues to induce cancer reversion assume that it is due to production of critical molecular morphogens or a change in gene activity. However, previous results have shown that tumor progression could be promoted or accelerated by altering the mechanics or structure of the ECM [5, 188, 193, 210], or by chemically altering the connective tissue stroma [87], suggesting that physical cues conveyed by the stroma may be equally important.

In this thesis I sought to elucidate the mechanism by which embryonic mesenchyme normalizes tumor cell behavior. We hypothesized that because insoluble ECM plays a dominant role in organ development in the embryo, this could translate to regulation

of mesenchymal cell induced normalization of tumor cells. To test this hypothesis, I isolated cell-derived ECM from embryonic mesenchyme and repopulated the matrix with tumor cells in 2D and 3D culture, assessing changes in cell organization and cell fate. Using this approach I found that the insoluble components, isolated using detergent extraction, were sufficient to induce tumor cell normalization to the same extent as live mesenchymal cells in co-culture. Tumor cells in 2D and 3D culture with mesenchymal ECM decreased their growth and increased expression of ERα. Mesenchymal ECM was also able to increase formation of hollow lumen structures in 3D culture, whereas co-culture with CAF cells or ECM had no affect. The versatility of these result was confirmed using multiple tumor cell lines isolated from different stages of tumor progression within the C3(1) SV40 T-antigen transgenic mouse model (M28: DCIS, M6: solid tumor, M6C: metastatic), another aggressive mammary tumor cell isolated from mice (4T1) as well as human breast cancer cells (MCF7). Further, injection of the embryonic ECM into fast growing mammary tumors significantly slowed tumor growth.

The goal of chapter 4 of this work was to determine which features of the embryonic ECM are required to induce tumor cell normalization. First, we were able to show that the efficacy of tumor cell normalization drops significantly for mesenchyme isolated at E14.5 compared to early stage mesenchyme isolated from either the mammary bud or the tooth germ. Then by comparing biochemical and mechanical properties of the ECM from four different embryonic mesenchymal cells and adult CAFs we were able to identify features which were specific to the embryonic ECMs. Specifically, AFM measurements revealed that the Young's modulus of inductive ECMs was significantly less than either MM14.5 or CAF ECM. However, more experiments are required to understand whether these differences in matrix compliance are playing a role in tumor normalization. Using proteomics analysis we were able to identify eleven proteins,

which were specific to embryonic matrices. Three of these proteins were shown to have the capacity to induce lumen formation in 3D culture, Collagen III, biglycan, and SPARC. However, it remains unclear how these three proteins act on the tumor cells to induce differentiation.

Collagen III is a fibrillar collagen found extensively in connective tissue, and it has been shown to be overexpressed in some breast tumors [94]. Collagen III expression is also increased in the stroma, particularly the adipose tissue, of mammary glands following irradiation treatments, which ultimately lead to tumor formation within the adjacent epithelium [211, 212]. However, the role of collagen III in breast cancer remains unclear. During embryonic morphogenesis collagen III is expressed in the clefts of branching organs. At the clefts, collagen III is thought to provide a rigid support to stabilize the structure and prevent continued growth and invasion [207]. Thus, collagen III may have different roles depending on the tissue context. Interestingly, both biglycan and SPARC have been shown to bind to collagen III, regulating fibrillogenesis, matrix remodeling and cell-matrix interactions [202, 208, 209].

SPARC has been implicated in regulation of epithelial and adipocyte cell behavior. SPARC-null mice develop age-related abnormalities due to unusual differentiation of epithelial cells as well as increased accumulation of white adipose tissue. The ECM remodeling associated with adipogenesis requires SPARC [213]. SPARC likely influences the expression, folding, post-translational modification, and secretion of collagens in white adipose tissue such as collagens VI and III, both found to be highly expressed in embryonic ECM. Further, SPARC has also been previously suggested as a tumor-suppressor [36], as it has been shown to inhibit cell adhesion and cell cycle progression [214–216]. Thus SPARC could be acting to regulate tumor cell behavior directly or through interaction with collagens. However, more studies would be required to fully understand the role of each of these proteins in mammary tumor

cell normalization.

5.1 Limitations

The findings presented in this thesis lend support to the idea that differentiation therapy could be a viable treatment option for solid tumors. However, these studies did not analyze whether continuous contact with embryonic ECM is required for tumor cell normalization and to what extent the differentiation is reversible. Extensive degradation and remodeling of ECM is a hallmark of tumors [217], suggesting that ECM introduced to the tumor microenvironment would not last long. Our *in vivo* studies required repeated injection of embryonic ECM in order to achieve continued suppression of tumor growth. Further, studies described in this thesis were carried out for only two weeks *in vitro* and ten days *in vivo*, leaving us to only speculate regarding the long term affects of this treatment on tumor cells. Previous reports show that tumor cells injected into the blastocyst can take part in normal development [108], and ultimately can be part of a variety of tissues in cancer-free adult mice [109]. But it will be critical to carry out long-term studies both *in vitro* and *in vivo* using multiple tumor models in order to determine the reversibility of the differentiation induced by mesenchymal ECM specifically.

While we tested the efficacy of embryonic ECM on a number of different mouse tumors and one human tumor cell line *in vitro* the generality of this approach remains unclear. One of the hardest human breast cancers to treat are aggressive triple-negative (ERα, PR, Her2/neu) tumors. Preliminary studies to evaluate more aggressive human breast cancer cell lines were inconclusive; some aggressive breast cancer lines (SKBR3, MDA-MB-231) fail to form spheroids in 3D culture, making traditional lumen formation analysis impossible. Further, *in vivo* studies were only carried out

with a highly aggressive and metastatic mouse mammary tumor cell (4T1). While embryonic ECM was able to slow progression of these tumors it could not induce full differentiation of the cells. In order to evaluate differentiation of more physiologically relevant tumors *in vivo* studies could be carried out using human breast cancer cells or early stage tumors in transgenic mice.

5.2 Tissue engineering approach to tumor therapy

It has become widely accepted that cancer is an irreversible and deadly disease that results from an accumulation of genetic mutations. This view has led to the use of toxic therapies that aim to completely eradicate all cancer cells, but which have significant side effects and often cause high morbidity in patients. However, it has long been suggested that malignant cells could differentiate into non-malignant cells by re-activating endogenous differentiation programs [3, 218]. Differentiation therapy is an attractive option theoretically, but it has been difficult not only due to our lack of understanding of differentiation pathways, but also our inability to envision a methodology that could restore or supersede a tumor's immutable genetic level mutations. However, over the past 50 years of treating patients it has become clear that conventional approaches are not sufficient in a significant proportion of cancer patients. According to projections from the American Cancer Society this year more than 500,000 Americans will die of cancer, accounting for one in four deaths in the United States [219]. Further, while the 5-year survival rate for patients diagnosed with cancer in the last ten years is 66%, up from 50% in the 1970s, this still means that one out of every three patients diagnosed with cancer will not be alive in five years [219]. Clearly there is reason to pursue all potential therapeutic options.

The promise of differentiation therapy is best characterized by the addition of

retinoids in the treatment of acute promyelocytic leukemia (APML). In most patients, APML cells have a chromosomal translocation that produces a fusion gene consisting of the promyelocytic leukemia (PML) and retinoic acid receptor α (RARα). PML-RARα plays a key role in pathogenesis by recruiting histone deacetylases (HDACs) and DNA methyltransferases. By treating with retinoids PML-RARα-HDAC complexes are triggered to dissociate, resulting in degradation of PML-RARα and differentiation of APML cells [220]. Prior to retinoic acid-based differentiation therapy the remission rates of APML progressively improved from 50 to 80%, of which only about 35% could expect long-term survival. However, now with the use of retinoic acid and chemotherapy more than 90% of patients achieve complete remission and about 75% can be cured [221–224]. However, APML is often posited as a simple case; the disease is addicted to the fusion gene and has minimal additional genetic abnormalities. The application of differentiation therapies for solid tumors has been more complicated.

Currently there are four primary modalities for cancer therapy: surgery, radiation, molecular inhibitors (drugs), and anti-angiogenesis therapy. And investigation of differentiation-based therapies has centered around identifying druggable differentiation pathways [225]. However, the finding that insoluble matrix can induce normalization of tumor epithelium suggests that there is another possibility; biomaterials and scaffolds currently used for tissue engineering applications could also be used for cancer therapy [184]. These materials would need to be carefully designed to mimic all structural, adhesive, molecular, chemical, and mechanical properties that embryonic tissues convey to induce cancer reversal. The findings presented in this thesis are a step in this direction.

While the adoption of a differentiation-based therapy may seem like a consolation with the current view of cancer, the potential for reversion of the malignant cancer phenotype to a more benign, or at least a lower grade of biologic aggressiveness, may

serve as a critical clinical transition. A once fatal cancer could be shifted into one which is more amenable to management or treatment. For example, expression of ERα is a key determinant in human breast cancer; many of our current therapies rely on estrogen responsiveness for treatment. Thus by reexpressing ERα in mammary tumor cells using embryonic ECM we may be opening the door for use of endocrine therapies. Importantly, for differentiation therapy to be successful it does not need to eliminate all cancer cells or even differentiation them all to 'normal,' even a change in pathological status accomplished using differentiation therapy could change the prognosis of patients with cancer by decades.

Bibliography

[1] J. J. DeCosse, C. L. Gossens, J. F. Kuzma, and B. R. Unsworth, "Breast cancer: induction of differentiation by embryonic tissue," *Science*, vol. 181, no. 104, pp. 1057–8, 1973.

[2] G. R. Cunha, H. Fujii, B. L. Neubauer, J. M. Shannon, L. Sawyer, and B. A. Reese, "Epithelial-mesenchymal interactions in prostatic development. i. morphological observations of prostatic induction by urogenital sinus mesenchyme in epithelium of the adult rodent urinary bladder," *J Cell Biol*, vol. 96, no. 6, pp. 1662–70, 1983.

[3] G. B. Pierce and C. Wallace, "Differentiation of malignant to benign cells," *Cancer Res*, vol. 31, no. 2, pp. 127–34, 1971.

[4] Y. C. Wong, G. R. Cunha, and N. Hayashi, "Effects of mesenchyme of the embryonic urogenital sinus and neonatal seminal vesicle on the cytodifferentiation of the dunning tumor: ultrastructural study," *Acta Anat (Basel)*, vol. 143, no. 2, pp. 139–50, 1992.

[5] D. E. Ingber, J. A. Madri, and J. D. Jamieson, "Role of basal lamina in neoplastic disorganization of tissue architecture," *Proc Natl Acad Sci U S A*, vol. 78, no. 6, pp. 3901–5, 1981.

[6] D. E. Ingber, J. A. Madri, and J. D. Jamieson, "Basement membrane as a spatial organizer of polarized epithelia. exogenous basement membrane reorients pancreatic epithelial tumor cells in vitro," *Am J Pathol*, vol. 122, no. 1, pp. 129–39, 1986.

[7] P. A. Kenny and M. J. Bissell, "Tumor reversion: correction of malignant behavior by microenvironmental cues," *Int J Cancer*, vol. 107, no. 5, pp. 688–95, 2003.

[8] T. K. Watanabe, L. J. Hansen, N. K. Reddy, Y. S. Kanwar, and J. K. Reddy, "Differentiation of pancreatic acinar carcinoma cells cultured on rat testicular seminiferous tubular basement membranes," *Cancer Res*, vol. 44, no. 11, pp. 5361–8, 1984.

[9] K. R. Levental, H. Yu, L. Kass, J. N. Lakins, M. Egeblad, J. T. Erler, S. F. Fong, K. Csiszar, A. Giaccia, W. Weninger, M. Yamauchi, D. L. Gasser, and V. M. Weaver, "Matrix crosslinking forces tumor progression by enhancing integrin signaling," *Cell*, vol. 139, no. 5, pp. 891–906, 2009.

[10] S. C. Li, G. F. Chen, P. S. Chan, H. L. Choi, S. M. Ho, and F. L. Chan, "Altered expression of extracellular matrix and proteinases in noble rat prostate gland after long-term treatment with sex steroids," *Prostate*, vol. 49, no. 1, pp. 58–71, 2001.

[11] S. Lu, M. Huang, Y. Kobayashi, A. Komiyama, X. Li, R. Katoh, and A. Kawaoi, "Alterations of basement membrane in di-isopropanolnitrosamine-induced carcinogenesis of the rat thyroid gland: an immunohistochemical study," *Virchows Arch*, vol. 436, no. 6, pp. 595–601, 2000.

[12] F. Guilak, D. M. Cohen, B. T. Estes, J. M. Gimble, W. Liedtke, and C. S. Chen, "Control of stem cell fate by physical interactions with the extracellular matrix," *Stem Cell*, vol. 5, no. 1, pp. 17–26, 2009.

[13] P. J. Keely, "Mechanisms by which the extracellular matrix and integrin signaling act to regulate the switch between tumor suppression and tumor promotion," *J Mammary Gland Biol Neoplasia*, vol. 16, no. 3, pp. 205–19, 2011.

[14] T. Rozario and D. W. DeSimone, "The extracellular matrix in development and morphogenesis: a dynamic view," *Dev Biol*, vol. 341, no. 1, pp. 126–40, 2010.

[15] C. M. Kielty, C. Baldock, D. Lee, M. J. Rock, J. L. Ashworth, and C. A. Shuttleworth, "Fibrillin: from microfibril assembly to biomechanical function," *Philos Trans R Soc Lond B Biol Sci*, vol. 357, no. 1418, pp. 207–17, 2002.

[16] E. Ruoslahti, "Fibronectin and its receptors," *Annu Rev Biochem*, vol. 57, pp. 375–413, 1988.

[17] C. M. Lo, H. B. Wang, M. Dembo, and Y. L. Wang, "Cell movement is guided by the rigidity of the substrate," *Biophys J*, vol. 79, no. 1, pp. 144–52, 2000.

[18] M. R. Ng, A. Besser, G. Danuser, and J. S. Brugge, "Substrate stiffness regulates cadherin-dependent collective migration through myosin-ii contractility," *J Cell Biol*, vol. 199, no. 3, pp. 545–63, 2012.

[19] J. Pelham, R. J. and Y. Wang, "Cell locomotion and focal adhesions are regulated by substrate flexibility," *Proc Natl Acad Sci U S A*, vol. 94, no. 25, pp. 13661–5, 1997.

[20] C. S. Chen, M. Mrksich, S. Huang, G. M. Whitesides, and D. E. Ingber, "Geometric control of cell life and death," *Science*, vol. 276, no. 5317, pp. 1425–8, 1997.

[21] L. E. Dike, C. S. Chen, M. Mrksich, J. Tien, G. M. Whitesides, and D. E. Ingber, "Geometric control of switching between growth, apoptosis, and differentiation during angiogenesis using micropatterned substrates," *In Vitro Cell Dev Biol Anim*, vol. 35, no. 8, pp. 441–8, 1999.

[22] A. J. Engler, S. Sen, H. L. Sweeney, and D. E. Discher, "Matrix elasticity directs stem cell lineage specification," *Cell*, vol. 126, no. 4, pp. 677–89, 2006.

[23] M. C. Brown, L. A. Cary, J. S. Jamieson, J. A. Cooper, and C. E. Turner, "Src and fak kinases cooperate to phosphorylate paxillin kinase linker, stimulate its focal adhesion localization, and regulate cell spreading and protrusiveness," *Mol Biol Cell*, vol. 16, no. 9, pp. 4316–28, 2005.

[24] S. K. Hanks, M. B. Calalb, M. C. Harper, and S. K. Patel, "Focal adhesion protein-tyrosine kinase phosphorylated in response to cell attachment to fibronectin," *Proc Natl Acad Sci U S A*, vol. 89, no. 18, pp. 8487–91, 1992.

[25] C. K. Thodeti, B. Matthews, A. Ravi, A. Mammoto, K. Ghosh, A. L. Bracha, and D. E. Ingber, "Trpv4 channels mediate cyclic strain-induced endothelial cell reorientation through integrin-to-integrin signaling," *Circ Res*, vol. 104, no. 9, pp. 1123–30, 2009.

[26] C. A. Kirkpatrick, B. D. Dimitroff, J. M. Rawson, and S. B. Selleck, "Spatial regulation of wingless morphogen distribution and signaling by dally-like protein," *Dev Cell*, vol. 7, no. 4, pp. 513–23, 2004.

[27] J. Kreuger, L. Perez, A. J. Giraldez, and S. M. Cohen, "Opposing activities of dally-like glypican at high and low levels of wingless morphogen activity," *Dev Cell*, vol. 7, no. 4, pp. 503–12, 2004.

[28] M. K. Gordon and R. A. Hahn, "Collagens," *Cell Tissue Res*, vol. 339, no. 1, pp. 247–57, 2010.

[29] B. P. Toole, "Hyaluronan in morphogenesis," *Semin Cell Dev Biol*, vol. 12, no. 2, pp. 79–87, 2001.

[30] P. Bianco, L. W. Fisher, M. F. Young, J. D. Termine, and P. G. Robey, "Expression and localization of the two small proteoglycans biglycan and decorin in developing human skeletal and non-skeletal tissues," *J Histochem Cytochem*, vol. 38, no. 11, pp. 1549–63, 1990.

[31] P. Bornstein and E. H. Sage, "Matricellular proteins: extracellular modulators of cell function," *Curr Opin Cell Biol*, vol. 14, no. 5, pp. 608–16, 2002.

[32] T. R. Kyriakides and P. Bornstein, "Matricellular proteins as modulators of wound healing and the foreign body response," *Thromb Haemost*, vol. 90, no. 6, pp. 986–92, 2003.

[33] P. Maurer, W. Gohring, T. Sasaki, K. Mann, R. Timpl, and R. Nischt, "Recombinant and tissue-derived mouse bm-40 bind to several collagen types and have increased affinities after proteolytic activation," *Cell Mol Life Sci*, vol. 53, no. 5, pp. 478–84, 1997.

[34] J. E. Murphy-Ullrich, T. F. Lane, M. A. Pallero, and E. H. Sage, "Sparc mediates focal adhesion disassembly in endothelial cells through a follistatin-like region and the ca(2+)-binding ef-hand," *J Cell Biochem*, vol. 57, no. 2, pp. 341–50, 1995.

[35] H. Sage, J. Tupper, and R. Bramson, "Endothelial cell injury in vitro is associated with increased secretion of an mr 43,000 glycoprotein ligand," *J Cell Physiol*, vol. 127, no. 3, pp. 373–87, 1986.

[36] G. P. Nagaraju and D. Sharma, "Anti-cancer role of sparc, an inhibitor of adipogenesis," *Cancer Treat Rev*, vol. 37, no. 7, pp. 559–66, 2011.

[37] E. Ruoslahti, "Rgd and other recognition sequences for integrins," *Annu Rev Cell Dev Biol*, vol. 12, pp. 697–715, 1996.

[38] S. S. Lee, V. Knott, J. Jovanovic, K. Harlos, J. M. Grimes, L. Choulier, H. J. Mardon, D. I. Stuart, and P. A. Handford, "Structure of the integrin binding fragment from fibrillin-1 gives new insights into microfibril organization," *Structure*, vol. 12, no. 4, pp. 717–29, 2004.

[39] V. N. Patel, S. M. Knox, K. M. Likar, C. A. Lathrop, R. Hossain, S. Eftekhari, J. M. Whitelock, M. Elkin, I. Vlodavsky, and M. P. Hoffman, "Heparanase cleavage of perlecan heparan sulfate modulates fgf10 activity during ex vivo submandibular gland branching morphogenesis," *Development*, vol. 134, no. 23, pp. 4177–86, 2007.

[40] E. Zcharia, R. Zilka, A. Yaar, O. Yacoby-Zeevi, A. Zetser, S. Metzger, R. Sarid, A. Naggi, B. Casu, N. Ilan, I. Vlodavsky, and R. Abramovitch, "Heparanase accelerates wound angiogenesis and wound healing in mouse and rat models," *FASEB J*, vol. 19, no. 2, pp. 211–21, 2005.

[41] J. I. Lopez, I. Kang, W. K. You, D. M. McDonald, and V. M. Weaver, "In situ force mapping of mammary gland transformation," *Integr Biol (Camb)*, vol. 3, no. 9, pp. 910–21, 2011.

[42] M. Dembo and Y. L. Wang, "Stresses at the cell-to-substrate interface during locomotion of fibroblasts," *Biophys J*, vol. 76, no. 4, pp. 2307–16, 1999.

[43] A. Mammoto, T. Mammoto, and D. E. Ingber, "Mechanosensitive mechanisms in transcriptional regulation," *J Cell Sci*, vol. 125, no. Pt 13, pp. 3061–73, 2012.

[44] D. E. Ingber, "Cellular mechanotransduction: putting all the pieces together again," *FASEB J*, vol. 20, no. 7, pp. 811–27, 2006.

[45] A. W. Orr, B. P. Helmke, B. R. Blackman, and M. A. Schwartz, "Mechanisms of mechanotransduction," *Dev Cell*, vol. 10, no. 1, pp. 11–20, 2006.

[46] B. D. Matthews, C. K. Thodeti, J. D. Tytell, A. Mammoto, D. R. Overby, and D. E. Ingber, "Ultra-rapid activation of trpv4 ion channels by mechanical forces applied to cell surface beta1 integrins," *Integr Biol (Camb)*, vol. 2, no. 9, pp. 435–42, 2010.

[47] A. Mammoto, S. Huang, and D. E. Ingber, "Filamin links cell shape and cytoskeletal structure to rho regulation by controlling accumulation of p190rhogap in lipid rafts," *J Cell Sci*, vol. 120, no. Pt 3, pp. 456–67, 2007.

[48] X. H. Zhao, C. Laschinger, P. Arora, K. Szaszi, A. Kapus, and C. A. McCulloch, "Force activates smooth muscle alpha-actin promoter activity through the rho signaling pathway," *J Cell Sci*, vol. 120, no. Pt 10, pp. 1801–9, 2007.

[49] F. J. Alenghat, J. D. Tytell, C. K. Thodeti, A. Derrien, and D. E. Ingber, "Mechanical control of camp signaling through integrins is mediated by the heterotrimeric galphas protein," *J Cell Biochem*, vol. 106, no. 4, pp. 529–38, 2009.

[50] J. L. Balligand, O. Feron, and C. Dessy, "enos activation by physical forces: from short-term regulation of contraction to chronic remodeling of cardiovascular tissues," *Physiol Rev*, vol. 89, no. 2, pp. 481–534, 2009.

[51] M. L. Mikkola, "Genetic basis of skin appendage development," *Semin Cell Dev Biol*, vol. 18, no. 2, pp. 225–36, 2007.

[52] J. Jernvall and I. Thesleff, "Reiterative signaling and patterning during mammalian tooth morphogenesis," *Mech Dev*, vol. 92, no. 1, pp. 19–29, 2000.

[53] E. J. Kollar and G. R. Baird, "Tissue interactions in embryonic mouse tooth germs. ii. the inductive role of the dental papilla," *J Embryol Exp Morphol*, vol. 24, no. 1, pp. 173–86, 1970.

[54] A. G. Lumsden, "Spatial organization of the epithelium and the role of neural crest cells in the initiation of the mammalian tooth germ," *Development*, vol. 103 Suppl, pp. 155–69, 1988.

[55] M. Mina and E. J. Kollar, "The induction of odontogenesis in non-dental mesenchyme combined with early murine mandibular arch epithelium," *Arch Oral Biol*, vol. 32, no. 2, pp. 123–7, 1987.

[56] C. Grobstein, "Mechanisms of organogenetic tissue interaction," *Natl Cancer Inst Monogr*, vol. 26, pp. 279–99, 1967.

[57] I. Thesleff, A. Vaahtokari, P. Kettunen, and T. Aberg, "Epithelial-mesenchymal signaling during tooth development," *Connect Tissue Res*, vol. 32, no. 1-4, pp. 9–15, 1995.

[58] T. Mammoto, A. Mammoto, Y. S. Torisawa, T. Tat, A. Gibbs, R. Derda, R. Mannix, M. de Bruijn, C. W. Yung, D. Huh, and D. E. Ingber, "Mechanochemical control of mesenchymal condensation and embryonic tooth organ formation," *Dev Cell*, vol. 21, no. 4, pp. 758–69, 2011.

[59] M. D. Sternlicht, "Key stages in mammary gland development: the cues that regulate ductal branching morphogenesis," *Breast Cancer Res*, vol. 8, no. 1, p. 201, 2006.

[60] P. Schedin, T. Mitrenga, S. McDaniel, and M. Kaeck, "Mammary ecm composition and function are altered by reproductive state," *Mol Carcinog*, vol. 41, no. 4, pp. 207–20, 2004.

[61] J. M. Veltmaat, A. A. Mailleux, J. P. Thiery, and S. Bellusci, "Mouse embryonic mammogenesis as a model for the molecular regulation of pattern formation," *Differentiation*, vol. 71, no. 1, pp. 1–17, 2003.

[62] C. J. Watson and W. T. Khaled, "Mammary development in the embryo and adult: a journey of morphogenesis and commitment," *Development*, vol. 135, no. 6, pp. 995–1003, 2008.

[63] A. Propper and L. Gomot, "[tissue interactions during organogenesis of the mammary gland in the rabbit embryo]," *C R Acad Sci Hebd Seances Acad Sci D*, vol. 264, no. 22, pp. 2573–5, 1967.

[64] A. Propper and L. Gomot, "Control of chick epidermis differentiation by rabbit mammary mesenchyme," *Experientia*, vol. 29, no. 12, pp. 1543–4, 1973.

[65] G. R. Cunha, P. Young, K. Christov, R. Guzman, S. Nandi, F. Talamantes, and G. Thordarson, "Mammary phenotypic expression induced in epidermal cells by embryonic mammary mesenchyme," *Acta Anat (Basel)*, vol. 152, no. 3, pp. 195–204, 1995.

[66] T. Sakakura, Y. Nishizuka, and C. J. Dawe, "Mesenchyme-dependent morphogenesis and epithelium-specific cytodifferentiation in mouse mammary gland," *Science*, vol. 194, no. 4272, pp. 1439–41, 1976.

[67] T. Sakakura, I. Kusano, M. Kusakabe, Y. Inaguma, and Y. Nishizuka, "Biology of mammary fat pad in fetal mouse: capacity to support development of various fetal epithelia in vivo," *Development*, vol. 100, no. 3, pp. 421–30, 1987.

[68] T. Sakakura, Y. Sakagami, and Y. Nishizuka, "Dual origin of mesenchymal tissues participating in mouse mammary gland embryogenesis," *Dev Biol*, vol. 91, no. 1, pp. 202–7, 1982.

[69] K. Kimata, T. Sakakura, Y. Inaguma, M. Kato, and Y. Nishizuka, "Participation of two different mesenchymes in the developing mouse mammary gland: synthesis of basement membrane components by fat pad precursor cells," *J Embryol Exp Morphol*, vol. 89, pp. 243–57, 1985.

[70] V. N. Patel, I. T. Rebustini, and M. P. Hoffman, "Salivary gland branching morphogenesis," *Differentiation*, vol. 74, no. 7, pp. 349–64, 2006.

[71] J. E. Fata, Z. Werb, and M. J. Bissell, "Regulation of mammary gland branching morphogenesis by the extracellular matrix and its remodeling enzymes," *Breast Cancer Res*, vol. 6, no. 1, pp. 1–11, 2004.

[72] G. B. Silberstein, P. Strickland, S. Coleman, and C. W. Daniel, "Epithelium-dependent extracellular matrix synthesis in transforming growth factor-beta 1-growth-inhibited mouse mammary gland," *J Cell Biol*, vol. 110, no. 6, pp. 2209–19, 1990.

[73] M. S. Wicha, L. A. Liotta, B. K. Vonderhaar, and W. R. Kidwell, "Effects of inhibition of basement membrane collagen deposition on rat mammary gland development," *Dev Biol*, vol. 80, no. 2, pp. 253–6, 1980.

[74] G. B. Silberstein and C. W. Daniel, "Glycosaminoglycans in the basal lamina and extracellular matrix of the developing mouse mammary duct," *Dev Biol*, vol. 90, no. 1, pp. 215–22, 1982.

[75] D. Alford, D. Baeckstrom, M. Geyp, P. Pitha, and J. Taylor-Papadimitriou, "Integrin-matrix interactions affect the form of the structures developing from

human mammary epithelial cells in collagen or fibrin gels," *J Cell Sci*, vol. 111 (Pt 4), pp. 521–32, 1998.

[76] L. Hinck and G. B. Silberstein, "Key stages in mammary gland development: the mammary end bud as a motile organ," *Breast Cancer Res*, vol. 7, no. 6, pp. 245–51, 2005.

[77] W. F. Vogel, A. Aszodi, F. Alves, and T. Pawson, "Discoidin domain receptor 1 tyrosine kinase has an essential role in mammary gland development," *Molecular and cellular biology*, vol. 21, no. 8, pp. 2906–17, 2001.

[78] Y. S. Kanwar, J. Wada, S. Lin, F. R. Danesh, S. S. Chugh, Q. Yang, T. Banerjee, and J. W. Lomasney, "Update of extracellular matrix, its receptors, and cell adhesion molecules in mammalian nephrogenesis," *Am J Physiol Renal Physiol*, vol. 286, no. 2, pp. F202–15, 2004.

[79] F. Berdichevsky, D. Alford, B. D'Souza, and J. Taylor-Papadimitriou, "Branching morphogenesis of human mammary epithelial cells in collagen gels," *J Cell Sci*, vol. 107 (Pt 12), pp. 3557–68, 1994.

[80] S. Stahl, S. Weitzman, and J. C. Jones, "The role of laminin-5 and its receptors in mammary epithelial cell branching morphogenesis," *J Cell Sci*, vol. 110 (Pt 1), pp. 55–63, 1997.

[81] K. A. Moore, T. Polte, S. Huang, B. Shi, E. Alsberg, M. E. Sunday, and D. E. Ingber, "Control of basement membrane remodeling and epithelial branching morphogenesis in embryonic lung by rho and cytoskeletal tension," *Dev Dyn*, vol. 232, no. 2, pp. 268–81, 2005.

[82] D. E. Ingber, J. A. Madri, and J. D. Jamieson, "Neoplastic disorganization of pancreatic epithelial cell-cell relations. role of basement membrane," *Am J Pathol*, vol. 121, no. 2, pp. 248–60, 1985.

[83] M. J. Bissell and D. Radisky, "Putting tumours in context," *Nat Rev Cancer*, vol. 1, no. 1, pp. 46–54, 2001.

[84] S. W. Hayward, G. D. Grossfeld, T. D. Tlsty, and G. R. Cunha, "Genetic and epigenetic influences in prostatic carcinogenesis (review)," *Int J Oncol*, vol. 13, no. 1, pp. 35–47, 1998.

[85] L. Ronnov-Jessen, O. W. Petersen, and M. J. Bissell, "Cellular changes involved in conversion of normal to malignant breast: importance of the stromal reaction," *Physiol Rev*, vol. 76, no. 1, pp. 69–125, 1996.

[86] M. H. Barcellos-Hoff and S. A. Ravani, "Irradiated mammary gland stroma promotes the expression of tumorigenic potential by unirradiated epithelial cells," *Cancer Res*, vol. 60, no. 5, pp. 1254–60, 2000.

[87] M. V. Maffini, A. M. Soto, J. M. Calabro, A. A. Ucci, and C. Sonnenschein, "The stroma as a crucial target in rat mammary gland carcinogenesis," *J Cell Sci*, vol. 117, no. Pt 8, pp. 1495–502, 2004.

[88] A. F. Olumi, G. D. Grossfeld, S. W. Hayward, P. R. Carroll, T. D. Tlsty, and G. R. Cunha, "Carcinoma-associated fibroblasts direct tumor progression of initiated human prostatic epithelium," *Cancer Res*, vol. 59, no. 19, pp. 5002–11, 1999.

[89] A. Orimo, P. B. Gupta, D. C. Sgroi, F. Arenzana-Seisdedos, T. Delaunay, R. Naeem, V. J. Carey, A. L. Richardson, and R. A. Weinberg, "Stromal fibroblasts present in invasive human breast carcinomas promote tumor growth and angiogenesis through elevated sdf-1/cxcl12 secretion," *Cell*, vol. 121, no. 3, pp. 335–48, 2005.

[90] A. P. Sappino, W. Schurch, and G. Gabbiani, "Differentiation repertoire of fibroblastic cells: expression of cytoskeletal proteins as marker of phenotypic modulations," *Lab Invest*, vol. 63, no. 2, pp. 144–61, 1990.

[91] R. A. Willis, "The unusual in tumour pathology," *Can Med Assoc J*, vol. 97, no. 24, pp. 1466–79, 1967.

[92] C. Frantz, K. M. Stewart, and V. M. Weaver, "The extracellular matrix at a glance," *J Cell Sci*, vol. 123, no. Pt 24, pp. 4195–200, 2010.

[93] I. J. Huijbers, M. Iravani, S. Popov, D. Robertson, S. Al-Sarraj, C. Jones, and C. M. Isacke, "A role for fibrillar collagen deposition and the collagen internalization receptor endo180 in glioma invasion," *PloS one*, vol. 5, no. 3, p. e9808, 2010.

[94] S. Kauppila, F. Stenback, J. Risteli, A. Jukkola, and L. Risteli, "Aberrant type i and type iii collagen gene expression in human breast cancer in vivo," *J Pathol*, vol. 186, no. 3, pp. 262–8, 1998.

[95] G. G. Zhu, L. Risteli, M. Makinen, J. Risteli, A. Kauppila, and F. Stenback, "Immunohistochemical study of type i collagen and type i pn-collagen in benign and malignant ovarian neoplasms," *Cancer*, vol. 75, no. 4, pp. 1010–7, 1995.

[96] T. Hasebe, S. Sasaki, S. Imoto, K. Mukai, T. Yokose, and A. Ochiai, "Prognostic significance of fibrotic focus in invasive ductal carcinoma of the breast: a prospective observational study," *Mod Pathol*, vol. 15, no. 5, pp. 502–16, 2002.

[97] P. P. Provenzano, K. W. Eliceiri, J. M. Campbell, D. R. Inman, J. G. White, and P. J. Keely, "Collagen reorganization at the tumor-stromal interface facilitates local invasion," *BMC Med*, vol. 4, no. 1, p. 38, 2006.

[98] C. J. Sympson, M. J. Bissell, and Z. Werb, "Mammary-gland tumor-formation in transgenic mice overexpressing stromelysin-1," *Semin Cancer Biol*, vol. 6, no. 3, pp. 159–163, 1995.

[99] C. J. Sympson, R. S. Talhouk, C. M. Alexander, J. R. Chin, S. M. Clift, M. J. Bissell, and Z. Werb, "Targeted expression of stromelysin-1 in mammary gland provides evidence for a role of proteinases in branching morphogenesis and the requirement for an intact basement membrane for tissue-specific gene expression," *J Cell Biol*, vol. 125, no. 3, pp. 681–93, 1994.

[100] G. Akiri, E. Sabo, H. Dafni, Z. Vadasz, Y. Kartvelishvily, N. Gan, O. Kessler, T. Cohen, M. Resnick, M. Neeman, and G. Neufeld, "Lysyl oxidase-related protein-1 promotes tumor fibrosis and tumor progression in vivo," *Cancer Res*, vol. 63, no. 7, pp. 1657–66, 2003.

[101] J. T. Erler, K. L. Bennewith, M. Nicolau, N. Dornhofer, C. Kong, Q. T. Le, J. T. Chi, S. S. Jeffrey, and A. J. Giaccia, "Lysyl oxidase is essential for hypoxia-induced metastasis," *Nature*, vol. 440, no. 7088, pp. 1222–6, 2006.

[102] I. G. Maroulakou, M. Anver, L. Garrett, and J. E. Green, "Prostate and mammary adenocarcinoma in transgenic mice carrying a rat c3(1) simian virus 40

large tumor antigen fusion gene," *Proc Natl Acad Sci U S A*, vol. 91, no. 23, pp. 11236–40, 1994.

[103] J. E. Green, M. A. Shibata, K. Yoshidome, M. L. Liu, C. Jorcyk, M. R. Anver, J. Wigginton, R. Wiltrout, E. Shibata, S. Kaczmarczyk, W. Wang, Z. Y. Liu, A. Calvo, and C. Couldrey, "The c3(1)/sv40 t-antigen transgenic mouse model of mammary cancer: ductal epithelial cell targeting with multistage progression to carcinoma," *Oncogene*, vol. 19, no. 8, pp. 1020–7, 2000.

[104] M. A. Shibata, I. G. Maroulakou, C. L. Jorcyk, L. G. Gold, J. M. Ward, and J. E. Green, "p53-independent apoptosis during mammary tumor progression in c3(1)/sv40 large t antigen transgenic mice: suppression of apoptosis during the transition from preneoplasia to carcinoma," *Cancer Res*, vol. 56, no. 13, pp. 2998–3003, 1996.

[105] K. Yoshidome, M. A. Shibata, C. Couldrey, K. S. Korach, and J. E. Green, "Estrogen promotes mammary tumor development in c3(1)/sv40 large t-antigen transgenic mice: paradoxical loss of estrogen receptoralpha expression during tumor progression," *Cancer Res*, vol. 60, no. 24, pp. 6901–10, 2000.

[106] G. M. Clark and W. L. McGuire, "Steroid receptors and other prognostic factors in primary breast cancer," *Semin Oncol*, vol. 15, no. 2 Suppl 1, pp. 20–5, 1988.

[107] G. M. Clark, C. K. Osborne, and W. L. McGuire, "Correlations between estrogen receptor, progesterone receptor, and patient characteristics in human breast cancer," *J Clin Oncol*, vol. 2, no. 10, pp. 1102–9, 1984.

[108] R. L. Brinster, "The effect of cells transferred into the mouse blastocyst on subsequent development," *J Exp Med*, vol. 140, no. 4, pp. 1049–56, 1974.

[109] B. Mintz and K. Illmensee, "Normal genetically mosaic mice produced from malignant teratocarcinoma cells," *Proc Natl Acad Sci U S A*, vol. 72, no. 9, pp. 3585–9, 1975.

[110] G. S. Martin, "Rous sarcoma virus: a function required for the maintenance of the transformed state," *Nature*, vol. 227, no. 5262, pp. 1021–3, 1970.

[111] P. Rous, "A sarcoma of the fowl transmissible by an agent separable from the tumor cells," *J Exp Med*, vol. 13, no. 4, pp. 397–411, 1911.

[112] D. S. Dolberg and M. J. Bissell, "Inability of rous sarcoma virus to cause sarcomas in the avian embryo," *Nature*, vol. 309, no. 5968, pp. 552–6, 1984.

[113] A. W. Stoker, C. Hatier, and M. J. Bissell, "The embryonic environment strongly attenuates v-src oncogenesis in mesenchymal and epithelial tissues, but not in endothelia," *J Cell Biol*, vol. 111, no. 1, pp. 217–28, 1990.

[114] J. J. DeCosse, C. Gossens, J. F. Kuzma, and B. R. Unsworth, "Embryonic inductive tissues that cause histologic differentiation of murine mammary carcinoma in vitro," *J Natl Cancer Inst*, vol. 54, no. 4, pp. 913–22, 1975.

[115] N. Hayashi and G. R. Cunha, "Mesenchyme-induced changes in the neoplastic characteristics of the dunning prostatic adenocarcinoma," *Cancer Res*, vol. 51, no. 18, pp. 4924–30, 1991.

[116] N. Hayashi, G. R. Cunha, and Y. C. Wong, "Influence of male genital tract mesenchymes on differentiation of dunning prostatic adenocarcinoma," *Cancer Res*, vol. 50, no. 15, pp. 4747–54, 1990.

[117] H. Fujii, G. R. Cunha, and J. T. Norman, "The induction of adenocarcinomatous differentiation in neoplastic bladder epithelium by an embryonic prostatic inductor," *J Urol*, vol. 128, no. 4, pp. 858–61, 1982.

[118] S. Sakaguchi, T. Takahashi, T. Sakakura, Y. Sakagami, Y. Nishizuka, and H. Tanaka, "Earlier appearance of murine mammary tumor virus-associated antigens in duct-alveolus nodules induced by transplantation of fetal salivary mesenchyme into c3h mouse mammary glands," *Gann*, vol. 72, no. 6, pp. 982–7, 1981.

[119] T. Sakakura, Y. Sakagami, and Y. Nishizuka, "Acceleration of mammary cancer development by grafting of fetal mammary mesenchymes in c3h mice," *Gann*, vol. 70, no. 4, pp. 459–66, 1979.

[120] T. Sakakura, Y. Sakagami, and Y. Nishizuka, "Accelerated mammary cancer development by fetal salivary mesenchyma isografted to adult mouse mammary epithelium," *J Natl Cancer Inst*, vol. 66, no. 5, pp. 953–9, 1981.

[121] M. Allinen, R. Beroukhim, L. Cai, C. Brennan, J. Lahti-Domenici, H. Huang, D. Porter, M. Hu, L. Chin, A. Richardson, S. Schnitt, W. R. Sellers, and

K. Polyak, "Molecular characterization of the tumor microenvironment in breast cancer," *Cancer Cell*, vol. 6, no. 1, pp. 17–32, 2004.

[122] R. E. Bachelder, M. A. Wendt, and A. M. Mercurio, "Vascular endothelial growth factor promotes breast carcinoma invasion in an autocrine manner by regulating the chemokine receptor cxcr4," *Cancer Res*, vol. 62, no. 24, pp. 7203–6, 2002.

[123] C. Kuperwasser, T. Chavarria, M. Wu, G. Magrane, J. W. Gray, L. Carey, A. Richardson, and R. A. Weinberg, "Reconstruction of functionally normal and malignant human breast tissues in mice," *Proc Natl Acad Sci U S A*, vol. 101, no. 14, pp. 4966–71, 2004.

[124] K. Matsumoto and T. Nakamura, "Hepatocyte growth factor and the met system as a mediator of tumor-stromal interactions," *Int J Cancer*, vol. 119, no. 3, pp. 477–83, 2006.

[125] M. Wu, L. Jung, A. B. Cooper, C. Fleet, L. Chen, L. Breault, K. Clark, Z. Cai, S. Vincent, S. Bottega, Q. Shen, A. Richardson, M. Bosenburg, S. P. Naber, R. A. DePinho, C. Kuperwasser, and M. O. Robinson, "Dissecting genetic requirements of human breast tumorigenesis in a tissue transgenic model of human breast cancer in mice," *Proc Natl Acad Sci U S A*, vol. 106, no. 17, pp. 7022–7, 2009.

[126] B. Y. Karlan, R. L. Baldwin, F. D. Cirisano, P. W. Mamula, J. Jones, and L. D. Lagasse, "Secreted ovarian stromal substance inhibits ovarian epithelial cell proliferation," *Gynecologic oncology*, vol. 59, no. 1, pp. 67–74, 1995.

[127] F. H. Paraguassu-Braga, R. Borojevic, L. F. Bouzas, M. A. Barcinski, and A. Bonomo, "Bone marrow stroma inhibits proliferation and apoptosis in leukemic cells through gap junction-mediated cell communication," *Cell Death Differ*, vol. 10, no. 9, pp. 1101–8, 2003.

[128] L. W. Chung, H. E. Zhau, and J. Y. Ro, "Morphologic and biochemical alterations in rat prostatic tumors induced by fetal urogenital sinus mesenchyme," *Prostate*, vol. 17, no. 2, pp. 165–74, 1990.

[129] T. Sakakura, Y. Sakagami, and Y. Nishizuka, "Persistence of responsiveness of adult mouse mammary gland to induction by embryonic mesenchyme," *Dev Biol*, vol. 72, no. 2, pp. 201–10, 1979.

[130] D. Tarin, "Tissue interactions in morphogenesis, morphostasis and carcinogenesis," *J Theor Biol*, vol. 34, no. 1, pp. 61–72, 1972.

[131] S. D. Banerjee, R. H. Cohn, and M. R. Bernfield, "Basal lamina of embryonic salivary epithelia. production by the epithelium and role in maintaining lobular morphology," *J Cell Biol*, vol. 73, no. 2, pp. 445–63, 1977.

[132] M. R. Bernfield, S. D. Banerjee, and R. H. Cohn, "Dependence of salivary epithelial morphology and branching morphogenesis upon acid mucopolysaccharide-protein (proteoglycan) at the epithelial surface," *J Cell Biol*, vol. 52, no. 3, pp. 674–89, 1972.

[133] S. Huang and D. E. Ingber, "The structural and mechanical complexity of cell-growth control," *Nat Cell Biol*, vol. 1, no. 5, pp. E131–8, 1999.

[134] B. K. Hall and T. Miyake, "The membranous skeleton: the role of cell condensations in vertebrate skeletogenesis," *Anat Embryol (Berl)*, vol. 186, no. 2, pp. 107–24, 1992.

[135] S. Christley, M. S. Alber, and S. A. Newman, "Patterns of mesenchymal condensation in a multiscale, discrete stochastic model," *PLoS computational biology*, vol. 3, no. 4, p. e76, 2007.

[136] S. A. Newman, S. Christley, T. Glimm, H. G. Hentschel, B. Kazmierczak, Y. T. Zhang, J. Zhu, and M. Alber, "Multiscale models for vertebrate limb development," *Curr Top Dev Biol*, vol. 81, pp. 311–40, 2008.

[137] A. E. Urban, X. Zhou, J. M. Ungos, D. W. Raible, C. R. Altmann, and P. D. Vize, "Fgf is essential for both condensation and mesenchymal-epithelial transition stages of pronephric kidney tubule development," *Dev Biol*, vol. 297, no. 1, pp. 103–17, 2006.

[138] S. A. Downie and S. A. Newman, "Different roles for fibronectin in the generation of fore and hind limb precartilage condensations," *Dev Biol*, vol. 172, no. 2, pp. 519–30, 1995.

[139] D. A. Frenz, N. S. Jaikaria, and S. A. Newman, "The mechanism of precartilage mesenchymal condensation: a major role for interaction of the cell surface with the amino-terminal heparin-binding domain of fibronectin," *Dev Biol*, vol. 136, no. 1, pp. 97–103, 1989.

[140] C. B. Knudson and B. P. Toole, "Changes in the pericellular matrix during differentiation of limb bud mesoderm," *Dev Biol*, vol. 112, no. 2, pp. 308–18, 1985.

[141] W. M. Kulyk, W. B. Upholt, and R. A. Kosher, "Fibronectin gene expression during limb cartilage differentiation," *Development*, vol. 106, no. 3, pp. 449–55, 1989.

[142] H. C. Ott, T. S. Matthiesen, S. K. Goh, L. D. Black, S. M. Kren, T. I. Netoff, and D. A. Taylor, "Perfusion-decellularized matrix: using nature's platform to engineer a bioartificial heart," *Nat Med*, vol. 14, no. 2, pp. 213–21, 2008.

[143] T. H. Petersen, E. A. Calle, L. Zhao, E. J. Lee, L. Gui, M. B. Raredon, K. Gavrilov, T. Yi, Z. W. Zhuang, C. Breuer, E. Herzog, and L. E. Niklason, "Tissue-engineered lungs for in vivo implantation," *Science*, vol. 329, no. 5991, pp. 538–41, 2010.

[144] B. E. Uygun, A. Soto-Gutierrez, H. Yagi, M. L. Izamis, M. A. Guzzardi, C. Shulman, J. Milwid, N. Kobayashi, A. Tilles, F. Berthiaume, M. Hertl, Y. Nahmias, M. L. Yarmush, and K. Uygun, "Organ reengineering through development of a transplantable recellularized liver graft using decellularized liver matrix," *Nat Med*, vol. 16, no. 7, pp. 814–20, 2010.

[145] E. Cukierman, "Cell migration analyses within fibroblast-derived 3-d matrices," *Methods Mol Biol*, vol. 294, pp. 79–93, 2005.

[146] J. Folkman, M. Klagsbrun, J. Sasse, M. Wadzinski, D. Ingber, and I. Vlodavsky, "A heparin-binding angiogenic protein–basic fibroblast growth factor–is stored within basement membrane," *Am J Pathol*, vol. 130, no. 2, pp. 393–400, 1988.

[147] C. L. Chu, J. A. Buczek-Thomas, and M. A. Nugent, "Heparan sulphate proteoglycans modulate fibroblast growth factor-2 binding through a lipid raft-mediated mechanism," *Biochem J*, vol. 379, no. Pt 2, pp. 331–41, 2004.

[148] M. Presta, J. A. Maier, M. Rusnati, and G. Ragnotti, "Basic fibroblast growth factor is released from endothelial extracellular matrix in a biologically active form," *J Cell Physiol*, vol. 140, no. 1, pp. 68–74, 1989.

[149] J. Folkman and A. Moscona, "Role of cell shape in growth control," *Nature*, vol. 273, no. 5661, pp. 345–9, 1978.

[150] D. E. Ingber and J. Folkman, "Mechanochemical switching between growth and differentiation during fibroblast growth factor-stimulated angiogenesis in vitro: role of extracellular matrix," *J Cell Biol*, vol. 109, no. 1, pp. 317–30, 1989.

[151] M. L. Li, J. Aggeler, D. A. Farson, C. Hatier, J. Hassell, and M. J. Bissell, "Influence of a reconstituted basement membrane and its components on casein gene expression and secretion in mouse mammary epithelial cells," *Proc Natl Acad Sci U S A*, vol. 84, no. 1, pp. 136–40, 1987.

[152] R. McBeath, D. M. Pirone, C. M. Nelson, K. Bhadriraju, and C. S. Chen, "Cell shape, cytoskeletal tension, and rhoa regulate stem cell lineage commitment," *Dev Cell*, vol. 6, no. 4, pp. 483–95, 2004.

[153] D. Mooney, L. Hansen, J. Vacanti, R. Langer, S. Farmer, and D. Ingber, "Switching from differentiation to growth in hepatocytes: control by extracellular matrix," *J Cell Physiol*, vol. 151, no. 3, pp. 497–505, 1992.

[154] M. Opas, "Expression of the differentiated phenotype by epithelial cells in vitro is regulated by both biochemistry and mechanics of the substratum," *Dev Biol*, vol. 131, no. 2, pp. 281–93, 1989.

[155] K. K. Parker, A. L. Brock, C. Brangwynne, R. J. Mannix, N. Wang, E. Ostuni, N. A. Geisse, J. C. Adams, G. M. Whitesides, and D. E. Ingber, "Directional control of lamellipodia extension by constraining cell shape and orienting cell tractional forces," *FASEB J*, vol. 16, no. 10, pp. 1195–204, 2002.

[156] H. Hertz, "Uber die beruhurung fester elastischer korper (on the contact of elastic solids)," *J Reini Angew Math*, vol. 5, pp. 12–23, 1881.

[157] K. Johnson, "Contact mechanics," *Cambridge: Cambridge University Press*, 1985.

[158] M. Kanapathipillai, A. Mammoto, T. Mammoto, J. H. Kang, E. Jiang, K. Ghosh, N. Korin, A. Gibbs, R. Mannix, and D. E. Ingber, "Inhibition of mammary tumor growth using lysyl oxidase-targeting nanoparticles to modify extracellular matrix," *Nano Lett*, vol. 12, no. 6, pp. 3213–7, 2012.

[159] K. Saha, A. J. Keung, E. F. Irwin, Y. Li, L. Little, D. V. Schaffer, and K. E. Healy, "Substrate modulus directs neural stem cell behavior," *Biophys J*, vol. 95, no. 9, pp. 4426–38, 2008.

[160] E. Hadjipanayi, V. Mudera, and R. A. Brown, "Close dependence of fibroblast proliferation on collagen scaffold matrix stiffness," *J Tissue Eng Regen Med*, vol. 3, no. 2, pp. 77–84, 2009.

[161] H. B. Wang, M. Dembo, and Y. L. Wang, "Substrate flexibility regulates growth and apoptosis of normal but not transformed cells," *Am J Physiol Cell Physiol*, vol. 279, no. 5, pp. C1345–50, 2000.

[162] W. H. Guo, M. T. Frey, N. A. Burnham, and Y. L. Wang, "Substrate rigidity regulates the formation and maintenance of tissues," *Biophys J*, vol. 90, no. 6, pp. 2213–20, 2006.

[163] A. Mammoto, K. M. Connor, T. Mammoto, C. W. Yung, D. Huh, C. M. Aderman, G. Mostoslavsky, L. E. Smith, and D. E. Ingber, "A mechanosensitive transcriptional mechanism that controls angiogenesis," *Nature*, vol. 457, no. 7233, pp. 1103–8, 2009.

[164] G. R. Cunha, N. Hayashi, and Y. C. Wong, "Regulation of differentiation and growth of normal adult and neoplastic epithelia by inductive mesenchyme," *Cancer Surv*, vol. 11, pp. 73–90, 1991.

[165] M. L. Ellison, E. J. Ambrose, and G. C. Easty, "Differentiation in a transplantable rat tumour maintained in organ culture," *Exp Cell Res*, vol. 55, no. 2, pp. 198–204, 1969.

[166] C. J. Dawe, W. D. Morgan, and M. S. Slatick, "Influence of epitheliomesenchymal interactions on tumor induction by polyoma virus," *Int J Cancer*, vol. 1, no. 5, pp. 419–50, 1966.

[167] C. J. Dawe, J. Whang-Peng, W. D. Morgan, E. C. Hearon, and T. Knutsen, "Epithelial origin of polyoma salivary tumors in mice: evidence based on chromosome-marked cells," *Science*, vol. 171, no. 3969, pp. 394–7, 1971.

[168] X. Dong-Le Bourhis, Y. Berthois, G. Millot, A. Degeorges, M. Sylvi, P. M. Martin, and F. Calvo, "Effect of stromal and epithelial cells derived from normal and tumorous breast tissue on the proliferation of human breast cancer cell lines in co-culture," *Int J Cancer*, vol. 71, no. 1, pp. 42–8, 1997.

[169] C. M. Verfaillie and P. Catanzaro, "Direct contact with stroma inhibits proliferation of human long-term culture initiating cells," *Leukemia*, vol. 10, no. 3, pp. 498–504, 1996.

[170] M. F. Rousseau-Merck, M. N. Lombard, C. Nezelof, and H. Mouly, "Limitation of the potentialities of nephroblastoma differentiation in vitro," *Eur J Cancer*, vol. 13, no. 2, pp. 163–70, 1977.

[171] K. R. Baumann and H. L. Hosick, "Replication of mouse mammary tumor cells in monolayer cultures stimulated with embryo extract," *Exp Cell Biol*, vol. 46, no. 6, pp. 325–37, 1978.

[172] M. Gleave, J. T. Hsieh, C. A. Gao, A. C. von Eschenbach, and L. W. Chung, "Acceleration of human prostate cancer growth in vivo by factors produced by prostate and bone fibroblasts," *Cancer Res*, vol. 51, no. 14, pp. 3753–61, 1991.

[173] S. Krause, M. V. Maffini, A. M. Soto, and C. Sonnenschein, "A novel 3d in vitro culture model to study stromal-epithelial interactions in the mammary gland," *Tissue Eng Part C Methods*, vol. 14, no. 3, pp. 261–71, 2008.

[174] S. Ali and R. C. Coombes, "Estrogen receptor alpha in human breast cancer: occurrence and significance," *J Mammary Gland Biol Neoplasia*, vol. 5, no. 3, pp. 271–81, 2000.

[175] T. Vargo-Gogola and J. M. Rosen, "Modelling breast cancer: one size does not fit all," *Nat Rev Cancer*, vol. 7, no. 9, pp. 659–72, 2007.

[176] A. E. Karnoub, A. B. Dash, A. P. Vo, A. Sullivan, M. W. Brooks, G. W. Bell, A. L. Richardson, K. Polyak, R. Tubo, and R. A. Weinberg, "Mesenchymal

stem cells within tumour stroma promote breast cancer metastasis," *Nature*, vol. 449, no. 7162, pp. 557–63, 2007.

[177] A. B. Jaffe and A. Hall, "Rho gtpases: biochemistry and biology," *Annu Rev Cell Dev Biol*, vol. 21, pp. 247–69, 2005.

[178] E. Pinney, M. Zimber, A. Schenone, M. Montes-Camacho, F. Ziegler, and G. Naughton, "Human embryonic-like ecm (hecm) stimulates proliferation and differentiation in stem cells while killing cancer cells," *International Journal of Stem Cells*, vol. 4, no. 1, pp. 70–75, 2011.

[179] S. Kidd, E. Spaeth, J. L. Dembinski, M. Dietrich, K. Watson, A. Klopp, V. L. Battula, M. Weil, M. Andreeff, and F. C. Marini, "Direct evidence of mesenchymal stem cell tropism for tumor and wounding microenvironments using in vivo bioluminescent imaging," *Stem Cells*, vol. 27, no. 10, pp. 2614–23, 2009.

[180] S. B. Coffelt, F. C. Marini, K. Watson, K. J. Zwezdaryk, J. L. Dembinski, H. L. LaMarca, S. L. Tomchuck, K. Honer zu Bentrup, E. S. Danka, S. L. Henkle, and A. B. Scandurro, "The pro-inflammatory peptide ll-37 promotes ovarian tumor progression through recruitment of multipotent mesenchymal stromal cells," *Proc Natl Acad Sci U S A*, vol. 106, no. 10, pp. 3806–11, 2009.

[181] N. C. Direkze, K. Hodivala-Dilke, R. Jeffery, T. Hunt, R. Poulsom, D. Oukrif, M. R. Alison, and N. A. Wright, "Bone marrow contribution to tumor-associated myofibroblasts and fibroblasts," *Cancer Res*, vol. 64, no. 23, pp. 8492–5, 2004.

[182] G. Ishii, T. Sangai, T. Oda, Y. Aoyagi, T. Hasebe, N. Kanomata, Y. Endoh, C. Okumura, Y. Okuhara, J. Magae, M. Emura, T. Ochiya, and A. Ochiai, "Bone-marrow-derived myofibroblasts contribute to the cancer-induced stromal reaction," *Biochem Biophys Res Commun*, vol. 309, no. 1, pp. 232–40, 2003.

[183] E. L. Spaeth, J. L. Dembinski, A. K. Sasser, K. Watson, A. Klopp, B. Hall, M. Andreeff, and F. Marini, "Mesenchymal stem cell transition to tumor-associated fibroblasts contributes to fibrovascular network expansion and tumor progression," *PloS one*, vol. 4, no. 4, p. e4992, 2009.

[184] D. E. Ingber, "Can cancer be reversed by engineering the tumor microenvironment?," *Semin Cancer Biol*, vol. 18, no. 5, pp. 356–64, 2008.

[185] A. W. James, A. A. Theologis, S. A. Brugmann, Y. Xu, A. L. Carre, P. Leucht, K. Hamilton, K. S. Korach, and M. T. Longaker, "Estrogen/estrogen receptor alpha signaling in mouse posterofrontal cranial suture fusion," *PloS one*, vol. 4, no. 9, p. e7120, 2009.

[186] R. G. Holzer, C. MacDougall, G. Cortright, K. Atwood, J. E. Green, and C. L. Jorcyk, "Development and characterization of a progressive series of mammary adenocarcinoma cell lines derived from the c3(1)/sv40 large t-antigen transgenic mouse model," *Breast Cancer Res Treat*, vol. 77, no. 1, pp. 65–76, 2003.

[187] J. G. Goetz, S. Minguet, I. Navarro-Lerida, J. J. Lazcano, R. Samaniego, E. Calvo, M. Tello, T. Osteso-Ibanez, T. Pellinen, A. Echarri, A. Cerezo, A. J. Klein-Szanto, R. Garcia, P. J. Keely, P. Sanchez-Mateos, E. Cukierman, and M. A. Del Pozo, "Biomechanical remodeling of the microenvironment by stromal caveolin-1 favors tumor invasion and metastasis," *Cell*, vol. 146, no. 1, pp. 148–63, 2011.

[188] M. J. Paszek, N. Zahir, K. R. Johnson, J. N. Lakins, G. I. Rozenberg, A. Gefen, C. A. Reinhart-King, S. S. Margulies, M. Dembo, D. Boettiger, D. A. Hammer, and V. M. Weaver, "Tensional homeostasis and the malignant phenotype," *Cancer Cell*, vol. 8, no. 3, pp. 241–54, 2005.

[189] P. P. Provenzano, D. R. Inman, K. W. Eliceiri, and P. J. Keely, "Matrix density-induced mechanoregulation of breast cell phenotype, signaling and gene expression through a fak-erk linkage," *Oncogene*, vol. 28, no. 49, pp. 4326–43, 2009.

[190] P. J. Keely, J. E. Wu, and S. A. Santoro, "The spatial and temporal expression of the alpha 2 beta 1 integrin and its ligands, collagen i, collagen iv, and laminin, suggest important roles in mouse mammary morphogenesis," *Differentiation*, vol. 59, no. 1, pp. 1–13, 1995.

[191] G. B. Silberstein and C. W. Daniel, "Glycosaminoglycans in the basal lamina and extracellular matrix of serially aged mouse mammary ducts," *Mech Ageing Dev*, vol. 24, no. 2, pp. 151–62, 1984.

[192] M. J. Warburton, D. Mitchell, E. J. Ormerod, and P. Rudland, "Distribution of myoepithelial cells and basement membrane proteins in the resting, pregnant, lactating, and involuting rat mammary gland," *J Histochem Cytochem*, vol. 30, no. 7, pp. 667–76, 1982.

[193] M. D. Sternlicht, A. Lochter, C. J. Sympson, B. Huey, J. P. Rougier, J. W. Gray, D. Pinkel, M. J. Bissell, and Z. Werb, "The stromal proteinase mmp3/stromelysin-1 promotes mammary carcinogenesis," *Cell*, vol. 98, no. 2, pp. 137–46, 1999.

[194] K. Gelse, E. Poschl, and T. Aigner, "Collagens–structure, function, and biosynthesis," *Adv Drug Deliv Rev*, vol. 55, no. 12, pp. 1531–46, 2003.

[195] S. Peyrol, M. Raccurt, F. Gerard, C. Gleyzal, J. A. Grimaud, and P. Sommer, "Lysyl oxidase gene expression in the stromal reaction to in situ and invasive ductal breast carcinoma," *Am J Pathol*, vol. 150, no. 2, pp. 497–507, 1997.

[196] L. Yuan, M. Siegel, K. Choi, C. Khosla, C. R. Miller, E. N. Jackson, D. Piwnica-Worms, and K. M. Rich, "Transglutaminase 2 inhibitor, kcc009, disrupts fibronectin assembly in the extracellular matrix and sensitizes orthotopic glioblastomas to chemotherapy," *Oncogene*, vol. 26, no. 18, pp. 2563–73, 2007.

[197] M. A. Carvalho, K. Arcanjo, L. C. Silva, and R. Borojevic, "The capacity of connective tissue stromas to sustain myelopoiesis depends both upon the growth factors and the local intercellular environment," *Biol Cell*, vol. 92, no. 8-9, pp. 605–14, 2000.

[198] M. Vigny, M. P. Ollier-Hartmann, M. Lavigne, N. Fayein, J. C. Jeanny, M. Laurent, and Y. Courtois, "Specific binding of basic fibroblast growth factor to basement membrane-like structures and to purified heparan sulfate proteoglycan of the ehs tumor," *J Cell Physiol*, vol. 137, no. 2, pp. 321–8, 1988.

[199] K. E. Kubow, E. Klotzsch, M. L. Smith, D. Gourdon, W. C. Little, and V. Vogel, "Crosslinking of cell-derived 3d scaffolds up-regulates the stretching and unfolding of new extracellular matrix assembled by reseeded cells," *Integr Biol (Camb)*, vol. 1, no. 11-12, pp. 635–48, 2009.

[200] A. Naba, K. R. Clauser, S. Hoersch, H. Liu, S. A. Carr, and R. O. Hynes, "The matrisome: in silico definition and in vivo characterization by proteomics of normal and tumor extracellular matrices," *Mol Cell Proteomics*, vol. 11, no. 4, p. M111 014647, 2012.

[201] H. Alimohamad, T. Habijanac, H. Larjava, and L. Hakkinen, "Colocalization of the collagen-binding proteoglycans decorin, biglycan, fibromodulin and lumican with different cells in human gingiva," *J Periodontal Res*, vol. 40, no. 1, pp. 73–86, 2005.

[202] T. Douglas, S. Heinemann, S. Bierbaum, D. Scharnweber, and H. Worch, "Fibrillogenesis of collagen types i, ii, and iii with small leucine-rich proteoglycans decorin and biglycan," *Biomacromolecules*, vol. 7, no. 8, pp. 2388–93, 2006.

[203] M. A. Nash, A. E. Loercher, and R. S. Freedman, "In vitro growth inhibition of ovarian cancer cells by decorin: synergism of action between decorin and carboplatin," *Cancer Res*, vol. 59, no. 24, pp. 6192–6, 1999.

[204] C. K. Weber, G. Sommer, P. Michl, H. Fensterer, M. Weimer, F. Gansauge, G. Leder, G. Adler, and T. M. Gress, "Biglycan is overexpressed in pancreatic cancer and induces g1-arrest in pancreatic cancer cell lines," *Gastroenterology*, vol. 121, no. 3, pp. 657–67, 2001.

[205] K. Yamamoto, N. Ohga, Y. Hida, N. Maishi, T. Kawamoto, K. Kitayama, K. Akiyama, T. Osawa, M. Kondoh, K. Matsuda, Y. Onodera, M. Fujie, K. Kaga, S. Hirano, N. Shinohara, M. Shindoh, and K. Hida, "Biglycan is a specific marker and an autocrine angiogenic factor of tumour endothelial cells," *Br J Cancer*, vol. 106, no. 6, pp. 1214–23, 2012.

[206] G. W. Robinson, A. B. Karpf, and K. Kratochwil, "Regulation of mammary gland development by tissue interaction," *J Mammary Gland Biol Neoplasia*, vol. 4, no. 1, pp. 9–19, 1999.

[207] Y. Nakanishi, H. Nogawa, Y. Hashimoto, J. Kishi, and T. Hayakawa, "Accumulation of collagen iii at the cleft points of developing mouse submandibular epithelium," *Development*, vol. 104, no. 1, pp. 51–9, 1988.

[208] R. A. Brekken and E. H. Sage, "Sparc, a matricellular protein: at the crossroads of cell-matrix," *Matrix biology : journal of the International Society for Matrix Biology*, vol. 19, no. 7, pp. 569–80, 2000.

[209] E. Hohenester, T. Sasaki, C. Giudici, R. W. Farndale, and H. P. Bachinger, "Structural basis of sequence-specific collagen recognition by sparc," *Proc Natl Acad Sci U S A*, vol. 105, no. 47, pp. 18273–7, 2008.

[210] S. Huang and D. E. Ingber, "Cell tension, matrix mechanics, and cancer development," *Cancer Cell*, vol. 8, no. 3, pp. 175–6, 2005.

[211] M. H. Barcellos-Hoff, "Radiation-induced transforming growth factor beta and subsequent extracellular matrix reorganization in murine mammary gland," *Cancer Res*, vol. 53, no. 17, pp. 3880–6, 1993.

[212] M. H. Barcellos-Hoff, R. Derynck, M. L. Tsang, and J. A. Weatherbee, "Transforming growth factor-beta activation in irradiated murine mammary gland," *J Clin Invest*, vol. 93, no. 2, pp. 892–9, 1994.

[213] A. D. Bradshaw, M. J. Reed, and E. H. Sage, "Sparc-null mice exhibit accelerated cutaneous wound closure," *J Histochem Cytochem*, vol. 50, no. 1, pp. 1–10, 2002.

[214] A. Chlenski, S. Liu, S. E. Crawford, O. V. Volpert, G. H. DeVries, A. Evangelista, Q. Yang, H. R. Salwen, R. Farrer, J. Bray, and S. L. Cohn, "Sparc is a key schwannian-derived inhibitor controlling neuroblastoma tumor angiogenesis," *Cancer Res*, vol. 62, no. 24, pp. 7357–63, 2002.

[215] N. Dhanesuan, J. A. Sharp, T. Blick, J. T. Price, and E. W. Thompson, "Doxycycline-inducible expression of sparc/osteonectin/bm40 in mda-mb-231 human breast cancer cells results in growth inhibition," *Breast Cancer Res Treat*, vol. 75, no. 1, pp. 73–85, 2002.

[216] I. T. Tai, M. Dai, D. A. Owen, and L. B. Chen, "Genome-wide expression analysis of therapy-resistant tumors reveals sparc as a novel target for cancer therapy," *J Clin Invest*, vol. 115, no. 6, pp. 1492–502, 2005.

[217] P. Lu, K. Takai, V. M. Weaver, and Z. Werb, "Extracellular matrix degradation and remodeling in development and disease," *Cold Spring Harb Perspect Biol*, vol. 3, no. 12, 2011.

[218] G. B. Pierce, "The cancer cell and its control by the embryo. rous-whipple award lecture," *Am J Pathol*, vol. 113, no. 1, pp. 117–24, 1983.

[219] R. Siegel, D. Naishadham, and A. Jemal, "Cancer statistics, 2013," *CA Cancer J Clin*, vol. 63, no. 1, pp. 11–30, 2013.

[220] I. Pitha-Rowe, W. J. Petty, S. Kitareewan, and E. Dmitrovsky, "Retinoid target genes in acute promyelocytic leukemia," *Leukemia*, vol. 17, no. 9, pp. 1723–30, 2003.

[221] I. Cunningham, T. S. Gee, L. M. Reich, S. J. Kempin, A. N. Naval, and B. D. Clarkson, "Acute promyelocytic leukemia: treatment results during a decade at memorial hospital," *Blood*, vol. 73, no. 5, pp. 1116–22, 1989.

[222] R. M. Stone, M. Maguire, M. A. Goldberg, J. H. Antin, D. S. Rosenthal, and R. J. Mayer, "Complete remission in acute promyelocytic leukemia despite persistence of abnormal bone marrow promyelocytes during induction therapy: experience in 34 patients," *Blood*, vol. 71, no. 3, pp. 690–6, 1988.

[223] M. S. Tallman, J. W. Andersen, C. A. Schiffer, F. R. Appelbaum, J. H. Feusner, A. Ogden, L. Shepherd, C. Willman, C. D. Bloomfield, J. M. Rowe, and P. H. Wiernik, "All-trans-retinoic acid in acute promyelocytic leukemia," *The New England journal of medicine*, vol. 337, no. 15, pp. 1021–8, 1997.

[224] M. S. Tallman, J. W. Andersen, C. A. Schiffer, F. R. Appelbaum, J. H. Feusner, W. G. Woods, A. Ogden, H. Weinstein, L. Shepherd, C. Willman, C. D. Bloomfield, J. M. Rowe, and P. H. Wiernik, "All-trans retinoic acid in acute promyelocytic leukemia: long-term outcome and prognostic factor analysis from the north american intergroup protocol," *Blood*, vol. 100, no. 13, pp. 4298–302, 2002.

[225] F. D. Cruz and I. Matushansky, "Solid tumor differentiation therapy - is it possible?," *Oncotarget*, vol. 3, no. 5, pp. 559–67, 2012.